

**UNIVERSITY OF SAO PAULO**  
**FACULTY OF PHARMACEUTICAL SCIENCES**  
Graduate Program in Drugs and Medicines  
Pharmaceutical Production and Control

Buparvaquone nanostructured lipid carrier development:  
physicochemical and *in vitro* leishmanicidal performances

Lis Marie Monteiro

A thesis submitted in fulfillment of the requirements for the degree of  
Doctor of Science  
Supervisor: Dr. Nádia Bou-Chacra

São Paulo  
2017

**UNIVERSITY OF SAO PAULO**  
**FACULTY OF PHARMACEUTICAL SCIENCES**  
Graduate Program in Drugs and Medicines  
Pharmaceutical Production and Control

Buparvaquone nanostructured lipid carrier development:  
physicochemical and *in vitro* leishmanicidal performances

Lis Marie Monteiro

Final version

A thesis submitted in fulfillment of the requirements for the degree of

Doctor of Science

Supervisor: Dr. Nádia Bou-Chacra

Co-supervisor: Dr. Paulo César Cotrim

São Paulo

2017

Ficha Catalográfica  
Elaborada pela Divisão de Biblioteca e  
Documentação do Conjunto das Químicas da USP

M772b Monteiro, Lis Marie  
Buparvaquone Nanostructured Lipid Carrier  
Development: Physicochemical and in vitro  
Leishmanicidal Performances / Lis Marie Monteiro. -  
São Paulo, 2017.  
109 p.

Tese (doutorado) - Faculdade de Ciências  
Farmacêuticas da Universidade de São Paulo.  
Departamento de Farmácia.  
Orientador: Bou-Chacra, Nadia  
Coorientador: Cotrim, Paulo Cesar

1. Buparvaquona. 2. Carrreadores lipídicos  
nanoestruturados. 3. Leishmanioses. 4. Doenças  
negligenciadas. I. T. II. Bou-Chacra, Nadia,  
orientador. III. Cotrim, Paulo Cesar, coorientador.

Lis Marie Monteiro

Buparvaquone nanostructured lipid carrier development:  
physicochemical and *in vitro* leishmanicidal performances

Referee Commission of the thesis submitted in fulfillment of  
the requirements for the degree of Doctor of Science

Supervisor: Dr. Raimar Löberberg

Dr. supervisor/chairwoman

Dr. Nádia Bou-Chacra

---

1<sup>st</sup> examiner

---

2<sup>nd</sup> examiner

---

3<sup>th</sup> examiner

São Paulo, \_\_\_\_\_

## Abstract

MONTEIRO, L. M. **Buparvaquone nanostructured lipid carrier development: physicochemical and *in vitro* leishmanicidal performances** 2017, 109p. Tese (Doutorado) – Faculdade de Ciências Farmacêuticas, Universidade de São Paulo, São Paulo, 2017.

Leishmaniasis is a group of diseases caused by parasites of the genus *Leishmania*. The estimated number of deaths from visceral leishmaniasis ranges from 20,000 to 50,000 annually. The most common treatment over the past 60 years has been pentavalent antimonials. Besides the doubtful effectiveness, they present several disadvantages such as the need for parenteral administration, large doses, long treatment, severe toxicity and parasite resistance. Buparvaquone (BPQ), a drug used for veterinary treatment of theileriosis, showed promising activity against *Leishmania spp.* However, due to its low aqueous solubility and bioavailability, it has failed in *in vivo* tests. The use of nanotechnologies has the potential to overcome these drawbacks due to the following advantages: increase in drug water-solubility, increase in therapeutic efficacy and treatment toxicity reduction. Therefore, the present work aimed the development, optimization, physical-chemical evaluation and *in vitro* performances of nanostructured lipid carriers (NLC) for BPQ encapsulation. The NLC preparation was performed by high pressure homogenization, and surface response and factorial design were applied to formulation optimization. *In vitro* dissolution profiles were evaluated in phosphate buffer pH 7.4 with tween 80 0.07% w/v or sodium dodecyl sulfate 1% w/v and simulated body fluid pH 7.4. Cytotoxicity was evaluated in mouse peritoneal macrophages and leishmanicidal activity in *L. infantum* amastigotes. Six optimized NLC were prepared and they showed solubility improvement from 1.5-fold to 611-fold when compared with free BPQ, depending on the formulation and medium. Dissolution profiles showed the NLC formulation suitability for BPQ regarding oral administration, the release could reach 83.29% of a 4mg dose in 30 minutes for formulation of 175.1 nm, while the free drug could be dissolved only 2.89% of the same dose after 4 hours. Moreover, formulation of 230.7 nm showed 81.42% of drug release in phosphate buffer pH 7.4 with dodecyl sulfate 1.0% w/v after 30 minutes, while BPQ did not dissolve. Cytotoxicity assay showed the safety of all formulations. The

CC<sub>50</sub> values were close to 500  $\mu$ M, while the IC<sub>50</sub> against amastigotes was only 456.5 nM for free BPQ. Developed NLCs showed an increase in IC<sub>50</sub> from 2.0 to 3.1-fold when compared to free drug in the *in vitro* leishmanicidal evaluation. Therefore, the NLC containing BPQ are a promising alternative for the treatment of leishmaniasis as oral and parenteral drug dosage forms. Additionally, they have a potential use for lymphatic targeted drug delivery, which can be an innovative approach for this neglected disease.

Keywords: Buparvaquone, Nanostructured Lipid Carrier, Leishmaniasis, Neglected Diseases.

## Resumo

MONTEIRO, L. M. **Desenvolvimento de carreadores lipídicos nanoestruturados contendo buparvaquona: caracterização físico-química e avaliação da atividade leishmanicida *in vitro*** 2017, 109f. Tese (Doutorado) – Faculdade de Ciências Farmacêuticas, Universidade de São Paulo, São Paulo, 2017.

Leishmanioses são um grupo de doenças causadas por parasitas do gênero *Leishmania*. O número estimado de óbitos por leishmaniose visceral varia entre 20.000 e 50.000 por ano. O tratamento mais comum nos últimos 60 anos tem sido os antimônios pentavalentes. Além da eficácia duvidosa, eles apresentam várias desvantagens, como a necessidade de administração parenteral, altas doses, tratamento prolongado, toxicidade severa e resistência parasitária. Buparvaquona (BPQ), um fármaco usado para tratamento veterinário da teileriose, mostrou atividade promissora contra *Leishmania donovani*. No entanto, devido à sua baixa solubilidade e biodisponibilidade aquosa, falhou em testes *in vivo*. O uso das nanotecnologias tem o potencial de superar esses obstáculos devido às seguintes vantagens: aumento da solubilidade em água, aumento da eficácia terapêutica e redução da toxicidade do tratamento. Portanto, o presente trabalho objetivou o desenvolvimento, otimização, avaliação físico-química e avaliação do desempenho *in vitro* de carreadores lipídicos nanoestruturados (NLC) para a encapsulação da BPQ. A preparação do NLC foi realizada por homogeneização de alta pressão e superfície de resposta e planejamento fatorial foram aplicados à otimização das formulações. Os perfis de dissolução *in vitro* foram avaliados em tampão fosfato pH 7.4 com tween 80 a 0.07% p/v ou dodecilsulfato de sódio 1.0% p/v e fluido corporal simulado pH 7.4. A citotoxicidade foi avaliada em macrófagos peritoneais de camundongos e atividade leishmanicida em amastigotas de *L. infantum*. Foram preparados quatro NLC otimizados e mostraram melhora da solubilidade de 1,5 a 611 vezes quando comparado com a BPQ livre, dependendo da formulação e do meio. Os perfis de dissolução mostraram a adequação da formulação NLC para BPQ em relação à administração oral. A dissolução pode atingir 83,29% de uma dose de 4.0 mg em 30 minutos para a formulação de 175,1 nm, enquanto o fármaco livre dissolveu apenas

2,89% da mesma dose após 4 horas. Além disso, a formulação de 230,7 nm mostrou 81,42% de liberação do fármaco em tampão fosfato pH 7.4 com dodecil sulfato de sódio 1.0% p/v após 30 minutos, enquanto o BPQ não se dissolveu. O teste de citotoxicidade mostrou a segurança de todas as formulações. Os valores  $CC_{50}$  foram próximos de 500  $\mu$ M, enquanto o  $IC_{50}$  em amastigotas foi de apenas 456,5 nM para BPQ livre. Os NLC desenvolvidos mostraram um aumento no  $IC_{50}$  de 2,0 a 3,1 vezes quando comparado ao fármaco livre na avaliação leishmanicida *in vitro*. Logo, as NLC contendo BPQ são uma alternativa promissora para o tratamento de leishmanioses como formas farmacêuticas oral e parenteral. Além disso, eles têm um uso potencial para a sítio-específico ao sistema linfático, o que pode ser uma abordagem inovadora para esta doença negligenciada.

Palavras-chave: Buparvaquona, Carreador Lipídico Nanoestruturado, Leishmanioses, Doenças Negligenciadas.



## Preface

This thesis is an original work by Lis Marie Monteiro completed under the supervision of Prof. Dr. Nadia Bou-Chacra at the University of São Paulo and Co-supervision of Prof. Dr. Paulo César Cotrim and Prof. Dr. Raimar Löbenberg. This work was performed in the Dr. Nádia Bou-Chacra lab facilities, Tropical Medicine Institute of São Paulo and Drug Development Innovation Center (DDIC) at University of Alberta.

**Chapter 2** of this thesis has been published as “Buparvaquone nanostructured lipid carrier: development of an affordable delivery system for the treatment of leishmaniasis” in **BioMed Research International** Volume 2017, Article ID 9781603, Lis Marie Monteiro is the first author and Dr. Nadia Bou-Chacra is the last and corresponding author, Dr. Gabriel Lima Barros de Araújo, Dr. Raimar Löbenberg and Dr. Paulo César Cotrim are collaborators regarding conception and design study, analysis of data and drafting of article and critical revision.

**Chapter 3** of this thesis has been submitted for publication as “Nanostructured lipid carrier enables oral administration of low water soluble buparvaquone: development by DoE, *in vitro* drug release and cytotoxicity” and Lis Marie Monteiro being the primary author and responsible for data collection, analysis and write up of this manuscript, Dr. Nadia Bou-Chacra was the supervisory author and was involved in the formulation of the concept, analysis and composition of the manuscript. The **Journal of Controlled Release** was selected for submission.

**Chapter 4** of this thesis has been submitted for publication as “Co-encapsulation of buparvaquone and polymyxin B in nanostructured lipid carrier as a delivery system for leishmaniasis treatment” and Lis Marie Monteiro was responsible for data collection, analysis and write up of this manuscript, Dr. Nadia Bou-Chacra was the supervisory author and was involved in the formulation of the concept, analysis and composition of the manuscript. The **International Journal of Antimicrobial Agents** was selected for submission

## **Acknowledgments**

I would like to greatly thank my supervisors, Dr. Nádia Araci Bou-Chacra, Dr. Raimar Löbenberg and Dr. Paulo César Cotrim for their guidance, help and support to my Ph.D research. I am extremely grateful for encouraging and inspiring all the way on my Ph.D study. Without their continuous support, my work could not have been done. Without their training, my academic writing and presentation delivery skills could not have been improved. I sincerely appreciate the valuable opportunity of 6-month study in the University of Alberta, provided by Dr. Löbenberg. I also would like to thank laboratory colleagues for their guidance and support.

My sincere thanks go to many brilliant scientists. I greatly thank MSc Edite Kanashiro and Mussya Rocha for the incredible guidance and help on leishmanicidal and cytotoxicity tests. Special thanks are dedicated to: MSc Ivan Cordova Morales for his help in the high-pressure homogenization and Megumi Nishitani for her support in the dual degree agreement.

My work could not have been done without the support of my family. They have been incredibly caring, understanding, encouraging and supportive. I really appreciate their love. My life would not have been complete without the amazing friends I have known. I am grateful to FAPESP and CNPq for the financial support.

## Table of Contents

<b>Abstract .....</b>	<b>iii</b>
<b>Resumo.....</b>	<b>v</b>
<b>Preface.....</b>	<b>vii</b>
<b>Acknowledgements.....</b>	<b>viii</b>
<b>Table of Contents.....</b>	<b>ix</b>
<b>List of Tables.....</b>	<b>xiv</b>
<b>List of Figures .....</b>	<b>xvii</b>
<b>List of Abbreviations.....</b>	<b>xviii</b>
<b>Chapter 1</b>	
<b>Introduction.....</b>	<b>1</b>
<b>1.1.1. Neglected diseases .....</b>	<b>1</b>
<b>1.1.2. Leishmaniasis: life cycle, clinical manifestations and chemotherapy....</b>	<b>2</b>
<b>1.1.3. Leishmaniasis life cycle.....</b>	<b>2</b>
<b>1.2.1. Clinical manifestations .....</b>	<b>4</b>
<b>1.2.1.1. Visceral leishmaniasis.....</b>	<b>4</b>
<b>1.2.1.2. Cutaneous leishmaniasis.....</b>	<b>5</b>
<b>1.2.2. Leishmaniasis chemotherapy .....</b>	<b>6</b>
<b>1.2.2.1. Buparvaquone.....</b>	<b>7</b>
<b>1.2.3. Biopharmaceutics Classification System (BCS) - permeability and solubility implications in new drugs and medicines development.....</b>	<b>8</b>
<b>1.2.4. Considerations on nanotechnology for drug delivery systems.....</b>	<b>11</b>
<b>1.2.4.1. Nanostructured lipid systems: liposome, nanoemulsion, solid lipid nanoparticle and nanostructured lipid carrier.....</b>	<b>13</b>
<b>1.2.4.2. Liposomes and nanoemulsions.....</b>	<b>13</b>
<b>1.2.4.3. Solid lipid nanoparticles and nanostructured lipid carriers.....</b>	<b>14</b>

1.2.5. Rational scientific basis for the application of nanostructured systems in the treatment of leishmaniases .....	18
Hypothesis.....	23
Objectives.....	23
Chapter 2	
Abstract.....	25
2.1. Introduction.....	26
2.2. Materials and methods.....	27
2.2.1. Chemicals.....	27
2.2.2. Selection of liquid and solid lipids for BPQ-NLCs preparation.....	28
2.2.3. Preparation of BPQ-NLC.....	29
2.2.4. NLC formulation and optimization by response surface design.....	29
2.2.5. Determination of z-average, polydispersity index and zeta potential...	30
2.2.6. Determination of BPQ solubility in liquid lipids and encapsulation efficiency.....	30
2.3. Results and Discussion.....	31
2.3.1. Evaluation of BPQ solubility in solid and liquid lipids.....	31
2.3.2. Preparation of BPQ-NCL.....	35
2.3.3. BPQ-NLC optimization by response surface design.....	36
2.3.4. Encapsulation efficiency (EE) .....	43
2.4. Conclusions.....	44
Chapter 3	
Abstract.....	46
3.1. Introduction.....	47
3.2. Material and Methods.....	48
3.2.1. Materials.....	48

3.2.2.	Analytical method for buparvaquone quantification by HPLC.....	49
3.2.3.	Development of BPQ-NLC by factorial design.....	49
3.2.4.	Determination of the Z-average, polydispersity index, particle size distribution and zeta potential.....	50
3.2.5.	Drug loading and encapsulation efficiency (%EE) .....	50
3.2.6.	BPQ-NLC morphology by transmission electron microscopy (TEM).....	51
3.2.7.	BPQ-NLC stability testing.....	51
3.2.9.	Free BPQ and BPQ-NLC dissolution profiles.....	51
3.2.10.	Free BPQ and BPQ-NLC cytotoxicity.....	52
3.2.11.	CC <sub>50</sub> and statistical analysis.....	52
3.3.	Result .....	52
3.3.1.	BPQ-NLC formulation development.....	52
3.2.1.	Determination of the Z-average, polydispersity index and particle size distribution.....	57
3.3.3.	Drug loading and encapsulation efficiency (%EE).....	58
3.3.4.	BPQ-NLC morphology by transmission electron microscopy.....	58
3.3.5.	BPQ-NLC Z-average and polydispersity index stability testing.....	59
3.3.6.	BPQ-NLC drug loading and encapsulation efficiency stability testing...	59
3.3.7.	BPQ-NLC solubility evaluation.....	60
3.3.8.	Free BPQ and BPQ- NLC dissolution profiles.....	61
3.3.9.	Free BPQ and BPQ- NLC cytotoxicity.....	63
3.4.	Discussion.....	63
3.4.1.	BPQ-NLC formulation development.....	63
3.4.2.	BPQ-NLC morphology by transmission electron microscopy.....	65
3.4.3.	BPQ-NLC Z-average polydispersity index stability testing.....	65
3.4.4.	BPQ-NLC drug loading and encapsulation efficiency stability testing...	66

3.4.5.	BPQ-NLC solubility evaluation.....	66
3.4.6.	BPQ- NLC dissolution profiles.....	66
3.4.7.	BPQ- NLC cytotoxicity.....	68
3.5.	Conclusions.....	68

## Chapter 4

Abstract.....	71
4.1 Introduction.....	72
4.2. Materials and methods.....	73
4.2.1. Materials.....	73
4.3. Methods.....	73
4.3.1. Analytical method for quantification of buparvaquone by HPLC.....	74
4.3.2. Preparation of buparvaquone nanostructured lipid carrier (BPQ-NLC)..	74
4.3.3. Preparation of BPQ and polymyxin B co-encapsulated in NLC (BPQ-NLC-POL) .....	74
4.3.4. Preparation of BPQ-NLC-POL coated with chitosan + dextran sulfate (BPQ-NLC-POL[-]) and BPQ-NLC-POL coated with DEAE-dextran (BPQNLC-POL[+]) .....	74
4.3.5. Determination of the Z-average, polydispersity index (PDI) and zeta potential (ZP) .....	75
4.3.6. Morphology by transmission electron microscopy (TEM) of BPQ-NLC, BPQ-NLC-POL[+] and BPQ-NLC-POL[-].....	75
4.3.7. Cytotoxicity and leishmanicidal activity of free BPQ, BPQ-NLC, BPQ-NLC-POL[-] and BPQ-NLC-POL [+] in L. infantum amastigotes.....	75
4.3.8. IC <sub>50</sub> , CC <sub>50</sub> and statistical analysis.....	76
4.4. Results.....	76
4.4.1. Preparation of buparvaquone nanostructured lipid carrier (BPQ-NLC)..	76
4.4.2. Preparation of BPQ-NLC with polymyxin B (BPQ-NLC-POL).....	76

4.4.3.	Preparation of BPQ-NLC-POL coated with chitosan and dextran sulfate (BPQ-NLC-POL[-]) and BPQ-NLC-POL coated with DEAE-dextran (BPQ-NLC-POL[+]).....	77
4.4.4.	Morphology by transmission electron microscopy (TEM) of BPQ-NLC, BPQ-NLC-POL[-] and BPQ-NLC-POL[+].....	77
4.4.5.	Cytotoxicity and leishmanicidal activity of free BPQ, BPQ-NLC, BPQ-NLC-POL[-] and BPQ-NLC-POL [+] in <i>L. infantum</i> amastigotes.....	78
4.5.	Discussion.....	79
4.5.1.	Preparation of buparvaquone nanostructured lipid carrier (BPQ-NLC)..	79
4.5.2.	Preparation of BPQ-NLC with polymyxin B (BPQ-NLC-POL) .....	79
4.5.3.	Preparation of BPQ-NLC-POL coated with chitosan and dextran sulfate (BPQ-NLC-POL[-]) and BPQ-NLC-POL coated with DEAE-dextran (BPQ-NLC-POL[+]) .....	80
4.5.4.	Morphology by transmission electron microscopy (TEM) of BPQ-NLC, BPQ-NLC-POL[+] and BPQ-NLC-POL[-] .....	80
4.5.5.	Cytotoxicity and leishmanicidal activity of free BPQ, BPQ-NLC, BPQ-NLC-POL[-] and BPQ-NLC-POL [+] in <i>L. infantum</i> amastigotes .....	80
4.6.	Conclusions.....	82
Chapter 5		
	General Conclusion.....	84
	Future prospective.....	86
	References .....	87
	Appendices.....	110

## List of Tables

Table 2.1. Buparvaquone solubility in liquid lipids.....	32
Table 2.2. Crystal evaluation by microscopy for buparvaquone solubility test.....	32
Table 2.3. Enthalpy of fusion (J g <sup>-1</sup> ) and crystallinity index for determining the solubility of buparvaquone in solids lipids by differential scanning calorimetry.....	35
Table 2.4. Experimental matrix and values of z-average and polydispersity (PDI) of buparvaquone nanostructured lipid carriers.....	37
Table 2.5. Analysis of variance for Z-average.....	38
Table 2.6. Coded coefficients of the linear model and p-value ( $\alpha=0.05$ ) with the variables: liquid and solid lipid ratio (SL:LL), Kolliphor® P188 (K188) and Tween® 80 (T80) .....	39
Table 2.7. Observed and predicted z-average, polydispersity index (PDI) and zeta potential (ZP) results from buparvaquone nanostructured lipid carriers...	42
Table 2.8. Theoretical and observed drug load and encapsulation efficiency of buparvaquone nanostructured lipid carriers .....	43
Table 3.1. Experimental design matrix, Z-average (Z-ave), polydispersity index (PDI) and zeta potential (ZP) of buparvaquone nanostructured lipid carrier development.....	53
Table 3.2. ANOVA from Z-average data of buparvaquone nanostructured lipid carrier development.....	54
Table 3.3. Coded coefficients and goodness-of-fit indexes from the Z-average data of buparvaquone nanostructured lipid carrier development.....	54
Table 3.4. Theoretical and experimental Z-average from formulations for mathematical model verification of buparvaquone nanostructured lipid carrier development.....	56
Table 3.5. Drug loading and encapsulation efficiency of V1 and V2 formulations from nanostructured lipid carrier development.....	58
Table 3.6. Z-average (nm) and particle size distribution of V1 and V2 formulations from stability testing.....	59
Table 3.7. Polydispersity index stability test of V1 and V2 formulations from nanostructured lipid carrier development.....	59



Table 3.8. Drug loading and encapsulation efficiency (%EE) stability test of V1 formulation from nanostructured lipid carrier development.....	60
Table 3.9. Drug loading and encapsulation efficiency (%EE) stability test of V2 formulation from nanostructured lipid carrier development.....	60
Table 3.10. BPQ-NLC solubility evaluation.....	60
Table 3.11 Solubility of buparvaquone (BPQ), and V1 and V2 formulations from nanostructured lipid carrier development.....	61
Table 4.1. Z-average, polydispersity index, zeta potential, buparvaquone (BPQ) drug loading and encapsulation efficiency BPQ-NLC-POL[-] and BPQ-NLC-POL[+] (n=3).....	77
Table 4.2. Cytotoxicity, amastigote activity against L.infantum (CC50 or IC50 and 95% IC) and selectivity index of free buparvaquone (BPQ), BPQ nanostructured lipid carrier (BPQ-NLC), BPQ nanostructured lipid carrier with polymyxin B coated with chitosan and dextran sulfate (BPQ-NLC-POL[-]) and BPQ nanostructured lipid carrier with polymyxin B coated with DEAE-dextran (BPQ-NLC-POL[+]).....	79

## List of Figures

Figure 1.1. The life cycle of Leishmania parasites. Source: KAYE AND SCOTT, 2011. (reproduced with permission).....	3
Figure 1.2. Initial stage of visceral leishmaniasis (Source: BRASIL, 2006) (reproduced with permission).....	5
Figure 1.3. Patients with cutaneous leishmaniasis. Source: FIOCRUZ, available at <a href="http://www.dbbm.fiocruz.br/tropical/leishman/leishext/html/leishmaniose_cut_nea.htm">http://www.dbbm.fiocruz.br/tropical/leishman/leishext/html/leishmaniose_cut_nea.htm</a> Accessed:19 May 2017 (reproduced with permission).....	6
Figure 1.4. Buparvaquone molecular structure. Source Reimão et al., 2012 (reproduced with permission).....	8
Figure 1.5. Diagrammatic representation of the Biopharmaceutics classification system (BCS), initially developed by Amidon et al. (1995) (Source: AVDEEF, 2012). (reproduced with permission).....	9
Figure 1.6. Solid lipid nanoparticles (SLN) and nanostructured lipid carriers (NLC) structures and NLC advantages. Source: BELOQUI et al., 2016 (reproduced with permission). ....	15
Figure 1.7. The human lymphatic system, showing the lymphatic vessels and lymphoid organs. Encyclopædia Britannica, inc., 2017.....	20
Figure 2.1. Optical microscopy from Softisan® 154 lipid samples mixed with buparvaquone A: (2 mg.g <sup>-1</sup> ) B: (1 mg.g <sup>-1</sup> ). 40X magnification.....	33
Figure 2.2. Thermoanalytical profiles of buparvaquone (BPQ), Softisan® 154 and BPQ physical mixture (PM) obtained at 10 °C min <sup>-1</sup> , under a dynamic nitrogen atmosphere (50 mL.min <sup>-1</sup> ). BPQ DSC curve (A) DSC Softisan® 154 curve (B) PM 1st run (C) PM 2nd run (D) TG: TG curves of PM (E). BPQ: buparvaquone; 1st run: first heat cycle; 2nd run: second heat cycle.....	34
Figure 2.3. Nanostructured lipid carrier for buparvaquone encapsulation: A and B, before and after high-pressure homogenization, respectively.....	36
Figure 2.4. Residuals analysis of the BPQ-NLC mathematical model for Z-average..	40
Figure 2.5. Contour plot of the BPQ-NLC mathematical model for z-average, containing the following variables: Solid and liquid ratio (SL:LL), Kolliphor® P188 and Tween® 80.....	41
Figure 2.6. Profile for predicted values and desirability function of the F1 z-average (201 nm), containing the following variables: solid and liquid lipid ratio (SL:LL) at 0.71, Kolliphor® P188 at 3.6% (w/w), Tween 80 at 0.37% (w/w).....	42

Figure 2.7. Profile for predicted values and desirability function of the F2 z-average (217 nm), containing the following variables: solid and liquid lipid ratio (SL:LL) at 2.06, Kolliphor® P188 at 3.6% (w/w), Tween 80 at 0.37% (w/w) .....	42
Figure 3.1. Main effects plots data from buparvaquone nanostructured lipid carrier development (Z-average).....	55
Figure 3.2. Contour plots from Z-average data evaluation of buparvaquone nanostructured lipid carrier development.....	56
Figure 3.3. Profile for predicted values and desirability function of the V1 Z-average (185.6 nm), containing the following variables: solid and liquid lipid ratio (SL:LL) at 1.0, poloxamer 188 at 4.0% w/w and lipid phase at 5.0% w/w.....	57
Figure 3.4. Profile for predicted values and desirability function of the V2 Z-average (232.4 nm), containing the following variables: solid and liquid lipid ratio (SL:LL) at 0.5, poloxamer 188 at 3.0% w/w and lipid phase at 15.0% w/w.....	57
Figure 3.5. Transmission electronic microscopy from formulation development V1: Z-average of 175.1 nm. Magnification 36kx. ....	58
Figure 3.6. Dissolution of free buparvaquone (BPQ) (black circles) and formulations V1 and V2 with (grey triangles) and without (black circles) pancrelipase, containing 4 mg of BPQ; using USP II apparatus (900 mL phosphate buffer pH 7.4 0.05M, tween 80 0.07% w/v), 50 rpm, 37 °C. (A) V1 Z-average: 175.1 nm. (B) V2 Z-average: 230.7 nm.....	62
Figure 3.7. Dissolution of free buparvaquone (BPQ) (black circles) and formulations V1 and V2 containing 4 mg of BPQ; using USP II apparatus (900 mL phosphate buffer pH 7.4 0.05 M, sodium dodecyl sulfate 1.0% w/v), 50 rpm, 37 °C. (A) V1 Z-average: 175.1 nm (gray inverted triangle). (B) V2 Z-average: 230.7 nm. (black diamond). ....	62
Figure 4.1. Transmission electron microscopy (36kx) of (A) Buparvaquone nanostructured lipid carrier (171.9±1.6 nm). (B) Buparvaquone nanostructured lipid carrier with polymyxin B coated with chitosan and dextran sulfate (183.8±4.5 nm). (C) Buparvaquone nanostructured lipid carrier with polymyxin B coated with DEAE-dextran (208.8± 2.6 nm).....	78

## List of Abbreviations

AMPs	Antimicrobial peptides
ANOVA	Analysis of variance
BCS	Biopharmaceutics classification system
BM	Binary mixture
BPQ	Buparvaquone
BPQ-NLC	Buparvaquone nanostructured lipid carrier
CI	Crystallinity index
CC <sub>50</sub>	Half maximal cytotoxicity concentration
DALY	Disability-adjusted life year
DSC	Differential scanning calorimetry
EE%	Encapsulation efficiency
EC <sub>50</sub>	Half maximal effective concentration
FaSSIF	Fasted state simulated intestinal fluid
FDA	United States Food and Drug Administration
FeSSIF	Fed state simulated intestinal fluid
GRAS	Generally recognized as safe
HED	Human equivalent dose
HPH	High-pressure homogenization
HPLC	High performance liquid chromatography,
LC	Cutaneous leishmaniasis
LL	Liquid lipid
LN <sub>s</sub>	Lymph nodes
Log D	Distribution coefficient
Log P	Partition-coefficient
LPS	Lipopolysaccharides
LS	Lymphatic system
MCT	Medium chain triglycerides - esters of capric and caprylic acids
MPS	Mononuclear phagocytic system
MR	Mannan receptors
MTT	3-methyl- [4-5-dimethylthiazol-2-yl] -2,5-diphenyltetrazolium bromide

NLCs	Nanostructured lipid carriers
NMP	N-Methyl-2-Pyrrolidone
NTDs	Neglected tropical diseases
PCS	Photon correlation spectroscopy
PDI	Polydispersity index
PVDF	Polyvinylidene fluoride
R <sup>2</sup>	Coefficient of determination
RH	Relative humidity
RSM	Response surface methodology
SD	Standard deviation
SL	Solid lipid
SL:LL	Solid lipid and liquid lipid ratio
SLNs	Solid lipid nanoparticles
TEM	Transmission electron microscopy
TG/DTG	Thermogravimetry/derivative thermogravimetry
USP	United States Pharmacopeia
VL	Visceral leishmaniasis
WHO	World Health Organization
ZP	Zeta potential

# Chapter 1

## **Introduction**

## **1.1 Introduction**

### **1.1.1. Neglected diseases**

Neglected Tropical Diseases (NTDs) are a set of diseases caused by a variety of pathogens, being a serious cause of chronic disability and death, primarily in the populations most affected by poverty (HOTEZ et. al, 2016). These diseases are endemic in Africa, Asia and the Americas. NTDs are estimated to cause the death of one million people annually. More than one billion people are affected, out of the 2.7 billion that live in extreme poverty (defined as those earning less than US\$ 2 a day) (BOISSON et al., 2016; NAKAGAWA et al., 2015). NTDs not only persist and spread under these conditions but can also exacerbate and perpetuate the poverty of affected communities (GARG, 2011).

As result of the deficiency of sanitary conditions, preventive and curative strategies, most NTDs have stable levels of endemicity. Therefore, no outbreaks or health crises rise and the NTDs remain a low priority for health policies (NAKAGAWA et al., 2015). The negligible presence of NTDs at developed countries leads to few private investments for the development of drugs, diagnostics and vaccines (POKHREL, 2011; MORAN et al., 2009). Moreover, public funding reached its lowest level since 2007. The United States government funding fell 3.0% in 2015, which is the lowest investment recorded by the project G-FINDER from George Institute for International Health (CHAPMAN et al., 2017; LIESE, ROSENBERG and SCHRATZ, 2010).

The disability-adjusted life year (DALY) is a tool that may be used to assess and compare the relative impact of several diseases locally and globally. The DALY is one of the rare metrics available that could completely show the chronic effects of NDTs. According to World Health Organization (WHO) (2010), the major NTDs have an impact of least 26 million DALYs (HOTEZ et. al, 2010). The main NTDs, referring to DALYs lost, embrace schistosomiasis, leishmaniases and hookworm infection. Additional to DALYs, these diseases have a profound and disproportionate impact in social stigma on the world's poorest people. Worker productivity and child development are also deeply affected (HOTEZ et. al, 2014; WHO, 2010).

In the last decade, new organizations and agendas are emerging for global elimination of the NTDs, e.g. WHO neglected tropical diseases programs and Drugs for Neglected Diseases initiative (DNDi). Nowadays, they are focused on lymphatic filariasis, trachoma, yaws preventive chemotherapy and mass treatment using currently available medicines. However, for most NTDs, drugs, vaccines, diagnostic tools and vector control technologies are scarce and have limited use due to toxicity, inefficacy or high rates of reinfection (HOTEZ et al., 2010).

### **1.1.2. Leishmaniasis: life cycle, clinical manifestations and chemotherapy**

Leishmaniasis is caused by protozoan parasites of the genus *Leishmania* and is transmitted to humans and other mammals by phlebotomine sandfly vectors. Around 350 million people in 88 countries globally are living at risk of developing one of the disease forms, mostly in South and Central America, Africa, Asia, and southern Europe (KAYE and SCOTT, 2011; NATEGHI ROSTAMI et al., 2016). Though, more than 90% of potentially fatal infections occur in just six regions: Brazil, Ethiopia, Sudan, South Sudan, India and Bangladesh (PIGOTT et al., 2014).

Leishmaniasis is classified as the second most prevalent disease among NTDs (MAROLI et al., 2013). Despite scientific advances they remain as a significant public health problem. Although estimated to cause the ninth largest disease burden among individual infectious, they are still classified as the "most neglected diseases" based on the limited investments in diagnosis, treatment, vaccines and vector control (ALVAR et al., 2012; de PAIVA-CAVALCANTI et al., 2015).

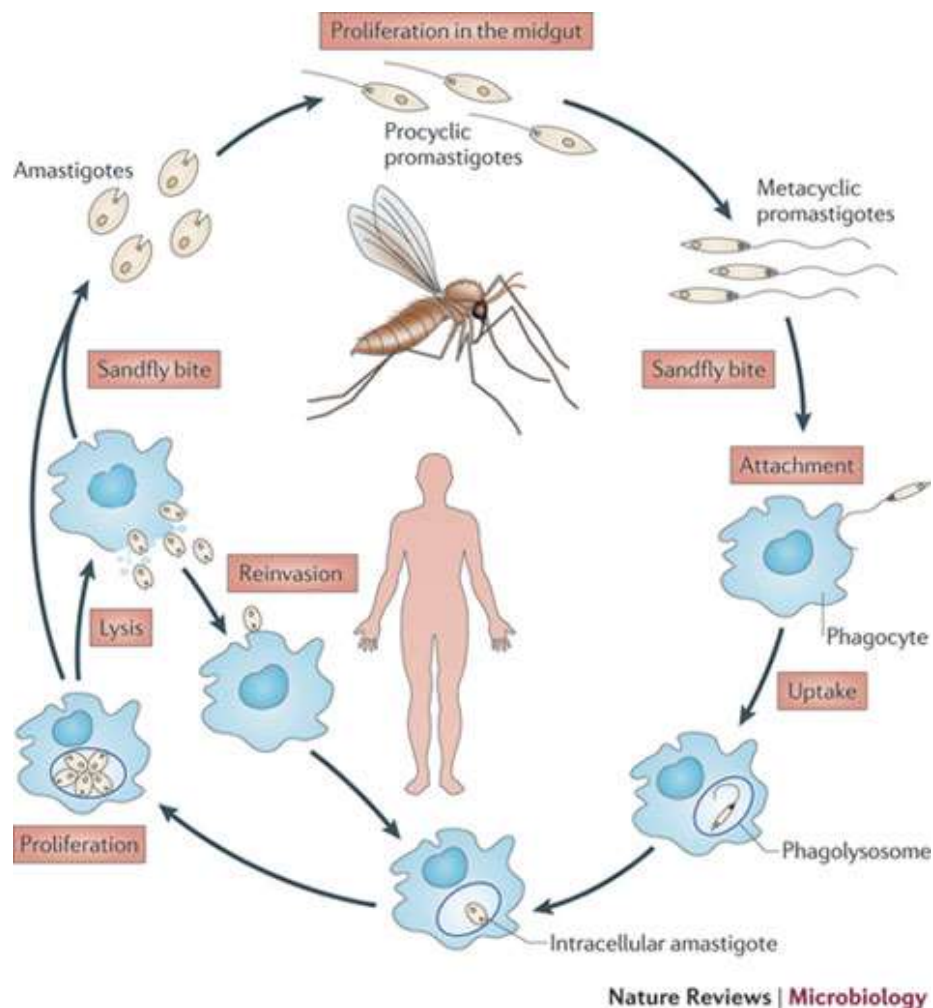
### **1.1.3. Leishmaniasis life cycle**

The transmission cycle of leishmaniasis (Figure 1.1) begins when the vector females pull the amastigote form present in blood monocytes from infected mammals. Then the parasites are released in the insect digestive tract, where the parasites multiply by binary division as promastigote form. Promastigotes differentiate into



paramastigotes, which colonize the esophagus and pharynx of the vector; in these places the parasites develop and give rise to the infective form called metacyclic promastigote. Infected females when performing a new bite in a vertebrate host, release the metacyclic promastigotes into the hosts skin. Then the parasites are phagocytosed by cells of the mononuclear phagocytic system (MPS), mostly by macrophages. The promastigote form differentiates into amastigotes and multiplies until cell disruption, resulting in the release of parasites that will be phagocytosed by new macrophages in a continuous process. In visceral leishmaniasis, dissemination occurs to other tissues rich in MPS cells, such as lymph nodes, liver, spleen and bone marrow (ALCOLEA et al., 2010; MCGWIRE and SATOSKAR, 2014; UENO and WILSON, 2012).

Figure 1.1. The life cycle of Leishmania parasites. Source: KAYE AND SCOTT, 2011.  
(reproduced with permission)



### **1.2.1. Clinical manifestations**

#### **1.2.1.1. Visceral leishmaniasis**

Visceral leishmaniasis (VL) is a systemic disease and it is fatal in more than 95% of cases if left untreated (WHO, 2017). VL can be characterized as an endemic, sporadic or epidemic disease, with different clinical features in each situation. In endemic areas, it tends to be relatively chronic and children are especially affected. The ages of 1 to 4 years are the most affected by visceral leishmaniasis caused by *L. infantum* in North Africa as well as West and Central Asia. However, since the start of HIV infections and increased use of immunosuppression from transplants and chemotherapy, half the cases in Europe affect adults (WHO, 2010).

*L. donovani* and *L. infantum* affect the spleen, liver, the small intestine mucosa, bone marrow, lymph nodes and other lymphoid tissues. In the initial stage (Figure 1.2) the symptomatology may vary from patient to patient, but in most cases includes fever lasting less than four weeks, skin paleness and hepatosplenomegaly. This clinical manifestation can be easily confused with other infectious processes of a benign nature, such as malaria and enteric fever, especially in endemic regions where the patients show a subtle clinical symptomatology. Low fever, mild cutaneous paleness, diarrhea, unproductive cough and small hepatosplenomegaly are some of the symptoms (WHO, 2013; BRASIL, 2006).

In the steady stage patients usually present intermittent fever generally associated with progressive thinning, skin paleness and increased hepatosplenomegaly. The final stage is reached when no treatment is initiated. Thus, the disease tends to get worse. Then symptoms of malnutrition, continuous fever and more severe impairment of the general state are observed. Other significant manifestations include bleeding (epistaxis, bleeding gum, and petechiae), jaundice and ascites. In these patients, death is usually determined by bacterial infections and bleeding (BRASIL, 2006).

Figure 1.2. Initial stage of visceral leishmaniasis (Source: BRASIL, 2006) (reproduced with permission).



#### 1.2.1.2. Cutaneous leishmaniasis

Cutaneous leishmaniasis (LC) affects the skin and mucous membranes. It is a worldwide public health problem and although it is not lethal, the disease compromises the physiology, social life and working capacity of those affected (BEN SALAH et. al, 2013). The clinical spectrum of cutaneous leishmaniasis is broad and may mimic other skin diseases such as staphylococcal or streptococcal infection, mycobacterial ulcer, leprosy, fungal infection, cancer, sarcoidosis, among others (WHO, 2010).

The clinical characteristics of cutaneous leishmaniasis (Figure 1.3) tend to vary intra and interregional, reflecting various species of parasites, zoonotic cycle and immunological factors (BEN SALAH et. al, 2013). The most common lesion begins with a papule at the site of inoculation; it usually grows for a week and reaches its final size up to 5 cm in diameter with a raised border and variable surrounding hardening, gradual resolution over months or years is usual (WHO, 2010).

There are three main forms of the disease: localized, disseminated and diffuse cutaneous. The skin is primarily affected in the localized form and is caused by *L. braziliensis*, *L. panamensis*, *L. guyanensis* and *L. peruviana*. The lesion is usually of the ulcer type with a predisposition to natural cure and good response to treatment. Those wounds can be single or multiple. The disseminated form is caused by *Leishmania (V.) braziliensis* and *Leishmania (L.) amazonensis*. Typically, acneiform appearance and multiple lesions affect several body segments, frequently involving face and chest. The number of wounds can reach hundreds. The diffuse cutaneous form is usually caused by *L. (L.) amazonensis*. It is a rare and severe clinical form that

occurs in patients with deficiency in the cellular immune response to *Leishmania* antigens, the response to therapy is poor or absent (BRASIL, 2007; WHO, 2010).

Figure 1.3. Patients with cutaneous leishmaniasis. Source: FIOCRUZ, available at [http://www.dbbm.fiocruz.br/tropical/leishman/leishext/html/leishmaniose\\_cut\\_nea.htm](http://www.dbbm.fiocruz.br/tropical/leishman/leishext/html/leishmaniose_cut_nea.htm) Accessed: 19 May 2017. (reproduced with permission).



### 1.2.2. Leishmaniases chemotherapy

Meglumine antimoniate and sodium stibogluconate are the two currently available pentavalent antimonials and can be administered directly into the lesion for the treatment of cutaneous leishmaniasis (OPS, 2013; BEN SALAH et al., 2013). Common adverse events are anorexia, vomiting, nausea, abdominal pain, malaise, myalgia, arthralgia, headache, metallic taste and lethargy. Cardiac changes are dependent on the dose and treatment length; sudden death may occur. Prolongation of the Q-T interval ( $> 0.5$  s) indicates the possible occurrence of severe and fatal cardiac arrhythmia (OLIVEIRA et al., 2011). Increased concentration of pancreatic and hepatic enzymes is common; also leukopenia and thrombocytopenia may be observed. Whole blood, serum and electrocardiogram tests should be monitored and if serious adverse events occur (in most cases hepatic or cardiotoxicity) treatment must be interrupted (WHO, 2010).

Amphotericin B, used as second-line treatment for cutaneous leishmaniasis, is a polyene antibiotic and its common side effects are reactions to infusion, including more severe fever, chills and thrombophlebitis of the vein used in the injection. Discontinuation of treatment is frequent due to nephrotoxicity. Other rare but serious toxic effects are hypokalemia and myocarditis. Treatment should always be hospital-based to allow continuous monitoring of patient's condition. Lipid formulations of amphotericin B are diverse formulations such as lipid complex and colloidal dispersion. They are similar to amphotericin B on their efficacy but are significantly less toxic (SUNDAR. and CHAKRAVARTY, 2010).

Paromomycin is an aminoglycoside antibiotic usually administered intramuscularly. Mild pain at the injection site is the most common adverse event. Reversible ototoxicity and renal toxicity are also found (BEN SALAH, 2013). Pentamidine isethionate is administered intramuscularly or preferably by intravenous infusion. Serious adverse effects such as severe diabetes mellitus, myocarditis and renal toxicity limit its use (BLUM et al., 2014).

Miltefosine was originally developed as an oral anticancer drug but has been shown to have leishmanicidal activity. The main side effects are nausea, vomiting and diarrhea, occasional hepatic- and nephrotoxicity. Due to the potential teratogenic effect it should not be used by women who are pregnant or of childbearing age (STROPPIA et al., 2017).

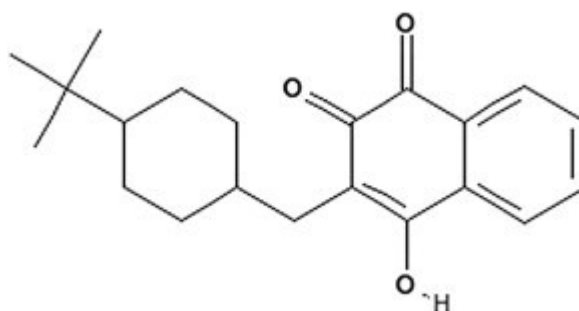
Regarding what has discussed above, successful treatment of leishmaniasis is impaired by several factors. The most prominent include drug parasite resistance and toxicity. Therefore, the search for new drugs and development of new delivery systems to overcome these issues are urgently required.

#### **1.2.2.1. Buparvaquone**

Buparvaquone (BPQ) (Figure 1.4), a hydroxynaphthoquinone, is currently marketed as Butalex® an intramuscular injection for the treatment of theileriosis in cattle. It was also originally developed as an anti-malarial compound but it showed leishmanicidal activity against *L. donovani* for the first time by Croft and colleagues (1992). In *in vitro* experiments the BPQ has proved to be 100-fold more effective

against amastigotes of *L. donovani* than other hydroxynaphthoquinones. The drug has very low water solubility ( $<300 \text{ ng.mL}^{-1}$ ) and therefore is poorly soluble in biological media such as gastric and interstitial fluids. This drug also has high lipophilicity. Due to these properties BPQ showed low *in vivo* activity against leishmaniasis via intramuscular injection (REIMÃO et al., 2012 and VENKATESH et al., 2010).

Figure 1.4. Buparvaquone molecular structure. Source Reimão et al., 2012 (reproduced with permission).



Buparvaquone mechanism of action has not been clarified but there are indications that it blocks the parasite respiratory chain (MÜLLER et al., 2016) similarly to atovaquone and other 1,4-naphthoquinones the most likely action is the inhibition of Complex III (b-c1 complex) (MÜLLER et al., 2015). Cytochrome complex III is a group of catalyzers responsible for electron transference to maintain the mitochondrial membrane potential. The effect on the ubiquinone biosynthesis has also been described which is also a critical component of mitochondrial respiratory chain. The blockage of these reactions seriously impairs the parasite ATP synthesis (SCHUCK et al., 2013).

### 1.2.3. Biopharmaceutics Classification System (BCS) - permeability and solubility implications in new drugs and medicines development

Biopharmaceutics Classification System (BCS) (Figure 1.5) was originally developed by Amidon and colleagues (1995). It has found widespread utility in drug discovery, product development and regulatory sciences as drugs must be sufficiently

soluble and permeable to reach their site of action (TSUME et al., 2014). Drug dose is a crucial factor in the BCS because highly soluble molecules are defined as those in which the highest dose will dissolve in 250 mL over the pH range of the gastrointestinal tract (i.e., pH 1–6.8) (BENET, 2013). Highly permeable compounds are defined as those that 85% or more are absorbed or where permeability was assessed by *in vitro* or *in vivo* methods (FDA, 2015).

The United States Food and Drug Administration (FDA) classifies drug substances into four groups based on aqueous solubility and intestinal membrane permeability (Figure 1.5). Class 1: high solubility and high permeability; Class 2: low solubility and high permeability; Class 3: high solubility and low permeability; Class 4: low solubility and low permeability. The BCS system was first proposed to provide a scientific basis for biowaivers based on a correlation of *in vitro* drug dissolution and *in vivo* drug absorption. The FDA BCS guidance allows biowaivers for BCS Class I drugs for immediate-release (IR) solid oral dosage forms (FDA, 2015).

Figure 1.5. Diagrammatic representation of the Biopharmaceutics classification system (BCS), initially developed by Amidon et al. (1995) (Source: AVDEEF, 2012). (reproduced with permission)

	HIGH SOLUBILITY	LOW SOLUBILITY
HIGH PERMEABILITY	<b>CLASS 1 (amphiphilic) <sup>a</sup></b> diltiazem antipyrine labetalol glucose captopril L-dopa enalapril metoprolol propranolol phenylalanine <b>1</b>	<b>CLASS 2 (lipophilic) <sup>b</sup></b> flurbiprofen ketoprofen naproxen desipramine diclofenac itraconazole piroxicam carbamazepine phenytoin verapamil <b>2</b>
LOW PERMEABILITY	<b>CLASS 3 (hydrophilic) <sup>c</sup></b> famotidine atenolol cimetidine acyclovir ranitidine nadolol hydrochlorothiazide <b>3</b>	<b>CLASS 4 <sup>d</sup></b> terfenadine furosemide cyclosporine <b>4</b>

<sup>a</sup> RATE OF DISSOLUTION limits *in vivo* absorption  
<sup>b</sup> SOLUBILITY limits absorption flux  
<sup>c</sup> PERMEABILITY is rate determining  
<sup>d</sup> No IVIV ( *in vitro* - *in vivo* ) correlation expected

BCS system has raised many discussions and subsequent variations, extension or sub-classifications had been proposed to develop a more science-based mechanistic *in vivo* predictive dissolution methodologies (WU and BENET, 2005; BUTLER and DRESSMAN, 2010; CHEN et al., 2011b). Therefore, those dissolution methods can be used to evaluate the probability of a formulation and dosage form to reach suitable bioavailability and pharmacological outcome (TSUME et al., 2014).

The number of failures of small-molecule drug candidates seems to have diminished significantly in recent years. The increased use of *in silico* screening is one of the main tools to select compounds with suitable physicochemical properties, such as size, lipophilicity, polarity, ionization, hydrogen bonding, aromaticity and shape. This method is based on analyses of data sets of approved oral administered drugs and investigational compounds (WARING et al., 2015; LEESON, 2016; NOGARA et al., 2015).

It is commonly recognized that the key factors affecting drugs permeability are its lipophilicity and protonation state. Log P (drug partitioning between octanol/water) is a measurement of lipophilicity. It is frequently described by the pH-dependent octanol/water partition coefficient, namely as log D, that combines the influence of lipophilicity (log P) and ionization in a single descriptor (HO et al., 2013; AVDEEF, 2012; GOSWAMI et al., 2013).

Christopher Lipinski and coworkers developed the Lipinski's rule of five (Ro5) in 1997. It affirms that poor absorption or permeation would occur when cLog P (calculated Log P) >5; molecular weight >500; hydrogen bond acceptors (O+N) >10; and hydrogen bond donors (OH+NH) >5. The Ro5 was proposed to passive permeation molecules, and it is 'violated' when two or more rules are broken (LEESON, 2016; MUNIR et al., 2016).

Besides the screening of new drugs, the Ro5 is a valuable tool to evaluate the suitability of compounds that already showed pharmacological effects in *in vitro* tests, but lack permeability and pharmacokinetic data. For buparvaquone, Ro5, combined with other *in silico* predictions, supported the potential use of this drug for leishmaniasis treatment. However, very low water solubility is still a critical matter for BPQ.

Solubility plays a major role in all pharmaceutical forms, including parenteral formulations. It is one of the most important parameters to achieve proper drug levels



in systemic circulation, resulting in a satisfactory pharmacological response. Low aqueous solubility is a critical issue in formulation development for new chemical molecules as well as the development of generic drugs (SAVJANI et al., 2012; WILLIAMS et al., 2013; JUNYAPRASERT and MORAKUL, 2015). Solubility is also required for the optimization of formulations, to predict *in vitro-in vivo* correlations as well to understand the dynamics of absorption, distribution, metabolism, excretion and toxicity (ADMET) (ZHOU et al., 2007; LIN and PEASE, 2016).

Problems related to solubility during the development of formulations are not expected for compounds with an aqueous solubility  $>0.1 \text{ mg.mL}^{-1}$ . However, for compounds with solubility between  $0.001$  and  $0.1 \text{ mg.mL}^{-1}$ , overcoming the poor absorption is the main goal. Drugs with an even lower solubility represent a real challenge (GLOMME et al., 2005), a condition which BPQ is included (water solubility  $<0.0003 \text{ mg.mL}^{-1}$ ). According to Williams and colleagues (2013), assuming moderate potency and permeability, issues from low water solubility ( $<50 \text{ mg.mL}^{-1}$ ) might be anticipated (WILLIAMS et al., 2013).

Typically, conventional formulations to improve solubility shows low bioavailability and poor pharmacokinetics and some approaches can rise systemic toxicity, as found using Cremophor® EL (CHEN et al., 2011a; SHEGOKAR and MÜLLER, 2010). Lately, various strategies to achieve nanometer-sized particles have been developed to increment the dissolution and bioavailability of poorly water-soluble drugs. These strategies include the increase the surface area/volume ratios, change the crystalline forms and design materials for controlled release. Decrease the drug particles to nanometer range can result in higher drug solubility and better pharmacokinetics, and it might also reduce the drug toxicity (XU, LING and ZHANG, 2013; THORAT and DALVI, 2012).

#### **1.2.4. Considerations on nanotechnology for drug delivery systems**

Long before the term nanotechnology is used, the Nobel Laureate physicist Richard Phillips Feynman (1918-1988) presented the ideas and concepts underlying nanoscience and nanotechnology at a meeting of the American Society of Physics at the California Institute of Technology on December 29, 1959. In his lecture entitled

"There is a lot of space down there," Feynman described a process which scientists would manipulate and control individual atoms and molecules (BHUSHAN, 2010; OZAK and OZKAN, 2013). Norio Taniguchi was first to use the term nanotechnology in 1974. This Japanese scientist defined nanotechnology as the process of separating, consolidating and deforming materials at the atomic or molecular level (MULVANEY, 2015; DEMETZOS, 2016).

The FDA (2014) defines nanotechnology as the process for the deliberate manipulation, manufacture or selection of materials having at least one size between 1 and 100 nm, despite this size restriction, this term commonly refers to structures up to several hundred nanometers (KATZ et al., 2015). Also, the nanometer-scale material must demonstrate physical, chemical and biological properties that allow innovative application of this material. These innovative properties must be attributed exclusively to their nanometric dimension. In the case of material consisting of particles larger than 100 and less than 1000 nm, but with innovative characteristics, this will be considered material obtained by nanotechnology (FDA, 2014).

The following features of nanometer-scale materials can be responsible for the innovative properties: gravitational forces become negligible, and therefore electromagnetic forces are dominant (e.g., Van der Waals forces, weak electromagnetic interactions). The nanoparticles motion can be described by mesoscopic system mechanics, while for particles in conventional dimension, classical mechanics better describe those particle features. For increased volume and surface ratio the nanoparticles Brownian motion becomes more prominent when compared to conventional particles (MCELFRESH, HOLCOMB and ECTOR, 2012; GAN, GAN and QIAO, 2011).

With the use of nanoparticles in drug delivery systems, it is possible to improve the solubility of poorly water-soluble drugs, prolong the systemic half-life, reduce immunogenicity, release the drug in a modified way (decreasing the frequency of administration) and at a specific site to minimize systemic side effects. Also, it is possible to develop a combination of two or more drugs to generate synergistic effects and consequently decrease drug resistance (BAMRUNGSAP et al., 2012; HE et al., 2011; VO et al., 2013; PAAVER, 2015).

#### **1.2.4.1. Nanostructured lipid systems: liposome, nanoemulsion, solid lipid nanoparticle and nanostructured lipid carrier**

Poorly water-soluble drug candidates are prevalent among new drug candidates in development pipelines, which limit formulation development, clinical application and marketability because of their low dissolution and poor bioavailability (VO et al., 2013; PAAVER, 2015). The use of nanostructured lipid systems (NLSs) as drug carriers is a promising method for overcoming these issues.

When compared to many other materials often used, particularly synthetic polymers, lipids are regarded as safer and high biocompatibility is expected (YINGCHONCHAROEN, KALINOWSKI and RICHARDSON, 2016; LIN et al., 2014b). NLSs have other advantages such as the viability of industrial scale production and low cost of lipids when compared to synthetic polymeric nanoparticles. Also, the manufacturing process does not require the use of organic solvents and, after sterilization by wet heat, their physicochemical characteristics remain unchanged. Like other nanostructured systems, these NLSs provide modified release of the drug, and targeted drug delivery systems can be achieved (TAMJID et al., 2013).

#### **1.2.4.2. Liposomes and nanoemulsions**

Liposomes are nanoparticulate lipidic vesicles prepared by hydration of surfactants when mixed with water under low shear force (SEZER, 2014). Phospholipids arrange themselves in sheets; by joining tails to tails, forming an aqueous core entrapped by one or more bilayers. Hydrophilic compounds can be encapsulated in the aqueous center and lipophilic ones, in the membrane (LIU and HUANG, 2013; GHARIB et al., 2015). However, the main disadvantages of this delivery system are the use of organic solvents, excessive cost of production process and materials, such as phospholipids. Due to low drug loading, drug leakage and fast drug release, serious stability problems during storage are found (TAMJID et al., 2013; TILA et al., 2015; AGARWAL et al., 2016).

Nanoemulsions are dispersions made up of two immiscible liquid phases which are mixed using mechanical shear and stabilized using an appropriate surfactant with

average diameters in the range of 50 to 1000 nm (BORRIN et al., 2016; SEZER, 2014). Nanoemulsions have much better stability to gravitational separation and aggregation than conventional emulsions (SINGH et al., 2017). They show toxicological safety, high content of the lipid phase and feasibility of large-scale production. However, they still undergo instabilities such as Ostwald ripening, flocculation, membrane permeability following premature drug release, creaming and particle aggregation during storage (SINGH et al., 2017; SEZER, 2014; HE et al., 2013). Irritation of gastrointestinal tract may occur because of high surfactant content (30-60%) and drug chemical instability (SEZER, 2014). Nanoemulsions are not able to solubilize compounds which have high melting points and price effectiveness of nanoemulsion is also a concern because expensive instruments are often involved (SINGH et al., 2017; SEZER, 2014).

#### **1.2.4.3. Solid lipid nanoparticles and nanostructured lipid carriers**

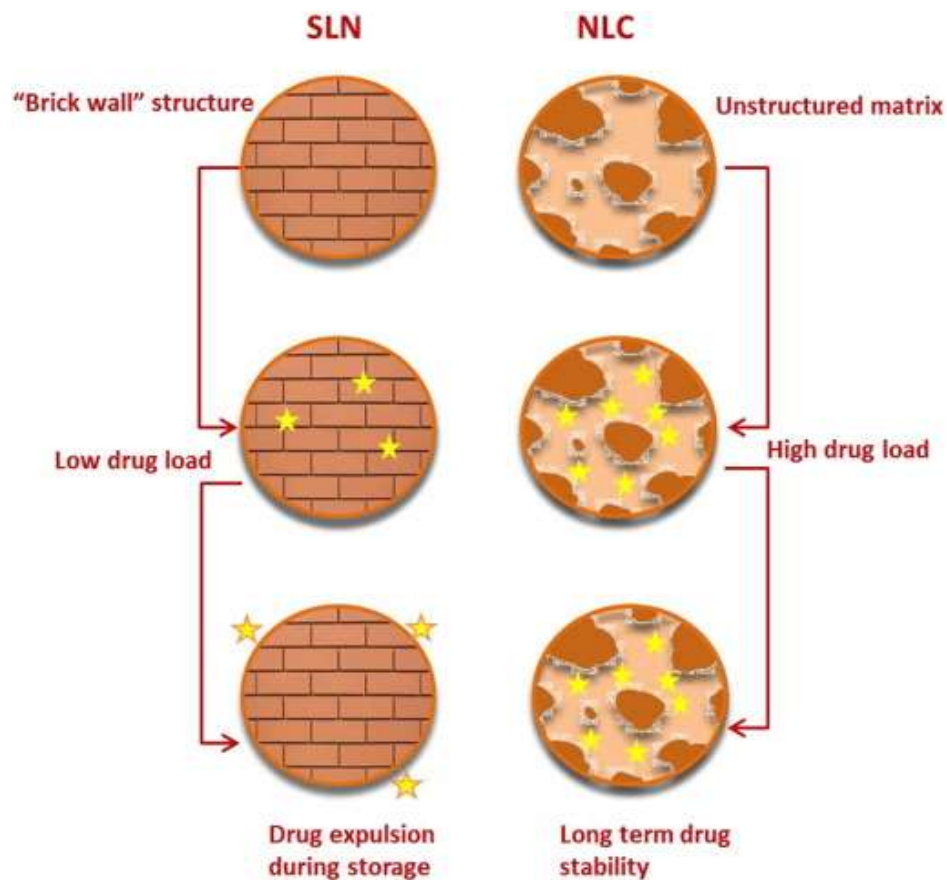
Solid lipid nanoparticles (SLNs) were developed by three working groups, Müller and colleagues, Gasco and colleagues and Westese in the 1990s (SCHWARZ et al.; 1994; FREITAS AND MÜLLER, 1999; MOREL et al., 1996; CAVALLI et al., 1997; SIEKMANN and WESTESEN; 1994; BUNJES, WESTESEN and KOCH, 1996). The objective was proposing alternatives to overcome drawbacks from nanoemulsions and liposomes, such as limited stability and inability to control the drug release, and at the same time, achieving formulations better tolerated than polymeric nanoparticles (DOKTOROVOVA, 2014). SLNs are similar to nanoemulsions but different as the nature of the lipids employed. The liquid lipid used in the emulsions is replaced by lipids, which are solid at room temperature. SLNs are composed of 0.1–30% (w/w) lipid phase dispersed in an aqueous solution of 0.5–5% (w/w) surfactant as a stabilizing agent. In this way, particles with diameters ranging from 50 to 1000 nm can be achieved (WEBER, ZIMMER and PARDEIKE, 2014).

Nevertheless, SLNs have a critical disadvantage due to the high crystallization mark of solid lipids. The low ordered lipid matrix progressively converts into a highly ordered crystalline structure ( $\beta$ -modification) during storage (WEBER, ZIMMER and PARDEIKE, 2014). This “perfect” structure is characterized by a crystal lattice with few imperfections and hence little room for drug accommodation. Therefore, the drug

incorporated into the SLNs at the production is expelled from the matrix during the storage. Besides the overall drug low solubility in solid lipids, when compared to liquid lipids, the polymorphic  $\beta$ -modification also explains the low drug loading of SLNs (SÁNCHEZ-LÓPEZ et al., 2017).

Regarding nanostructured lipid carrier (NLCs), these constitute the second generation of lipid nanoparticles (WANG et al., 2015). The NLCs present the following advantages when compared to SLNs (Figure 7): higher encapsulation efficiency, better control of drug release and lower drug expulsion during product storage (LIN et al., 2014; SÁNCHEZ-LÓPEZ et al., 2017). Thus, these nanocarriers have been used in the preparation of low water solubility drugs to increase the efficacy and reduce toxicity (BEH et al., 2017)

Figure 1.6. Solid lipid nanoparticles (SLN) and nanostructured lipid carriers (NLC) structures and NLC advantages. Source: BELOQUI et al., 2016 (reproduced with permission).



NLCs are prepared by mixing solid and liquid lipids and dispersing them in an aqueous surfactant solution (HENTSCHEL et al., 2008). The resulting matrix particles exhibit lower melting points compared to the first solid lipid but remains solid at room and body temperature (DOKTOROVOVA, 2014). Due to the differences in the structures of the solid and liquid lipids, there is a formation of the imperfect and disordered matrix. Therefore, the mixture accommodates drugs in molecular or amorphous forms in the clusters. As a consequence of these imperfections, the encapsulation efficiency is superior when compared to the SLNs (RANPISE, KORABU and GHODAKE, 2014).

The conventional method for the preparation of NLCs is high-pressure homogenization (HPH) (CORRIAS and LAI, 2011). This method has been used for years in the production of nanoemulsions for parenteral nutrition. High-pressure homogenizers force the liquid to pass through a small orifice a few micrometers wide. The fluid accelerates on a very short distance to high velocity. High shear stress, cavitation forces, turbulence and impact with solid surfaces disrupt the particles down to the submicron range (HEBISHY et al., 2015; MEHNERT and MÄDER, 2001).

Even though there are other methods available for NLC preparation, such as solvent diffusion method (HU et al., 2006), microemulsion, high shear homogenization and ultrasonication (UNER, 2006), the HPH presents some advantages when compared with the above cited. For temperature-sensitive drugs it can be performed using cold homogenization technique. Products with a low content of microparticles, narrow particle size distribution and higher oil phase content can be achieved. This method can be organic solvent free, and general industrial equipment is required, which make HPH well accepted by the regulatory authorities. The scale-up feasibility, a wide production range (150 and 2000 l.h<sup>-1</sup>) and the availability of homogenization production lines in the industry make HPH a desirable method for NLCs production (UNER, 2006).

Throughout literature, different combinations of lipids and surfactants have been described. Most of the lipids and surfactants are commercially available products and approved by various regulatory agencies, and usually, they are called as GRAS (Generally Recognized As Safe) by FDA. The most common solid lipids for NLCs preparation are stearic acid (SACHAN, GUPTA and ARORA, 2016), cetyl palmitate (KOVACEVIC et al., 2011; SCHWARZ et al., 2013; WANG, 2017), glyceryl

palmitostearate (Precirol ATO®5) (PARDEIKE et al, 2016; KHAN et al., 2016 ); glyceryl dibehenate (compritol®888 ATO) (ESPOSITO et al, 2014; BRUGÈ et al, 2015; ELMOWAFY et al., 2016) and tripalmitin (Dynasan®116) (TEERANACHAIDEEKUL, CHANTABURANAN and JUNYAPRASERT, 2017; AMASYA et al, 2016; GARCIA-FUENTES et al., 2005).

The most common liquid lipids for NLCs preparation are oleic acid (PARDEIKE et al, 2016; KHAN et al., 2016) triglycerides of medium-chain fatty acids, as caprylic and capric acids esters (Miglyol® 812) (MENDES et al., 2013; YOSTAWONKUL et al., 2017; BALGURI, ADELLI and MAJUMDAR, 2016); glyceryl monocaprylate (Capmul 808G) (NEGI, JAGGI and TALEGAONKAR, 2014; KHAN et al., 2016; KAITHWAS et al., 2017), and ethyl oleate (ZHANG et al., 2016; OTAROLA et al., 2015). Among these, medium chain triglycerides have a higher solvent capacity and are less susceptible to oxidation (LE BARS et al., 2015).

Among the surfactants for NLCs preparation, the most used are polysorbates (Tween®20, Tween®80) (MADANE and MAHAJAN, 2016; CHANBUREE and TIYABOONCHAI, 2017; LIN et al., 2007), poloxamers (188, 407) (Lutrol®F68, Lutrol®F127) (GARG et al., 2016; PEZESHKI et al., 2014; RAVANI et al., 2013); macrogol-15-hydroxystearate (Solutol®HS 15) (RAJINIKANTH and CHELLIAN, 2016; LIU et al., 2016a; LIU et al., 2016b); soy lecithin (MADANE and MAHAJAN, 2016; YU et al., 2017; NGUYEN, 2016); and polyoxyl castor oil (Cremophor EL) (SHETE and PATRAVALE, 2013; CHEN et al., 2014; ALJAEID and HOSNY, 2016).

Commercial veterinary formulation for BPQ is available from Merck Animal Health. Butalex is a drug dosage form for injection and is composed of 50 – 60% of N-Methyl-2-Pyrrolidone (NMP). This organic solvent is used as a strong solubilizing agent, and it is applied for subcutaneous or local injection in humans, but can be utilized as a cosolvent in parenteral formulations and as an enhancer in topical dosage forms (STRICKLEY, 2004). However, NMP is classified as a teratogenic compound. Twelve bioassays reported its effects on living organisms. Furthermore, NMP has cardiovascular toxicity due to induced arterial pressure changes after injection (JOUYBAN, 2010). Therefore, this formulation would not be feasible for human use of BPQ, even if the product had suitable *in vivo* effectiveness against leishmaniasis, which was not found in by Vexenat and colleagues (1998).

Even though some approaches have been proposed for BPQ (VENKATESH et al., 2010; da COSTA-SILVA and SONI, 2017), such formulations show some drawbacks, as toxicity from Cremophor EL (GELDERBLOM et al., 2001), low stability and the prohibitive cost of liposome production. Also, solid lipid nanoparticles are not suitable for this drug due to the low solubility, which leads to low drug loading and poor formulation stability. Furthermore, the high content of surfactants from emulsions and self-microemulsifying drug delivery systems may limit the use of these formulations for parenteral use (LOVELYN and ATTAMA, 2011; BOUYER et al., 2012.)

#### **1.2.5. Rational scientific basis for the application of nanostructured systems in the treatment of leishmaniasis**

If possible, the drugs should be released close the site of action to reduce the systemic effects and mainly because most the drugs act on intracellular receptors or directly in the tissues (PARVEEN, MISRA and SAHOO, 2012). Another concern is the existence of systems that limit the entry of the drug into the cell, reduce the cytosolic concentration through the action of elimination or degradation mechanisms. Nanoparticles can avoid these problems because they can protect the drug and act as the intracellular reservoir (FARAJI and WIPF, 2009).

The parasite's ability to survive and multiply within phagocytic cells is a prominent issue in developing new active compounds and drug-delivery systems for leishmaniasis. The intracellular parasites can protect themselves from exposure to drugs that do not readily diffuse into cells (HOLMES et al., 1996; CARRYN et al., 2003). Therefore, the use of drug carriers, such as nanoparticles, can improve the therapeutic efficacy by releasing leishmanicidal compounds in its site of action (COSTA LIMA et al., 2012). Nanoparticles are preferentially taken up by macrophages following systemic or local administration. The adsorption of serum protein on the nanoparticle surface (opsonization) is a major factor, which allows macrophages to recognize and internalize these particles, much more efficiently than the free drug (SHUKLA, PATRA and DUBEY, 2012; ALMOUAZEN et al., 2012). Accordingly, this mechanism would be useful for the effective treatment of leishmaniasis.



Macrophages are predominantly involved in bloodstream clearance and degradation of nanoparticles (LUNOV et al., 2011). *In vitro*, the uptake of nanoparticles by J-744 macrophages occurred through endocytosis process, and the particles were localized in lysosomal compartments. (CHELLAT et al., 2005). Considering such a feature, the use of nanoparticles in modified drug delivery systems targeting macrophages is particularly attractive, especially in the treatment of diseases in which macrophages act as host cells for parasites and bacteria, such as leishmaniasis.

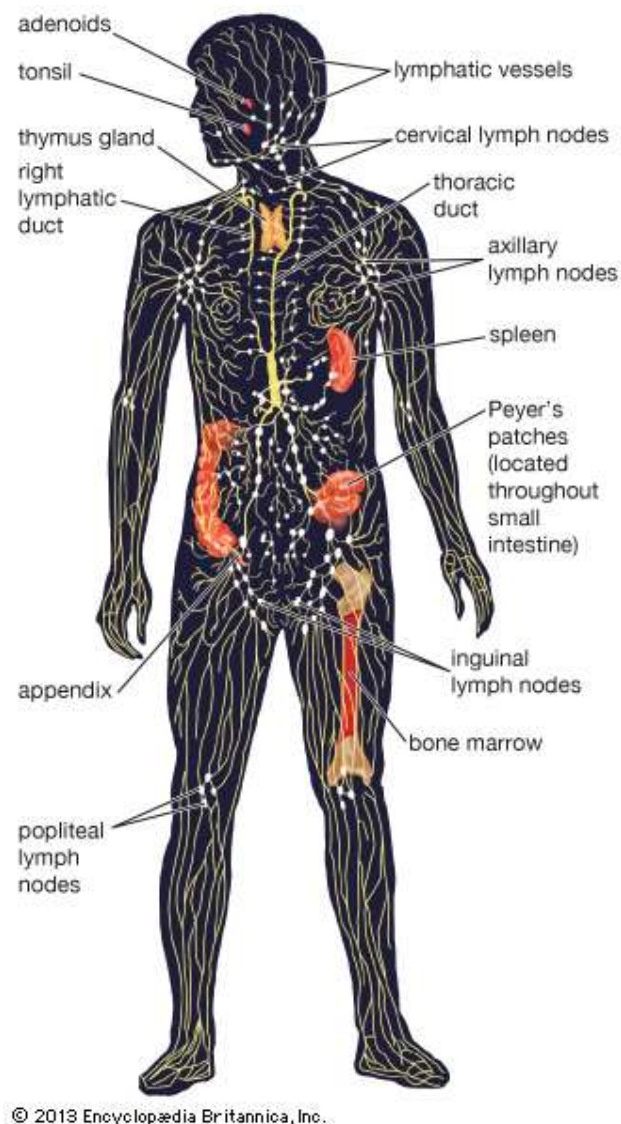
This fact motivated several groups of researchers to develop nanocarriers for the release of the drug directly into the macrophages to increase their bioavailability. Furthermore, encapsulation of drugs with leishmanicidal action is desired to minimize its adverse effects. Nahar and colleagues (2010) prepared gelatin nanoparticles loaded with amphotericin B and tested them against J774 macrophage infected with *Leishmania*. They found an increase in the EC<sub>50</sub> of 5.4-fold than the free drug (NAHAR et al., 2010). Van de Ven and colleagues (2012) prepared saponin-loaded PLGA nanoparticles and tested against *Leishmania donovani* infected macrophages; the increase in the activity was 2-fold.

It is well known that the lymphatic system (LS) is involved in the development and spread of leishmaniasis (REUS et al., 2005; CARVALHO et al., 2012; LAURENTI et al., 2013). After the vector bite, parasites are dispersed through the vascular and lymphatic systems, infecting MPS cells (WASAN et al., 2010). The LS is an open tubular system having capillaries and vessels that transport lymph fluid. The lymphoid organs are bone marrow, thymus, spleen, Peyer's patches and lymph nodes (LNs). The lymphatic vessels coming from the draining area (gut system or skin) (Figure 1.7) are responsible for transportation of fluid, proteins, lipids and different cell populations of the immune system to the LNs (BUETTNER and BODE, 2012)

The lipid-based formulations can be applied as lymphatic targeted drug delivery systems. The LS is involved in the absorption of lipids from intestines and their transportation to the systemic circulation by the wide LS drainage network (YÁÑEZ et al., 2010; KALEPU, MANTHINA and PADAVALA, 2013). Therefore, NLSs can promote oral absorption of the encapsulated drugs via selective lymphatic uptake (CHARMAN, 2000; HOLM et al., 2002; PORTER and CHARMAN, 2001) and direct these drugs and lipids to spleen and liver.

Additionally, those formulations can influence the absorption and bioavailability of low water solubility drugs by other mechanisms, such as modified and sustained drug release, change the composition of the intestinal environment, interaction with enterocyte-based transport processes and particle internalization by epithelial cells or lymphoid tissues in Peyer's patches (FRICKER et al., 2010). Therefore, the drug delivery systems targeted to lymphatic structures is a novel approach for leishmaniasis treatment and should be explored to develop new effective and safe pharmaceutical dosage forms.

Figure 1.7. The human lymphatic system, showing the lymphatic vessels and lymphoid organs. Encyclopædia Britannica, inc., 2017.



Regarding the use NLSs for parenteral administration, Asthana and colleagues (2013) prepared lipid nanoparticles coated with chitosan. They found increased antileishmanial properties and upregulation of tumor necrosis factor alpha (TNF- $\alpha$ ), interleukin-12 (IL-12), inducible nitric oxide synthase and downregulation of transforming growth factor  $\beta$  (TGF- $\beta$ ), IL-10, and IL-4. The chitosan was previously reported to be able to stimulate the production and release of various pro-inflammatory cytokines and to induce immunologic adjuvant effects by active binding to the specific receptors on macrophages (FENG et al., 2004; SEO et al., 2000), which can be explored for developing coated nanoparticles for leishmaniasis treatment.

Another polysaccharide that has potential use for macrophage target is dextran. The SIGN-R1 and mannan receptors (MR) from macrophages recognize various polysaccharides, such as dextran. These receptors interact with lipopolysaccharides from Gram-negative bacteria for pathogen recognition, uptake and further induction of immune responses (CHIEPPA et al., 2003; KAWAUCHI, KURODA and KOJIMA, 2014; TAKAHARA et al., 2011). Kang and colleagues have (2003) demonstrated the selective dextran uptake by SIGN-R1-expressing macrophages. Likewise, Choi and colleagues (2010) and other authors (PUSTYLNIKOV et al., 2014; TAKAHARA et al., 2011; KAWAUCHI, KURODA and KOJIMA, 2012; CHOI et al., 2011) have already investigated the interaction of dextran and macrophage receptors. In many cases the immune modulation from infected cells is beneficial for pathogens; interactions with SIGN-R1 receptors suppress T-helper type 1 (Th1) immune responses, which are crucial for defense against intracellular pathogens. Dextran as an inert ligand of MR and SIGN-R1 could reduce this unfavorable action by the blockage of these receptors (PUSTYLNIKOV et al., 2014). Moreover, Takahara and colleagues (2004) demonstrated that carbohydrate SIGN-R1 activation enhances cellular oxidative burst response against *C. albicans*, which is crucial for macrophage functions in response to pathogens, like *Leishmania*.

Antimicrobial peptides (AMPs), such polymyxin B, are compounds that possess immunomodulatory activities of the innate immune system of multicellular organisms and can be used for protection against pathogenic microorganisms (LOUTET and VALVANO, 2011). Properties of AMPs on *Leishmania* include the disruption of the plasma membrane and following increased cell permeability, interaction with intracellular targets and stimulation of biochemical modifications and apoptosis. As a

result of the AMPs, the parasite can be eliminated. Inside mammalian hosts, AMPs can recruit inflammatory cells to sites of parasite infection (MARR, MCGWIRE and MCMASTER, 2012; LOUTET and VALVANO, 2011). Therefore, those compounds can be explored for leishmaniasis treatment. Polymyxin B was tested against *Leishmania amazonensis* by our research group and showed potential activity use for leishmaniasis treatment. Therefore, this antibiotic was applied in this work for the development of nanostructured lipid carriers coating targeted to macrophages.

Successful treatment of leishmaniasis is impaired by several factors; the most notable are drug parasite resistance, toxicity and lack of effective prophylactic vaccines against leishmaniasis infections. Those issues make the discovery and development of new therapeutic agents a priority. Therefore, this work describes the development of buparvaquone nanostructured lipid carrier (BPQ-NLC) using safe and commercial available excipients to address the need for low cost, safety and effective medicines for leishmaniasis treatment.

## Hypothesis

Is it possible to develop buparvaquone nanostructured lipid carriers with features aiming to improve leishmaniasis treatment?

### Objectives

The study covers the following objectives

- (i) Selection the most suitable solid and liquid lipids for buparvaquone solubilization.
- (ii) Preparation of BPQ-NLC using statistic tools for formulation understanding and optimization.
- (iii) BPQ-NLC physicochemical characterization.
- (iv) Evaluation of BPQ-NLC solubility and *in vitro* drug release.
- (v) Evaluation of *in vitro* cytotoxicity and leishmanicidal activity

**Chapter 2** discusses in detail the selection of lipids and proposed a formulation using poloxamer and tween 80 as surfactants using statistic tools. This chapter try to achieve the **first objective** and partially the **second objective**.

**Chapter 3** covers the statistical development of formulation using poloxamer 188 as single surfactant and it try to achieve the **first, second, third and fourth objectives**.

**Chapter 4** covers the development of co-encapsulated buparvaquone and polymyxin B coated with biopolymers chitosan and dextran. This chapter try to achieve **the first, third, four and fifth objectives**.

## Chapter 2

### **Buparvaquone nanostructured lipid carrier: development of an affordable delivery system for the treatment of leishmaniases**

This study has already been published as Lis Marie Monteiro, Raimar Löbenberg, Paulo Cesar Cotrim, Gabriel Lima Barros de Araújo, Nádia Bou-Chacra. Buparvaquone nanostructured lipid carrier: development of an affordable delivery system for the treatment of leishmaniases. BioMed Research International. Volume 2017, Article ID 9781603, 11 pages.

## ABSTRACT

Buparvaquone (BPQ), a veterinary drug, was formulated as nanostructured lipid carriers (NLC) for leishmaniasis treatment. The formulation design addressed poor water solubility of BPQ and lack of human drug delivery system. The DSC/TG and microscopy methods were used for solid lipids screening. Softisan® 154 showed highest BPQ solubility in both methods. The BPQ solubility in liquid lipids using HPLC revealed Miglyol 812 as the best option. Response surface methodology (RSM) was used to identify the optimal Softisan®154:Miglyol®812 ratios (7:10 to 2:1) and Kolliphor® P188 and Tween 80 concentration (>3.0 % w/w) aiming z-average in the range of 100-300 nm for macrophage delivery. The NLC obtained by high-pressure homogenization showed low z-averages (<350 nm), polydispersity (<0.3) and encapsulation efficiency close to 100%. DSC/TG and microscopy in combination proved to be a powerful tool to select the solid lipid. The relationship among the variables, demonstrated by a linear mathematical model using RSM, allowed generating a design space. This design space showed the limits in which changes in the variables influenced the z-average. Therefore, these drug delivery systems have the potential to improve the availability of affordable medicines due to the low-cost of raw materials, using well established, reliable and feasible to scale-up technology.

Keywords: nanoparticles, buparvaquone, nanostructured lipid carrier, leishmaniasis, differential scanning calorimetry, surface response.

## 2.1.Introduction

Over the past decades, improper prescription and lack of patient compliance, due to severe toxicity of conventional medicines, have caused the development of widespread parasite resistance in leishmaniasis. Also, no new drug substances have been introduced in the therapy, and there are no effective vaccines available to prevent or heal this neglected tropical disease (LINDOSO, et al., 2012; ALVAR et al., 2013). Buparvaquone (BPQ) is used in the treatment of blood parasites in cattle and showed promising antileishmanial *in vitro* activity. Even though there is a formulation for veterinary use, no suitable pharmaceutical dosage form for a human is available. Also, the low water solubility of BPQ limits its bioavailability, which is the main challenge for developing a drug delivery system for enhancing its therapeutic efficacy.

The development of lipid nanoparticles is one of the most promising alternatives to overcome this limitation. Such delivery systems have the ability to overcome biological barriers, increase therapeutic efficacy, reduce toxicity and allow drug release at the specific site (KOBETS, GREKOV and LIPOLDOV, 2012; TIUMAN et al., 2011). Moreover, these colloidal carriers are quickly taken up by cells from the mononuclear phagocyte system (SINGH et al., 2012), which are the host cells of the leishmaniasis parasite infection. This mechanism makes nanoparticles an attractive vector for passive targeting of antileishmanial drug substances (VAN DE VEN et al., 2012). Therefore, lipid-based nanoparticles represent an opportunity to improve the leishmaniasis therapy.

Recently, biocompatible lipids have attracted attention for development of delivery systems for poorly soluble drugs (DAS, NG and TAN, 2012). Lipid-based nanoparticles include nanoemulsions (NE), solid lipid nanoparticles (SLN) and nanostructured lipid carriers (NLC). The NE present some advantages; they can be used in various dosage forms such as creams, liquids, sprays and foams. However, the main challenges are the low stability of the systems, use of a large concentration of surfactant for stabilizing the nanodroplets and limited solubilizing capacity for high-melting point substances (SEZER, 2014).

SLN present disadvantages, such as low drug loading capacity and drug expulsion during storage. The low ordered lipid matrix tends to be reorganized to



highly ordered structure. As a consequence, the perfect crystal lattice cannot accommodate the drug (WEBER, ZIMMER and PARDEIKE, 2014). The addition of a liquid phase can disorder the lipid matrix, which avoids lipid polymorphism and leads to enhanced drug loading capacity (CHEN, HUANG and PANG, 2013).

NLC have been introduced as an alternative to traditional colloidal carriers such as liposomes and polymeric nanoparticles due to the lower cost of raw materials, in comparison with phospholipids used to prepare liposomes. These NLC can provide formulations with higher physical stability, high encapsulation efficiency and feasible industrial scale-up (CIRRI et al., 2012). Furthermore, the NCL combine the advantages of polymeric nanoparticles due to the presence of a solid matrix, which can protect chemically unstable drugs and allow controlled release. As well, NLC bear the advantage of low *in vivo* toxic, owing to the use of biocompatible and biodegradable materials (CIRRI et al., 2012).

Recently, the formulation design of salicylic acid and lidocaine-prilocaine NLC, using the design of experiments (DoE), was reported to address the low water solubility of these drugs (RIBEIRO et al., 2016; KOVÁCS et al., 2017). The DoE is superior to the traditional change-one-at-a-time approach because it is a systematic multivariate method. This powerful statistical tool can be used to create a design space aiming to achieve an in-depth knowledge of the formulation and process understanding. Design space is defined as the multidimensional combination and interaction of input variables (e.g., material attributes) and process parameters that have been demonstrated to provide assurance of quality (ICH, 2009).

Considering the leishmaniasis therapeutic scenario, new drug substances, and affordable drug delivery systems are urgently needed. Therefore, BPQ-NLC are promising formulations to achieve high therapeutic efficacy and safety for leishmaniasis treatment. This work is focused on the comparison of two methods for BPQ solid lipid solubility studies (DSC/TG and microscopy) in the preformulation stage, and development and optimization of BPQ-NLC, using central composite experimental design.

## **2.2. Materials and methods**

### **2.2.1. Chemicals**

BPQ was purchased from Uniwise (China). Softisan<sup>®</sup> 154, Dynasan<sup>®</sup> P60, Dynasan<sup>®</sup> 118, Witepsol<sup>®</sup> E85, were kindly donated by CREMER Oleo Division (Germany). Gelucire<sup>®</sup> 44/13, Compritol<sup>®</sup> 888, Gelucire<sup>®</sup> 50/14, Precirol<sup>®</sup> ATO 5 were kindly donated by Gattefossé (France). Sterotex<sup>®</sup> HM, oleic acid, glyceryl monocaprylate, medium chain triglycerides (MCT) were kindly donated by Abitec (USA). Super refined cottonseed, safflower, corn, olive, soybean and sesame oils were kindly donated by Croda (UK). Kolliphor<sup>®</sup> P188 was acquired from BASF (Germany) and Tween 80 from Sigma–Aldrich (Spain). Purified water was of Milli-Q quality (Millipore, USA). All other reagents were at least of analytical grade and were used without further purification.

### **2.2.2. Selection of liquid and solid lipids for BPQ-NLCs preparation**

Regarding the liquid lipids, BPQ in excess was added to the liquid lipid and placed in orbital shaker at 25 °C. After 24 hours, aliquots were filtered through a PVDF membrane of 0.22 µm pore size and were injected into HPLC to determine the amount of solubilized BPQ, using the method described below.

BPQ solubility in solid lipids was evaluated according to Kasongo and colleagues (2011). Briefly, buparvaquone was added to the solid lipid in a concentration of 0.001% (w/w), this preparation was heated 10° C above the melting point of each lipid, under constant shaking for 24 hours. Aliquots were taken and observed by optical microscope; the BPQ concentration was adjusted until crystals observation. The results were ranked by the amount of crystals, the higher position in the rank, the lower amount of crystals was observed.

Drug solubility and crystallization behavior in solid lipids were carried out by using DSC/TG. The BPQ thermal behavior and solid lipids and 1:1 physical mixtures (PM) were characterized in a DSC 4,000 Perkin Elmer cell (Perkin Elmer Corp., Norwalk, CT, USA), under a dynamic N<sub>2</sub> atmosphere (50 mL.min<sup>-1</sup>), using sealed aluminum capsules with about 2 mg of samples. DSC curves were obtained at a heating rate of 10 °C min<sup>-1</sup> in the temperature range from 25 to 290 °C. An empty sealed pan was used as a reference.

TG/DTG curves were obtained with a thermobalance model Exstar-7200 (Hitachi High-Tech Science Corporation, Tokyo, Japan) in the temperature range 25-600°C using platinum crucibles DSC Exstar-7020 (Hitachi High-Tech Science Corporation, Tokyo, Japan).

The onset temperature, maximum peak in the melting range ( $T_{peak}$ ), and melting enthalpy ( $\Delta H_m$ ) were calculated using the software provided by PerkinElmer. The crystallinity indexes (CI) of BPQ were calculated in percentage according to Equation 2.1 (SOUTO and MÜLLER, 2005; FREITAS and MÜLLER, 1999; JUNYAPRASERT et al., 2009; SEVERINO, SANTANA and SOUTO, 2012):

$$CI(\%) = \frac{\Delta H_{BPQ\ PM * D}}{\Delta H_{BPQ\ 100\%}} * 100 \quad \text{Equation 2.1}$$

where:  $\Delta H_{BPQ\ PM}$  is the enthalpy of fusion ( $J.mg^{-1}$ ) of BPQ in the binary physical mixture of BPQ and solid lipid.  $\Delta H_{BPQ\ 100\%}$  is the enthalpy of fusion ( $J.mg^{-1}$ ) of pure drug. D is the dilution of BPQ in the PM, e.g. 1:1: dilution of 2.

### 2.2.3. Preparation of BPQ-NLC

After lipids selection, a mixture of solid (SL) and liquid (LL) lipids was tested in different ratios of SL:LL, from 1.5 (3:2 SL:LL) to 4 (4:1). The melting point of the mixture was determined by DSC as described above. The optical homogeneity was accessed by smearing the mixture in glass slides and observation of liquid drops or solid crumbs. The homogeneous mixtures of melting point above 40°C were selected for BPQ-NLC preparation.

The NLC preparation was performing as proposed by Muchow and colleagues (2013) by dispersing the lipid phase in the aqueous phase. The system was mixed by a mechanical homogenizer at 8000 rpm (Ultraturrax, IKA) for 5 min. The pre-emulsion was passed through a temperature-controlled high-pressure homogenizer (Nano DeBEE, BEE International), 60 bar and five cycles.

### 2.2.4. NLC formulation and optimization by response surface design

A three factor ( $2^3$ ) central composite design was employed for optimization of the nanostructured lipid carriers. The study was performed to evaluate the influence of following independent variables: solid and liquid lipids ratio (SL:LL) and surfactants concentrations (independent variables) in the z-average (response or dependent variable). The response surface method was applied to define the optimal conditions of the process and identification of relevant variables and their working range. The SL:LL range was 1.5 (3:2) (w/w) to 4.0 (4:1) (w/w), the surfactants concentrations were from 1.0 to 3.0% (w/w). Minitab® 17 software was used to generated the design matrix and data analyses.

The desirability method was used for the optimization process. The desirability function is based on the optimization techniques developed by Derringer and Suich (1980). In this approach, each response  $Y_i$  is first converted into a  $DY$  of each desirability function ranging between 0 and 1 ( $0 \leq d_i \leq 1$ ). Where  $D(Y) = 0$  represents an entirely undesirable value  $Y_i$ , while  $D(Y_i) = 1$  represents a completely desirable or ideal response value. The DI individual values are then combined using a geometric mean to give a general desirability function  $D$  (NATARAJAN, PERIYANAN and YANG, 2011).

#### **2.2.5. Determination of z-average, polydispersity index and zeta potential**

The Z-average of the nanostructured lipid carriers was determined immediately after high-pressure homogenization and was assessed by photon correlation spectroscopy (PCS) using Zetasizer ZS90 (Malvern Instruments, Malvern, UK) at 25 °C and 90° ( $n = 10$ ). The PCS technique calculates the z-average as light-weighted intensity and polydispersity index (PDI) as a measure for the width of the z-average distribution. The equipment was also used to measure the zeta potential (ZP). ZP measurements were carried out in purified water with a conductivity adjusted to 50  $\mu\text{S} \cdot \text{cm}^{-1}$  by the addition of NaCl 0.1% (w/v), to avoid ZP fluctuations caused by the difference in conductivity ( $n = 3$ ). The pH was adjusted to  $6.5 \pm 0.2$  by the addition of 0.01 N HCl or 0.01 N NaOH solution.

### **2.2.6. Determination of BPQ solubility in liquid lipids and encapsulation efficiency**

The method described by Venkatesh and colleagues (2010) was used as a basis for quantification method for solubility in liquid lipids and encapsulation efficiency. In brief, C4 250 mm × 4.6 mm ID, 5 µm particle size column; 1% glacial acetic acid in water, acetonitrile, and methanol 30:60:10 (v/v/v) mobile phase,  $\lambda$  = 251 nm, 50 µL injection volume, 35 °C column temperature. The final conditions were: column Waters Xterra, C8 100 x 4.6 mm, 3.5 µm particle size. A mobile phase of 1% glacial acetic acid, acetonitrile and methanol (25:65:10), a column temperature of 35 °C, injection volume 50 µL and UV detection  $\lambda$  = 251 nm.

The sample to assess the total drug amount was prepared as the following steps: acetonitrile were added to the NLCs and sonicated for 30 minutes. After cooling, the volume was completed with the same solvent, an aliquot was centrifuged at 376 RCF for 15 min, and the supernatant was diluted with mobile phase to appropriate concentration. Aliquots of the NLC were filtered through Amicon Ultra-0.5 mL Ultracel-10 membrane 50 kDa centrifugal filters (Millipore Merck). The filter was checked for BPQ adsorption previously. The filtrate was directly injected to quantify the supernatant content. Both samples were analyzed by HPLC as described above (n=3). Buparvaquone encapsulation efficiency was calculated by the difference between total BPQ amount and the content in the supernatant.

In the matter to test if the NLC structure could increase the drug loading, two formulations with augmented amount of BPQ were prepared, and their encapsulation efficiency was determined. A stability study was conducted at 8°C for three months; the samples were stored in 8 mL borosilicate sealed vials.

## **2.3. Results and Discussion**

### **2.3.1. Evaluation of BPQ solubility in solid and liquid lipids**

Table 2.1 shows the results of BPQ solubility in liquid lipids determined by HPLC. Miglyol® 182 presented the highest solubility (11.55 g.kg<sup>-1</sup>). This lipid is widely used for parenteral, oral and topical formulations; it is resistant to oxidation and it is a

synthesized medium-chain triglyceride, which ensures uniformity of product batch by batch.

Table 2.1. Buparvaquone solubility in liquid lipids.

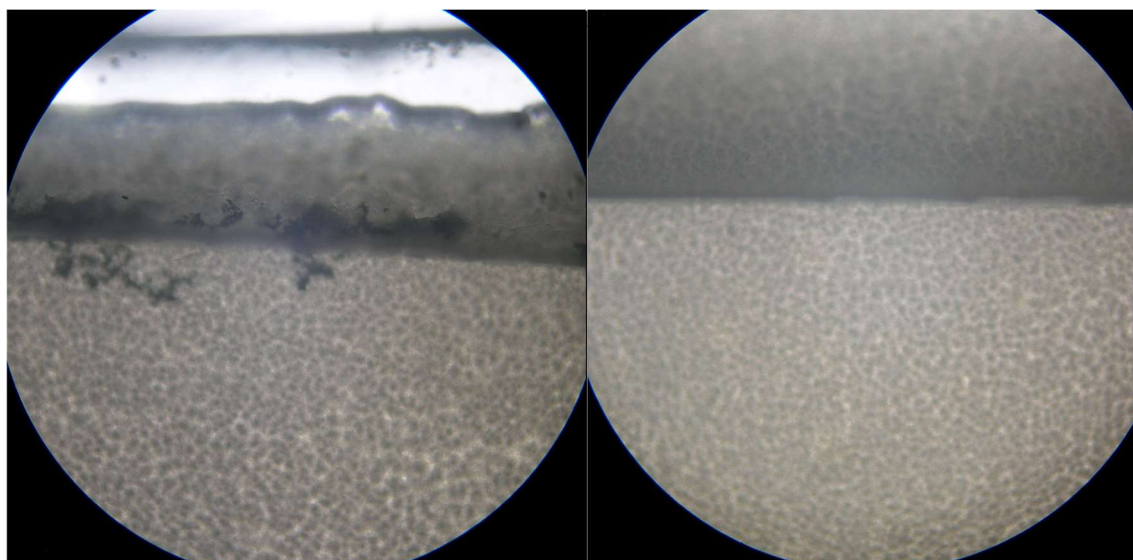
Liquid lipid	Solubility (g.kg <sup>-1</sup> )	RSD (%)
<b>Miglyol® 182</b>	11.55	1.9
<b>Glyceryl monocaprylate</b>	7.43	1.3
<b>Safflower purified Oil</b>	6.48	1.6
<b>Corn purified oil</b>	6.51	0.6
<b>Olive purified oil</b>	6.21	1.6
<b>Sesame purified oil</b>	5.96	7.4
<b>Cottonseed purified oil</b>	6.01	0.5
<b>Soy purified oil</b>	5.43	7.3
<b>Oleic acid</b>	5.21	2.4

Table 2.2 shows the results for solid lipids using the microscopy method. The lipids were ranked by the likely presence of crystals. The Figure 2.1 (A and B) shows the criteria for crystals observation in the mixture. Figure 1A shows the lipid mixture, which BPQ was not soluble and Figure 2.1B shows the lipid mixture, which BPQ was soluble.

Table 2.2 Crystal evaluation by microscopy for buparvaquone solubility test

Crystals Rank	Lipid	Soluble at 1mg.g <sup>-1</sup>	Soluble at 2mg.g <sup>-1</sup>	Melting Point (°C)
1 <sup>st</sup>	Softisan® 154	Yes	No	53-58
2 <sup>nd</sup>	Gelucire® 44/14	No	No	44
3 <sup>th</sup>	Dynasan® P60	No	No	58-62
4 <sup>th</sup>	Compritol® 888	No	No	70
5 <sup>th</sup>	Dynasan® 118	No	No	72-75
6 <sup>th</sup>	Sterotex® HM	No	No	69
7 <sup>th</sup>	Witepsol® E85	No	No	42-44
8 <sup>th</sup>	Gelucire® 50/13	No	No	50
9 <sup>th</sup>	Precirol® ATO 5	No	No	56

Figure 2.1. Optical microscopy from Softisan® 154 lipid samples mixed with buparvaquone A: (2 mg.g<sup>-1</sup>) B: (1 mg.g<sup>-1</sup>). 40X magnification.



Microscopic assessment for the determination of drug solubility in a solid lipid was used by several authors (MÜLLER et al., 2006; NIKOLIĆ, et al., 2011; MENDES et al., 2013; DEVKAR, TEKADE and KHANDELWAL, 2014; PATIL-GADHE and POKHARKAR, 2014; PARDEIKE et al., 2011). However, is time-consuming, the results are semi-quantitative and the interpretation can vary depending on the qualification of the analyst.

To find a potential substitute or an auxiliary method for microscopic evaluation, differential scanning calorimetry and thermogravimetry (DSC/TG) were used as a faster and reproducible approach for evaluating the ability of the solid lipids to solubilize BPQ. Kasongo and colleagues (2011), Severino and colleagues (2011) and Liu and colleagues (2014), in their studies, provided the rational for the correlation of DSC data with solubility. The greater reduction in CI of a drug peak, in a physical mixture with the SL, the better is the ability of the lipid to solubilize the drug.

Table 2.3 shows CI of BPQ and SL mixtures. Figure 2.2 shows Softisan® 154 DSC/TG thermograms. For the other lipids, the same approach was performed. In the first heating cycle, the drug was more soluble in Gelucire® 50/13 and Witepsol® E85. The crystallinity index of BPQ was reduced to 40.6 and 48.8% for these lipids, respectively. In the second heating cycle, the Witepsol® E85 and Softisan® 154

showed almost the same CI, 49.0 and 49.1%, respectively. A second heating cycle was studied to simulate the manufacturing conditions of NLC by high-pressure homogenization (KASONGO et al., 2011; MENDES et al., 2013). By quench cooling the sample, the contact time between drug and molten lipid is increased, and it is possible to evaluate better the capacity of the lipid to solubilize the drug. Additionally, it is possible to evaluate the drug and lipid recrystallization behavior. This method can also provide information about drug degradation and or drug-lipid incompatibility.

Figure 2.2. Thermoanalytical profiles of buparvaquone (BPQ), Softisan® 154 and BPQ physical mixture (PM) obtained at 10 °C min<sup>-1</sup>, under a dynamic nitrogen atmosphere (50 mL.min<sup>-1</sup>). BPQ DSC curve (A) DSC Softisan® 154 curve (B) PM 1<sup>st</sup> run (C) PM 2<sup>nd</sup> run (D) TG: TG curves of PM (E). BPQ: buparvaquone; 1<sup>st</sup> run: first heat cycle; 2<sup>nd</sup> run: second heat cycle.

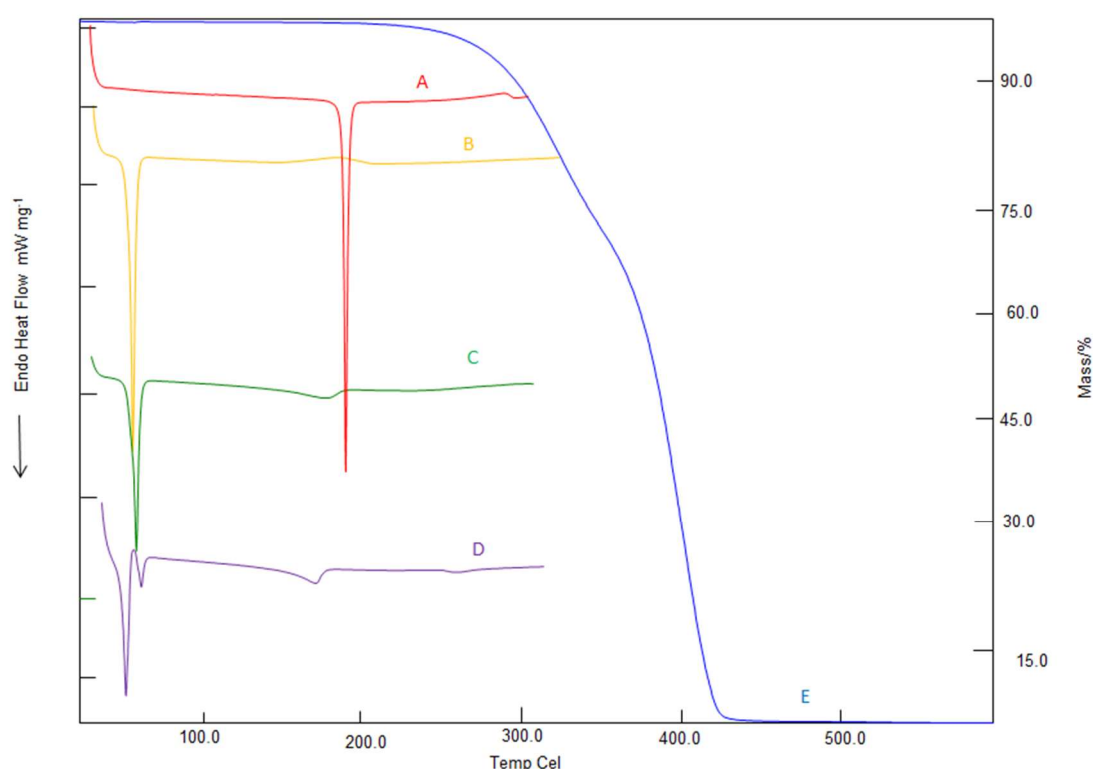




Table 2.3. Enthalpy of fusion ( $\text{J g}^{-1}$ ) and crystallinity index for determining the solubility of buparvaquone in solids lipids by differential scanning calorimetry.

Lipid	$\Delta H_{\text{BPQ}}$ ( $\text{J.mg}^{-1}$ )	$\Delta H_{\text{BPQ-PM}}$ ( $\text{J. mg}^{-1}$ ) 1 <sup>st</sup>	$\Delta H_{\text{BPQ-PM}}$ ( $\text{J. mg}^{-1}$ ) 2 <sup>nd</sup>	CI (%) 1 <sup>st</sup>	CI (%) 2 <sup>nd</sup>
<b>Witepsol® E85</b>	136.0	33.2	33.3	48.8	49.0
<b>Softisan® 154</b>	136.0	42.2	33.4	62.1	49.1
<b>Gelucire® 50/13</b>	136.0	59.4	34.4	40.6	50.6
<b>Gelucire® 44/14</b>	136.0	47.6	35.5	70.0	52.2
<b>Precirol® ATO 5</b>	136.0	54.9	37.7	80.7	55.4
<b>Sterotex® HM</b>	136.0	51.5	44.0	75.7	64.7
<b>Dynsan® P60</b>	136.0	59.4	57.9	87.4	85.1
<b>Compritrol® 888</b>	136.0	66.5	67.3	97.8	99.0

BPQ: buparvaquone; BPQ-PM: BPQ and lipid physical mixture; CI: crystallinity index =  $(\text{BPQ enthalpy in lipid mixture (J.mg}^{-1}) * D (\text{proportion of BPQ and lipid}) / \text{BPQ enthalpy of fusion (J.mg}^{-1})) \times 100$ ; 1<sup>st</sup> and 2<sup>nd</sup> heating cycles.

Microscopy revealed that Softisan® 154, among the other tested lipids, presented highest BPQ solubility. However, the DSC results confirmed its high solubility as the second rank being the first Witepsol® (Table 2.3). The divergence in the results revealed the relevance of the two methods.

By these findings, a rational for using the combined methods involves two steps: the screening of a high number of lipids with DSC/TG and microscopy evaluation for the most suitable ones to confirm and determine the drug amount that is soluble in the lipid. This combination of methods can save time, materials, work labor and can generate important information about the drug and lipids.

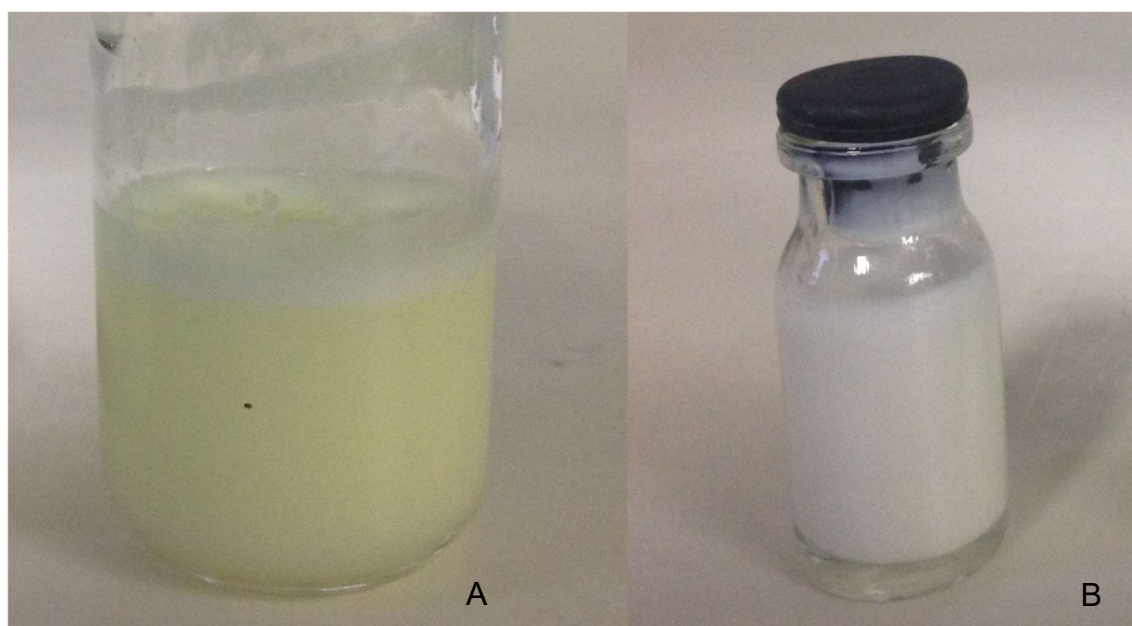
### 2.3.2. Preparation of BPQ-NCL

The Softisan® 154 (SL) and Miglyol® 182 (LL) were mixed in different ratios to determine the maximum proportion of Miglyol® 182. The SL:LL mixtures were visually homogeneous (no phase separation), and their melting points (MP) were above

40°C. For example, or SL:LL 1.5 (3:2), the MP was 48.8°C. The SL:LL ratios which the mixtures showed melting points higher than 40°C were selected to ensure the NLC solid matrix structure (AVERINA et al., 2011).

Figure 2.3 shows visual aspect of the formulations, before (Fig 2.3A) and after homogenization (Fig 2.3B). The high-pressure homogenization proved to be reliable for BPQ-NLC preparation, all formulations showed low z-averages <350 nm and low polydispersity <0.3 (Table 2.4). The yellow color of the drug was not observed after homogenization for F1 (Figure 2.3), indicating the drug internalization into the lipid matrix, which was confirmed by encapsulation efficiency. The stability of the formulations was accessed; all of them presented z-average and polydispersity variation less than 10.0% during three months (data now shown).

Figure 2.3. Nanostructured lipid carrier for buparvaquone encapsulation: A and B, before and after high-pressure homogenization, respectively.



### 2.3.3. BPQ-NLC optimization by response surface design

The response surface methodology (RSM) is an efficient and powerful statistical method to optimize processes. Using the RSM, it is possible to reduce the

number of experimental tests, with consequent savings in time and materials. The statistical design identifies component interactions and critical process parameters. The methodology involves three steps: (1) the development of rotary central composed design; (2) the response surface modeling by regression analysis (ANOVA); and (3) the optimization of the process using the model (WANG et al., 2012).

For this work, 20 experiments (Table 2.4) were used to evaluate the influence of the SL:LL and concentrations of Kolliphor® P188 and Tween 80 in the z-average. The best fitting model from ANOVA was selected based on the comparison of statistical parameters including the R-square ( $R^2$ ), adjusted R-square ( $\text{adj-}R^2$ ), predicted R-square ( $\text{pred-}R^2$ ), lack-of-fit test and p-values. The linear model and its significance were revealed by the  $p\text{-value} < 0.05$  ( $\alpha = 0.05$ ) for each term (Table 2.5).

Table 2.4. Experimental matrix and values of z-average and polydispersity (PDI) of buparvaquone nanostructured lipid carriers.

Form	Order	SL:LL	% Tween 80 (w/w)	% Kolliphor® P188 (w/w)	Z-average (nm)	PDI
12	1	2.75	2.00	2.00	263.2	0.198
2	2	4.00	1.00	1.00	323.1	0.252
6	3	4.00	1.00	3.00	257.3	0.214
9	4	2.75	2.00	2.00	266.9	0.194
5	5	1.50	1.00	3.00	234.6	0.154
8	6	4.00	3.00	3.00	243.9	0.228
7	7	1.50	3.00	3.00	217.7	0.210
1	8	1.50	1.00	1.00	286.0	0.193
11	9	2.75	2.00	2.00	261.3	0.224
10	10	2.75	2.00	2.00	259.4	0.207
3	11	1.50	3.00	1.00	239.7	0.179
4	12	4.00	3.00	1.00	265.9	0.190
20	13	2.75	2.00	2.00	251.4	0.192
18	14	2.75	2.00	3.63	234.2	0.193
16	15	2.75	3.63	2.00	240.5	0.220
14	16	4.79	2.00	2.00	277.2	0.212
17	17	2.75	2.00	0.37	289.0	0.178
19	18	2.75	2.00	2.00	261.2	0.198
13	19	0.71	2.00	2.00	224.8	0.162
15	20	2.75	0.37	2.00	268.8	0.157

Form: formulation; Order: preparation order; SL:LL: solid and liquid lipid ratio.

Table 2.5. Analysis of variance for Z-average.

Source of variation	DF	SS (adj)	MS (adj)	F-value	p-value
<b>Model</b>	4	9807.0	2451.74	63.33	0.000
<b>Linear</b>	3	8868.9	2956.29	76.36	0.000
<b>SL:LL</b>	1	1744.6	1744.56	45.06	0.000
<b>Tween® 80</b>	1	1419.4	1419.38	36.66	0.000
<b>Kolliphor® P188</b>	1	5704.9	5704.95	147.36	0.000
<b>Tween 80*Kolliphor®P188</b>	1	938.1	938.09	24.23	0.000
<b>Error</b>	15	580.7	38.71		
<b>Lack of fit</b>	10	274.6	27.46	0.45	0.869
<b>Pure error</b>	5	306.1	61.22	*	*
<b>Total SS</b>	19	10387.7			

DF: degrees of freedom; SS: sum of squares; F-value: statistic F-test; MS (adj) adjusted mean square; p-value: statistical significance. SL:LL solid and liquid ratio.

If the experimental environment is very noisy or significant variables are not considered in the experiment, it is possible that fraction of the observed data cannot be representative of the product/process. No significant lack-of-fit alone does not assure model adequacy and therefore, measures of overall performance, referred to as R-squares ( $R^2$ ) were evaluated. For this work, the  $R^2$  of 94.41%, adjusted  $R^2$  (adj- $R^2$ ) of 92.92% and predicted  $R^2$  (pred- $R^2$ ) of 91.04% show a suitable model from the data collected (Table 2.6).

When  $R^2$ , adj- $R^2$  and pred- $R^2$  differ dramatically, there is an indication that non-significant terms were included in the model (TRINH and KANG, 2011). For the developed Z-average model, the three  $R^2$  values are close (Table 6), which means the model is representative of the data and variables were representative of the product, regarding z-average.

Additionally, the pred- $R^2$  indicates the high probability of the practical values being close to the theoretical calculations from the model. In the present study, the observed values were within the predicted range (95% CI) (Table 2.6). Therefore, the model can predict the z-average as a function of SL:LL ratio and surfactants concentrations. The z-average is a critical quality attribute for intravenous administration and macrophage uptake. It was found that nanoparticles between 100

and 300 nm are more appropriate for macrophage internalization by phagocytosis (LIN et al., 2012; FANG et al., 2006). Smaller particles (<100 nm) tend to be taken up by endocytosis, a process which occurs in virtually all cells.

Table 2.6. Coded coefficients of the linear model and p-value ( $\alpha=0.05$ ) with the variables: liquid and solid lipid ratio (SL:LL), Kolliphor® P188 (K188) and Tween® 80 (T80).

Terms	Coefficient	C- DP	T-value	p-value	VIF
<b>Constant</b>	253.30	1.39	182.06	0.000	
<b>SL:LL</b>	18.68	2.78	6.71	0.000	1.00
<b>T80</b>	-16.85	2.78	-6.05	0.000	1.00
<b>KP188</b>	-33.78	2.78	-12.14	0.000	1.00
<b>T80*K188</b>	28.88	5.87	4.92	0.000	1.00
<b>SD= 6.22210    R<sup>2</sup>= 94.41%    adj-R<sup>2</sup>= 92.92%    pred-R<sup>2</sup>= 91.04%</b>					

R<sup>2</sup>: R-squared; adj-R<sup>2</sup>: adjusted R-squared; pred-R<sup>2</sup>: predicted R-squared. C-SD: coefficient standard deviation.

$$Z = 333.5 + 9.15 \text{ SL/LL} - 31.98\text{T80} - 42.34\text{K188} + 10.83\text{T80} * \text{K188} \quad \text{Equation 2}$$

where Z is the z-average; SL:LL is the solid and liquid ratio; T80 is the % of Tween 80 (w/v); K188 is the % of Kolliphor® P188 (w/v).

Residuals investigation is an essential part of all statistical modeling. The residual analysis for the ANOVA model was verified by the normal probability plot and the histogram (Figure 2.4). In normal probability plot, the residue is represented according to its expected value, calculated from the assumption that the residues follow a normal distribution (MONTGOMERY, 2004). Considering the results, the location of points on the probability curve and the histogram, the normality assumption is valid. Also, the graph of the individual observations showed the random behavior of the residuals. There was no phenomenon of heteroscedasticity. The analysis of the residuals confirmed that the choice of this model was appropriate (MONTGOMERY, 2004).

Figure 2.4. Residuals analysis of the BPQ-NLC mathematical model for Z-average

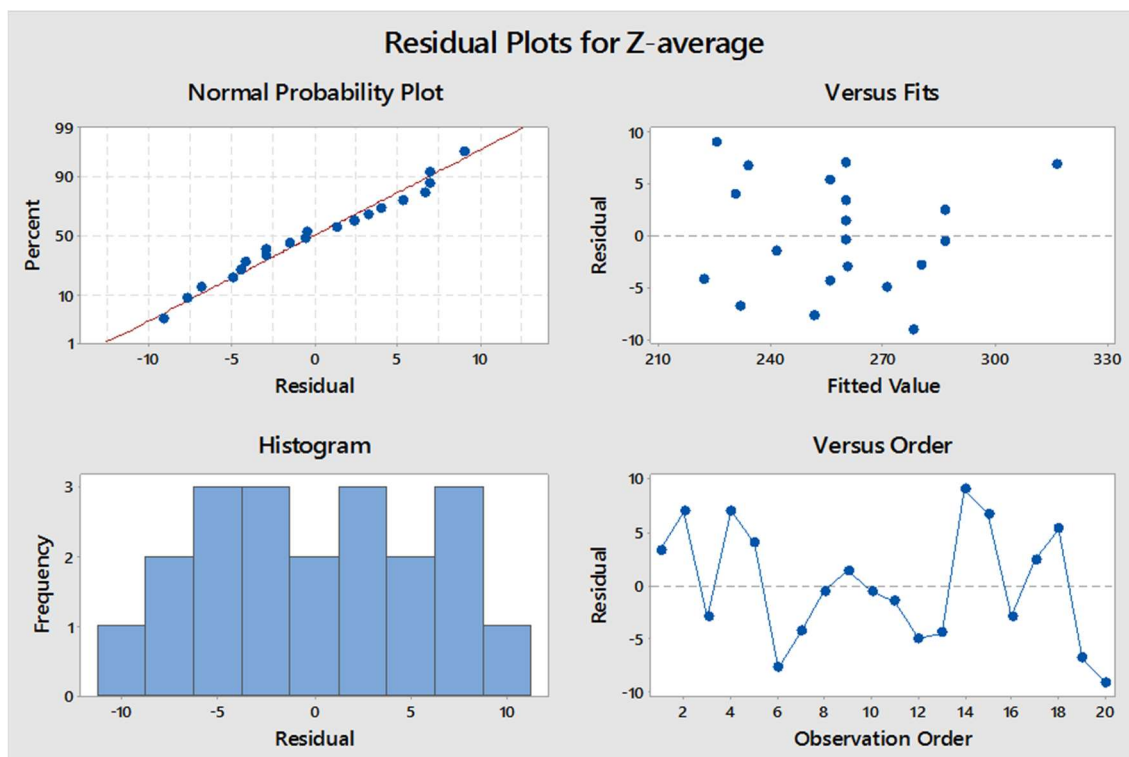


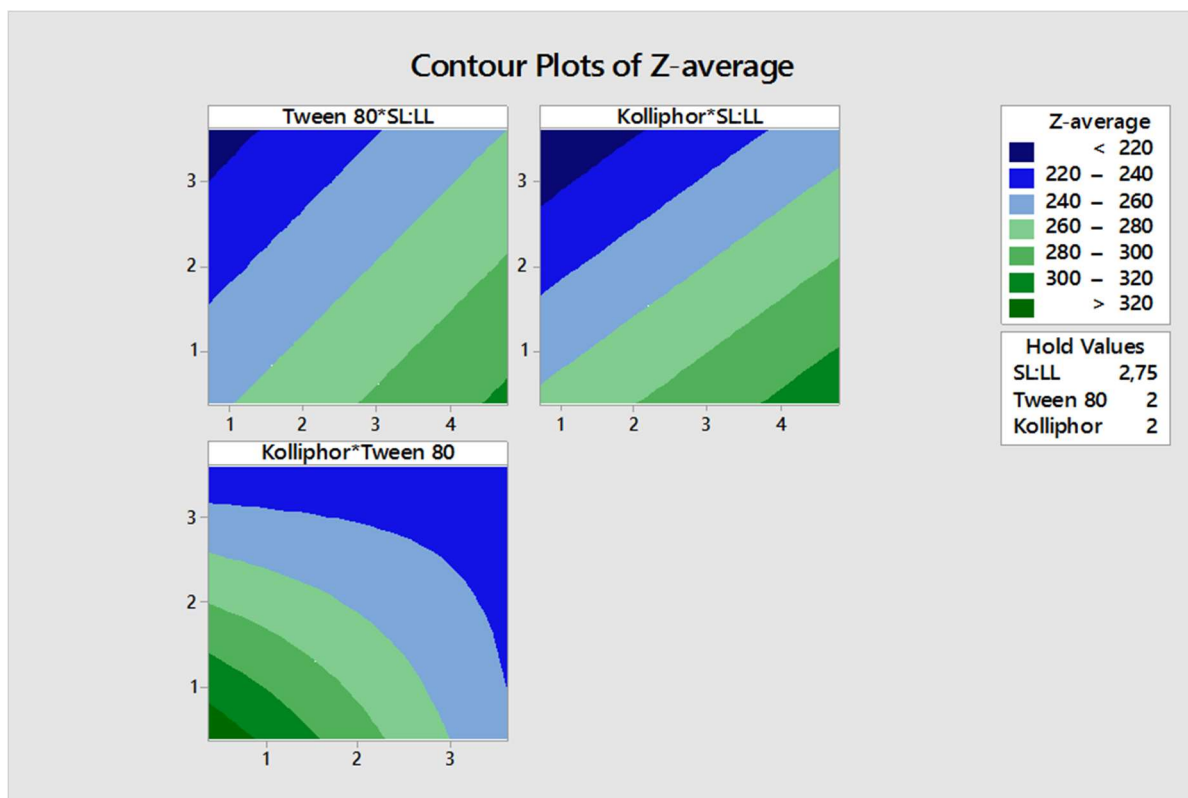
Figure 2.5 showed that Kolliphor® P188 reduced z-average at a lower concentration than Tween® 80. The result showed the area of z-average < 220 nm for Kolliphor® P188 is larger than Tween® 80. Likewise, the coded coefficient for Kolliphor® P188 and Tween® 80 are -33.78 and -16.85 (Table 6), which means that in the same concentration, the formulation prepared using Kolliphor® P188 will present lower z-average than one prepared using Tween® 80.

This finding can be explained by the longer central hydrophobic chain of polyoxypropylene from Kolliphor. Cohesive energy of lipophilic chain is stronger when compared to short lipophilic chain from Tween® 80 (KUNIEDA et al., 1998; MOLOUGHNEY and WEISLEDER, 2012). Moreover, two hydrophilic chains of polyoxyethylene oxide (PEO) exhibit gelation phenomena when heated (HAO et al., 2014), which contributes to integrity and stability of the surfactant film.

According to the Figure 2.5, when adjusting the SL:LL ratio to 2.75 (11:4), surfactants above 3.0% (w/w) are required to reach low Z-averages. The interaction between surfactants can be observed by the plot Kolliphor\*Tween and by the Kolliphor\*Tween coefficient interaction term, which presents a positive value of +28.88 (Table 2.6). As a consequence, for the optimization, low amounts of Tween

80 were applied to reduce the impact of this interaction. Furthermore, it can be seen that z-average < 220 nm are only achieved at low ratios of SL:LL (< 2.5).

Figure 2.5. Contour plot of the BPQ-NLC mathematical model for z-average, containing the following variables: Solid and liquid ratio (SL:LL), Kolliphor® P188 and Tween® 80.



For the mathematical model confirmation, two formulations were prepared: F1 and F2, according to Figure 2.6 and Figure 2.7, respectively. The measured values of z-average for F1 were: 215.4 nm  $\pm$  1.7% (183.8 to 217.4 nm; CI 95%). For F2, it was: 231.2 nm  $\pm$  1.0% (200.8 to 232.4 nm; CI 95%), which are within the predicted range (Table 2.7), confirming the validity of the mathematical model.

Figure 2.6. Profile for predicted values and desirability function of the F1 z-average (201 nm), containing the following variables: solid and liquid lipid ratio (SL:LL) at 0.71, Kolliphor® P188 at 3.6% (w/w), Tween 80 at 0.37% (w/w).

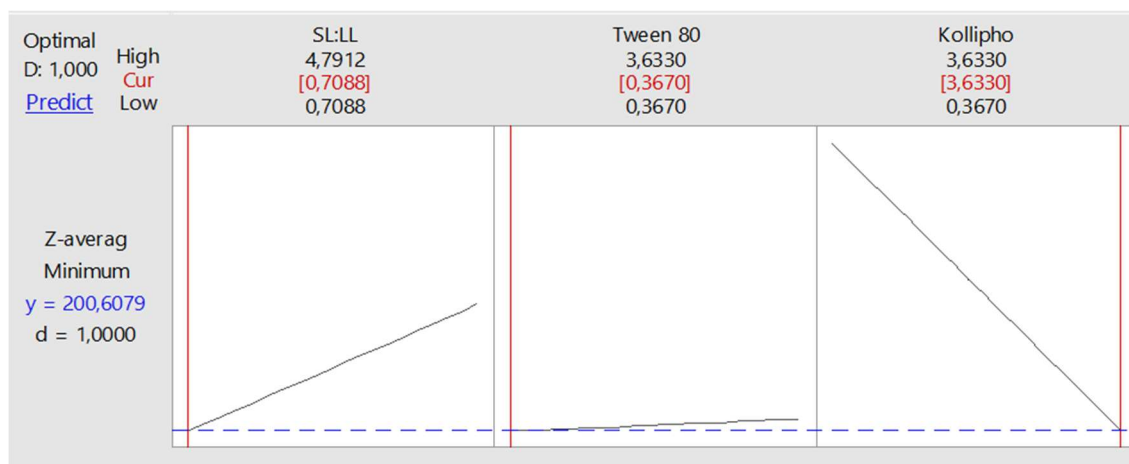


Figure 2.7. Profile for predicted values and desirability function of the F2 z-average (217 nm), containing the following variables: solid and liquid lipid ratio (SL:LL) at 2.06, Kolliphor® P188 at 3.6% (w/w), Tween 80 at 0.37% (w/w).

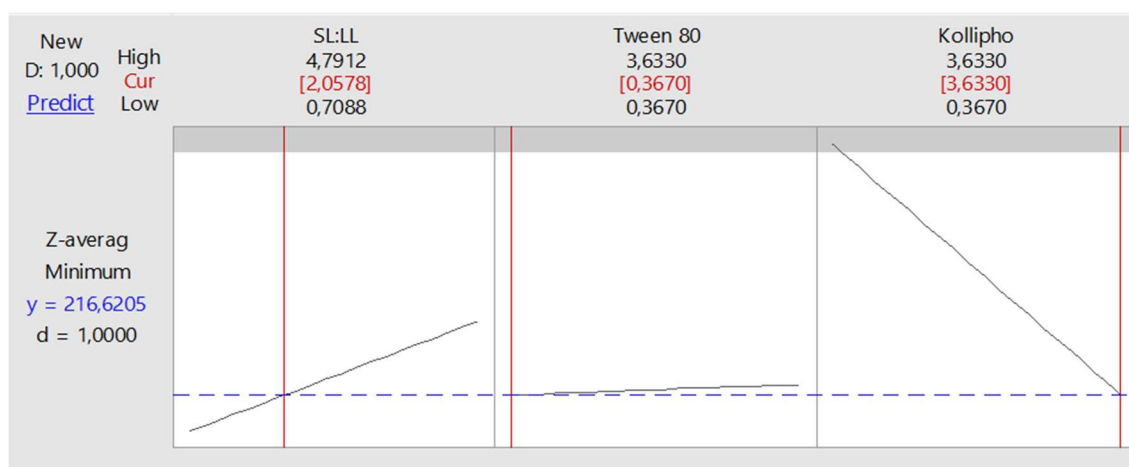


Table 2.7. Observed and predicted z-average, polydispersity index (PDI) and zeta potential (ZP) results from buparvaquone nanostructured lipid carriers

	Observed z-average (nm) ± RSD (%)	Predicted z-average (nm) (α=0.05)	PDI ± RSD (%)	ZP (mV) ± RSD (%)
<b>F1</b>	215.4± 1.7	183.8 to 217.4	0.152±7.6	-20.3± 4.7
<b>F2</b>	231.2± 1.0	200.8 to 232.4	0.136± 4.9	-20.9± 1.0

F1: SL:LL: 0.71; Tween 80: 0.37% (w/w); Kolliphor® P188: 3.63% (w/w); F2: SL:LL: 2.06; Tween 80: 0.37% (w/w); Kolliphor® P188: 3.63% (w/w).



### 2.3.4. Encapsulation efficiency (EE)

Table 2.8 shows the BPQ EEs for three formulations containing 320 (F1), 400 (F3) and 500  $\mu\text{g.mL}^{-1}$  (F4) of BPQ. These formulations were prepared using the same SL:LL ratio and surfactant concentration. They were prepared aiming to increase the drug loading since the structure of the matrix is disorganized by the presence of the liquid lipid and more drug could be accommodated, as reported by Chinsriwongkul and colleagues (2012) and Yuan and colleagues (2007). For these three formulations, the EEs were close to 100%, even in the F4, which was prepared with 156% of calculated drug loading. At the end of 3 months of stability, for all formulations, no drug was precipitated and no significant changes in the EE were found (data not shown).

These findings revealed the role of NLCs for BPQ encapsulation, comparing to SLN and NE. The preparation of SLN would compromise the drug loading and encapsulation efficiency during stability since BPQ has low solubility in solid lipids. The development of NE could increase the drug loading for using only liquid lipid. However, the stability of the nanoparticles and the increasing amount of surfactants, or even a required replacement for more sophisticated and expensive surfactants, such as lecithin, would lead to complex formulations, and consequently, expensive medicines, which is a big concern for neglected diseases.

Table 2.8. Theoretical and observed drug load and encapsulation efficiency of buparvaquone nanostructured lipid carriers

	<b>BPQ theoretical concentration (<math>\mu\text{g.mL}^{-1}</math>) (n=3)</b>	<b>Total observed BPQ concentration (<math>\mu\text{g.mL}^{-1}</math>)</b>	<b>Supernatant BPQ (<math>\mu\text{g.mL}^{-1}</math>)</b>	<b>Encapsulation efficiency (%)</b>
<b>F1</b>	320	312.5 $\pm$ 1.4	0.13 $\pm$ 0.02	99.96 $\pm$ 0.06%
<b>F3</b>	400	403.57 $\pm$ 5.0	<limit of detection	100.00%
<b>F4</b>	500	477.87 $\pm$ 1.9	0.06 $\pm$ 0.01	99.99 $\pm$ 0.02%

## 2.4. Conclusions

DSC/TG method revealed BPQ best solubility using Witepsol® E85 and Softisan® 154 as solid lipid. Microscopy supported Softisan® 154 suitability for NLC preparation. Both techniques, in combination, proved to be a powerful and consistent tool to select the appropriate solid lipids in the preformulation studies. The Miglyol® 182 allowed a drug loading up to 0.5 mg/mL due to the high solubility of BPQ (11.55 g.kg<sup>-1</sup>) in this liquid lipid.

The response surface methodology identified the critical surfactants concentration and Softisan® 154 Miglyol® 812 ratios and the interaction between Kolliphor® P188 and Tween® 80. The relationship among these variables, demonstrated by a linear mathematical model, allowed generating a design space. This design space revealed the limits in the variables for the achievement of z-averages at submicron size range.

The developed nanostructured lipid carriers showed low z-averages (<350 nm), polydispersity (<0.3) and encapsulation efficiency close to 100%, even when the BPQ amount was raised 156%, endorsing the ability of the NCL to increase the drug loading of lipid-based nanoparticles.

Thus, these findings showed the successful development of buparvaquone nanostructured lipid carriers, which are promising formulations for the treatment of leishmaniasis. This drug delivery system has the potential to improve the availability of affordable medicines due to the low-cost of raw materials, using technology with well-established reliability, efficacy and scale-up feasibility.

## Chapter 3

**Nanostructured lipid carrier enables oral administration of low water soluble buparvaquone: development by DoE, *in vitro* drug release and cytotoxicity.**

This study was submitted as Lis Marie Monteiro, Raimar Löbenberg, Paulo Cesar Cotrim, Nádia Bou-Chacra. Nanostructured lipid carrier enables oral administration of low water soluble buparvaquone: development by DoE, *in vitro* drug release and cytotoxicity at Journal of Controlled Release.

## Abstract

Leishmaniasis are a neglected tropical parasitic disease, and the most common treatment over the past 60 years has been pentavalent antimonials. However, they have several drawbacks such as the need for parenteral administration, prolonged treatment, and severe toxicity. Buparvaquone (BPQ), a drug used for the veterinary handling of theileriosis, showed promising activity against *Leishmania spp in vitro*. Nevertheless, due to its low aqueous solubility, it has failed in *in vivo* tests. The use of nanotechnologies could increase BPQ solubility and overcome leishmaniasis therapeutic limitations. Therefore, the objectives of this work were development, optimization and physicochemical evaluation of BPQ nanostructured lipid carrier (BPQ-NLC). The preparation was performed by high-pressure homogenization, and  $2^3$  factorial design was applied to evaluate the solid and liquid lipid ratios, surfactant concentration and lipid phase content. Two optimized formulations were prepared using the mathematical model, V1 of  $173.9 \pm 1.6$  nm and V2 of  $232.4 \pm 1.6$  nm. Cytotoxicity was evaluated in mouse peritoneal macrophages. Optimized formulations showed solubility improvement from 1.5-fold to 611-fold when compared with free BPQ, depending on the media tested. Dissolution profiles in phosphate buffer pH 7.4 with tween 80 0.07% revealed the suitability of the formulations when pancrelipase was present. The V1 release could reach 83.29% of a 4mg dose in 30 minutes, while the free drug could be dissolved only 2.89% of the same dose after 4 hours. Cytotoxicity test showed the safety of V1 which has the higher amount of surfactant. Therefore, the BPQ-NLC is a promising alternative for the treatment of leishmaniasis. Additionally, they have potential use for lymphatic targeted drug delivery, which can be an innovative approach.

Keywords: Buparvaquone, Nanostructured Lipid Carrier, Leishmaniasis, Neglected Diseases.

### 3.1. Introduction

Leishmaniasis are among the leading neglected tropical diseases (NTDs) responsible for the second highest number of deaths due to parasitic infection worldwide. They are highly associated with poverty (COSTA et al., 2011) and prevalent in 98 countries, in three of the five continents. Around 1.3 million new cases occurred annually, and the likely number of deaths from visceral leishmaniasis ranges from 20,000 to 50,000 per year (WHO, 2015).

As an obligate intracellular parasite, *Leishmania* is protected from conventional chemotherapy, which is not readily diffuse through the host cellular membrane. The pentavalent antimonials such as meglumine antimoniate or sodium stibogluconate drug substances have persisted as the first line of treatment for more than 60 years, with a success rate varying between 60% and 80%. Thereby, the therapy for the visceral leishmaniasis requires hospitalization for monitoring the severe adverse effects due to the parenteral administration of large and repeated doses of antimonials, during 20 to 40 days. (COSTA LIMA et al., 2012).

Meeting the leishmaniasis therapy needs, the development of nanostructured delivery systems is one of the most promising alternatives to conventional antimicrobial treatments. The nanoformulations advantages include enhancement of the solubility of poorly water-soluble drugs, allow the development of modified and site-specific drug delivery systems, which increase the therapeutic efficacy and reduce the toxicity of the therapy. (KOBETS et al., 2012; TIUMAN et al., 2011).

It is well known that the lymphatic system (LS) is involved in the development and spread of leishmaniasis (REUS et al., 2005; CARVALHO et al., 2013; LAURENTI et al., 2013). After the vector bite, parasites are dispersed through the vascular and lymphatic systems, infecting phagocytic cells (WASAN et al., 2010). The LS is involved in the absorption of lipids and lipophilic compounds from intestines and their transportation to the systemic circulation by the extensive LS drainage network (YÁÑEZ et al., 2010; KALEPU, MANTHINA, PADAVALA, 2013). Due to this mechanism, lipid nanoparticles can promote oral absorption of the encapsulated drugs via selective lymphatic uptake (CHARMAN, 2000; HOLM et al., 2002; PORTER, CHARMAN, 2001) and direct these drugs and lipids to spleen and liver. Therefore, the drug delivery systems targeted to lymphatic structures is a novel approach for

leishmaniasis treatment and should be explored to develop new effective and safe pharmaceutical dosage forms.

Among the nanostructured lipid systems, NLC In the recent past, biocompatible lipids have attracted the attention of formulation scientists as vehicles for release systems of poorly water-soluble drugs (DAS, NG, and TAN, 2012). These carriers have been introduced as alternatives to traditional colloidal carriers, such as liposomes and polymer nanoparticles, due to improved physical and chemical stability, the feasibility of industrial scale and lower cost of raw materials, especially compared to phospholipids (CIRRI et al., 2012).

As part of a program to discover new drugs for the treatment of leishmaniasis, a series of hydroxynaphthoquinones were tested against *Leishmania donovani*. In *in vitro* experiments, buparvaquone (BPQ) showed 100-fold increased activity against amastigotes compared to other hydroxynaphthoquinones (VEXENAT et al., 1998). However, in dogs infected with *L. (L.) infantum*, the negligible effect was observed. The aqueous solubility of buparvaquone is very low ( $<1 \text{ mg.L}^{-1}$ ) and therefore, it is poorly soluble in biological media, such as gastric and interstitial fluids, which explains its low bioavailability and limited *in vivo* efficacy (REIMÃO et al., 2012).

In this work, we show the development of nanostructured lipid carriers for BPQ encapsulation aiming lymphatic site-specific drug delivery, their physicochemical evaluation, *in vitro* drug release and *in vitro* leishmanicidal activity.

## **3.2. Material and Methods**

### **3.2.1. Materials**

Softisan® 154, was kindly donated by CREMER Oleo Division (Germany) and glyceryl monocaprylate, medium chain triglycerides (MCT) were kindly donated by Abitec (USA). Kolliphor® P188 was acquired from BASF (Germany) and Tween 80 from MilliporeSigma (Germany). Culture medium M199 and RPMI 1640, MTT reagent (3-(4,5-dimethylthiazol-2-yl)-2,5-diphenyl tetrazolium bromide) were purchased from MerckSigma (Germany). Pancreatin was obtained from MerckSigma (Germany). Purified water was obtained by Milli-Q system from Merck Millipore (Germany).

Organic solvents were HPLC grade, and all other chemicals used were of the at least analytical grade.

### **3.2.2. Analytical method for buparvaquone quantification by HPLC**

The HPLC method was described by Monteiro et al. (2017). Briefly, column Licrospher 100 RP8 100 x 4.6 mm endcapped, particle size five  $\mu\text{m}$  (Merck KGaA, Frankfurt, Germany). Mobile phase of 1.0% (v/v) glacial acetic acid, acetonitrile and methanol (25:65:10), 35 °C column temperature, 50  $\mu\text{L}$  injection volume and UV detection  $\lambda=252\text{ nm}$ .

### **3.2.3. Development of BPQ-NLC by factorial design**

After the lipids selection described by Monteiro and colleagues (2017), the buparvaquone nanostructured lipid carrier (BPQ-NLC) formulations were prepared by dispersing the heated lipid phase in the aqueous phase (70 °C). Pre-homogenization was performed using high-performance disperser (8.000 RPM for 5 min) (T25 digital ULTRA-TURRAX, IKA, Staufen, Germany). Afterward, the emulsion was passed through a high-pressure homogenizer (Nano DeBEE 45-2, Bee International, South Easton, MA, USA) at 600 bars for five cycles. The solid lipid, liquid lipid, and the surfactant were Softisan 154, MCT (capric/caprylic triglyceride) (1:2) and poloxamer 188, respectively.

Full factorial  $2^3$  design, with three center points, was carried out to evaluate the influence liquid to solid lipid ratio, surfactant concentration, and lipid phase amount in Z-average, aiming to define the optimal conditions of the formulation. The design matrix describes the order and the amount of materials used in the experiments. The levels of 0.5 (-1), 1.75 (0) and 3 (+1) were defined for the ratio of solid and liquid lipids (SL:LL), 1.0 (-1), 2.5 (0), 4.0 (+1) % w/w for poloxamer 188 and 5.0 (-1), 10.0 (0), 15.0 (+1) % w/w for lipid phase. Minitab 17 software was used to define the matrix and statistical analysis.

The mathematical model was verified by preparation of two formulations predicted by the model. Formulation V1 was prepared with 4.0% of poloxamer, SL:LL of 0.5, % lipid phase of 5.0% w/w. Formulation V2 was prepared with 3.0% of

poloxamer, SL:LL of 0.5 and % lipid phase of 15.0% w/w. Also, these two formulations were considered optimized formulations because of their Z-average < 300 nm, PDI<0.3 and monomodal particle size distribution.

#### **3.2.4. Determination of the Z-average, polydispersity index, particle size distribution and zeta potential**

The Z-average, polydispersity index, particle size distribution and zeta potential of BPQ-NLC were determined immediately after homogenization and periodically for stability study. The method was photon correlation spectroscopy (PCS) using Zetasizer Nano ZS90 (Malvern Instruments, Malvern, UK) at 25 °C and 90 °C angle (n = 10). The measurements were carried out in purified water (n=3), with conductivity adjusted to 50  $\mu\text{S.cm}^{-1}$ , by the addition of NaCl 0.1% w/v, aiming to avoid fluctuations in ZP caused by the changes in conductivity. The pH was adjusted to  $6.5 \pm 0.2$  by the addition of 0.01 M HCl or 0.01 M NaOH solution.

#### **3.2.5. Drug loading and encapsulation efficiency (%EE)**

Buparvaquone was quantified by HPLC method described in item 3.2.2. The drug loading samples were prepared as follow: nanoparticle aliquots were diluted to a volumetric flask to a BPQ concentration of 0.005  $\text{mg.mL}^{-1}$  and diluted with mobile phase. The final preparations were filtered with PVFD membrane, 0.45  $\mu\text{M}$  of pore size. Each formulation was evaluated in replicates of three.

The samples for %EE of not encapsulated BPQ, namely as supernatant, were prepared as follow: an aliquot of each formulation was placed in EMD Millipore Amicon™ centrifuge filter units, 100 Kd MWCO. The samples were centrifuged at 20 °C, 14000 g, for 30 minutes. The formulations were evaluated in replicates of three and the %EE was calculated as Equation 3.1:

$$\%EE = \frac{\text{drug loading (mg.mL}^{-1}) - \text{supernatant BPQ (mg.mL}^{-1})}{\{(\text{drug loading (mg.mL}^{-1})\}} \times 100 \quad \text{Equation 3.1}$$



### **3.2.6. BPQ-NLC morphology by transmission electron microscopy (TEM)**

Images were acquired using a Morgagni 268 transmission electron microscope with Gatan Digital Camera (Philips/FEI, Hillsboro, Oregon, USA). The samples were diluted in purified water in the ratio of 1:20. The diluted samples were placed over regular TEM grids and allowed to set for 15 seconds. The background was stained with phosphotungstic acid solution 10.0 % w/v (Sigma-Aldrich, St. Louis, Missouri, USA) for additional 15 seconds.

### **3.2.7. BPQ-NLC stability testing**

Right after high-pressure homogenization, formulations were stored at  $8 \pm 2^\circ \text{C}$ , in 8 mL clear glass vials. Drug loading, encapsulation efficiency, Z-average, particle size distribution and PDI were evaluated for six months, in replicates of three.

### **3.2.8. Free BPQ and BPQ-NLC solubility evaluation**

Free BPQ and BPQ-NLC solubility were evaluated in the following media: pH 1.2; 4.5; 6.8; 7.2; 7.4; 7.8 prepared accordingly to USP 32. FeSSIF and FaSSIF prepared as Jogia and colleagues (2014). Phosphate buffer 0.05 M pH 7.4 and dodecyl sodium sulfate 0.1%; 0.5%, 1.0% w/v. Phosphate buffer 0.05M (pH 7.4) and Tween 80 0.07% w/v. After 24 hours of shaking at  $37^\circ \text{C}$ , the samples were filtered with PVDF 0.1  $\mu\text{m}$  pore size membrane and diluted with mobile phase at least 2-fold. The quantification was performed as described in item 3.2.2.

### **3.2.9. Free BPQ and BPQ-NLC dissolution profiles**

The media were: phosphate buffer 0.05M pH 7.4 with Tween 80 0.07% w/v, phosphate buffer 0.05M pH 7.4 with sodium dodecyl sulfate 1.0% w/v, with or without pancrelipase, according to USP 32 monograph for fenofibrate capsules (0.1% w/v). The final method was: medium volume of 900 mL, apparatus II (paddle), 50 rpm, a sample volume of 2.0 mL, with media replacement. The samples were filtered with a

saturated membrane of PVDF 0.1  $\mu$ M pore size and diluted with mobile phase at least 3-fold. For each formulation and medium, the tests were performed in replicates of six. The BPQ quantification was performed as described before in item 3.2.2.

#### **3.2.10. Free BPQ and BPQ-NLC cytotoxicity**

Cell viability was determined by the MTT method (3-methyl- [4-5-dimethylthiazol-2-yl] -2,5-diphenyltetrazolium bromide) as described by Monteiro et al., 2017. Briefly, Mouse peritoneum macrophages were incubated for 24h at 37 °C ( $2 \times 10^5$ ). Increasing concentrations of free BPQ and BPQ-NLC were added to each well. After 24 hours, MTT solution was added, and the plate was incubated at 37 °C, 5% CO<sub>2</sub>, 95% RH, for 4 hours. The optical density was performed in ELISA plate reader ( $\lambda$  = 595 nm). Each treatment was evaluated with replicates of six. Cell-free and culture medium containing macrophages were used as a negative and positive control, respectively.

#### **3.2.11. CC<sub>50</sub> and statistical analysis**

The CC<sub>50</sub> value was expressed as the concentration of BPQ when the cell viability reaches 50%, and it was calculated by non-linear regression analysis using GraphPad Prism version 5.01. The p-value of <0.05 was considered statistically significant.

### **3.3. Result**

#### **3.3.1. BPQ-NLC formulation development**

The full 2<sup>3</sup> factorial design was applied for BPQ-NLC formulation development. With this tool, it was possible to evaluate the three variables with only 11 tests, including three replicates from the central point (F11, F9, F10), which can be used to evaluate the intrinsic variability of the process. Table 3.1 shows the design matrix and the experimental results of Z-average, polydispersity and zeta potential for each formulation.

Table 3.1. Experimental design matrix, Z-average (Z-ave), polydispersity index (PDI) and zeta potential (ZP) of buparvaquone nanostructured lipid carrier development.

SO	Level			SL:LL	% POL	% LP	Z-ave (nm)	PDI	ZP (mV)
	SL:LL	%POL	%LP						
<b>F11</b>	0	0	0	1.75	2.5	10.0	231.8	0.164	-22.1
<b>F9</b>	0	0	0	1.75	2.5	10.0	235.5	0.155	-12.8
<b>F8</b>	+1	+1	+1	3.00	4.0	15.0	229.3	0.147	-15.3
<b>F1</b>	-1	-1	-1	0.50	1.0	5.0	239.9	0.158	-20.4
<b>F5</b>	-1	-1	+1	0.50	1.0	15.0	366.9	0.241	-30.6
<b>F4</b>	+1	+1	-1	3.00	4.0	5.0	198.1	0.192	-19.3
<b>F7</b>	-1	+1	+1	0.50	4.0	15.0	208.3	0.164	-24.0
<b>F6</b>	+1	-1	+1	3.00	1.0	15.0	390.6	0.250	-43.7
<b>F10</b>	0	0	0	1.75	2.5	10.0	232.6	0.143	-27.0
<b>F2</b>	+1	-1	-1	3.00	1.0	5.0	267.7	0.223	-28.2
<b>F3</b>	-1	+1	-1	0.50	4.0	5.0	180.6	0.180	-25.3

SL:LL: solid lipid to liquid lipid ratio; SO: standard order; % POL: percentage of poloxamer 188 (w/w); % LP: percentage of lipid phase (w/w).

The most reliable method to evaluate the suitability of the mathematical model is the application of analysis of variance (ANOVA). The ANOVA compares the variation due to the treatment (change in the combination of variable levels) with the variation due to random errors inherent in the measurement of the generated responses. From this comparison, it is possible to evaluate the significance of the regression used to predict responses considering the sources of experimental variation. A model will be well-fitted to the experimental data if it presents a significant regression coefficient and a non-significant lack-of-fit (MYERS, 2009). Table 2 shows the ANOVA analysis from BPQ-NLC development regarding Z-average.

Table 3.2. ANOVA from Z-average data of buparvaquone nanostructured lipid carrier development.

Source	DF	SS (adj)	MS (adj)	F test	p-value
<b>Model</b>	4	42681.4	10670.4	39.80	0.001
<b>Linear</b>	3	38122.9	12707.6	47.40	0.001
<b>SL:LL</b>	1	1011.8	1011.8	3.77	0.100
<b>Poloxamer 188®</b>	1	25188.9	25188.9	93.95	0.001
<b>% lipid phase</b>	1	11922.3	11922.3	44.47	0.001
<b>Two factor interactions</b>	1	4558.5	4558.5	17.00	0.006
<b>Poloxamer 188 *% lipid phase</b>	1	4558.5	4558.5	17.00	0.006
<b>Error</b>	6	1608.6	268.1		
<b>Lack-of-fit</b>	3	28.0	9.3	2.48	0.301
<b>Pure error</b>	2	7.5	3.8		
<b>Total</b>	10	44290.0			

DF: degrees of freedom; SS(adj): the adjusted sum of squares; MS (adj): adjusted mean of squares, SL:LL solid and liquid lipid ratio.

Table 3.3 shows the coded coefficients of the mathematical model from ANOVA. Equation 3.2 shows the uncoded mathematical model for Z-average and Figure 3.1 shows the main effect plots.

Table 3.3. Coded coefficients and goodness-of-fit indexes from the Z-average data of buparvaquone nanostructured lipid carrier development.

Terms	Coefficient	T test	p-value
<b>Constant</b>	252.84	51.21	0.001
<b>SL:LL</b>	11.25	1.94	0.100
<b>%POL</b>	-56.11	-9.69	0.001
<b>% lipid phase</b>	38.60	6.67	0.001
<b>%POL*% lipid phase</b>	-23.87	-4.12	0.006
R <sup>2</sup> : 96.37%    R <sup>2</sup> (adj): 93.95%    R <sup>2</sup> (pred):90.69%			

Goodness-of-fit indexes: R<sup>2</sup>: coefficient of determination; R<sup>2</sup> (adj): adjusted coefficient of determination; R<sup>2</sup> (pred): predicted coefficient of determination of the adjusted model; %POL: poloxamer 188; SL:LL solid and liquid lipid ratio.

### Equation 3.2

$$Z - ave = 173.8 + 9.0 \text{ SL:LL} - 5.6 \%POL + 15.7 \%LP - 3.2 \%POL \times \%LP$$

Z-ave: Z-average (nm); % POL: percentage of Poloxamer 188 w/w; % LP: percentage of lipid phase (w/w).

Figure 3.1. Main effects plots data from buparvaquone nanostructured lipid carrier development (Z-average).

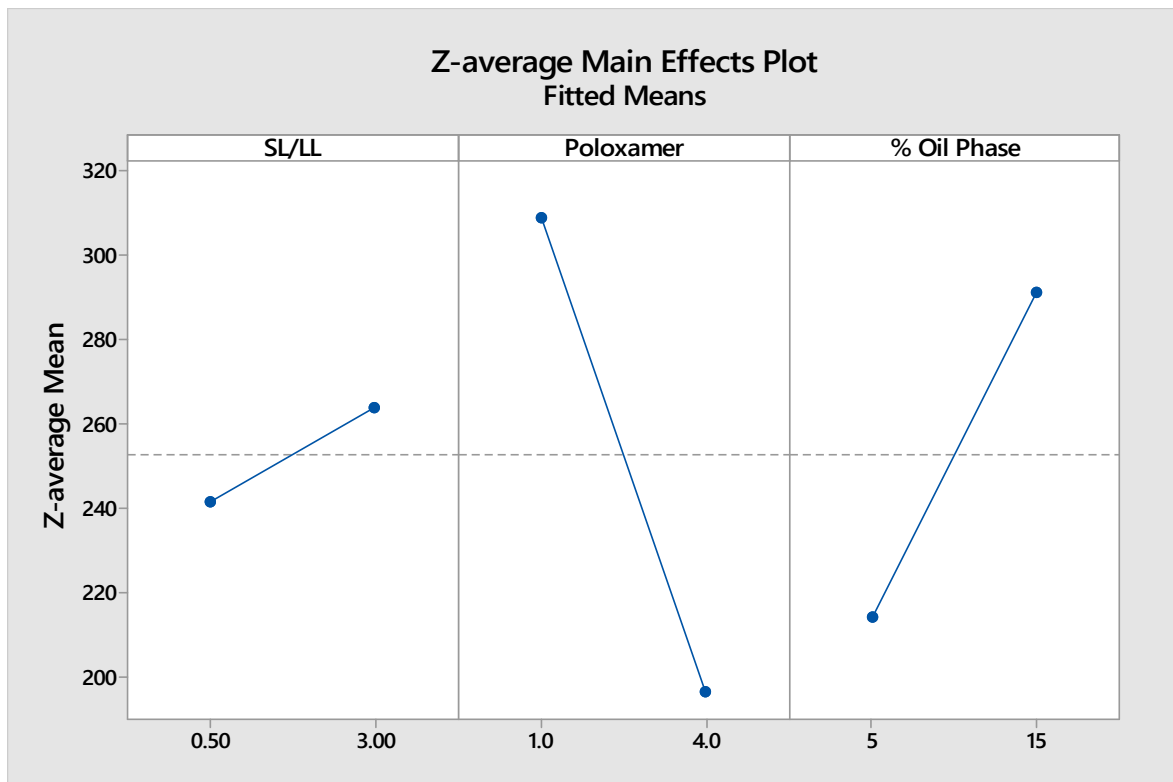
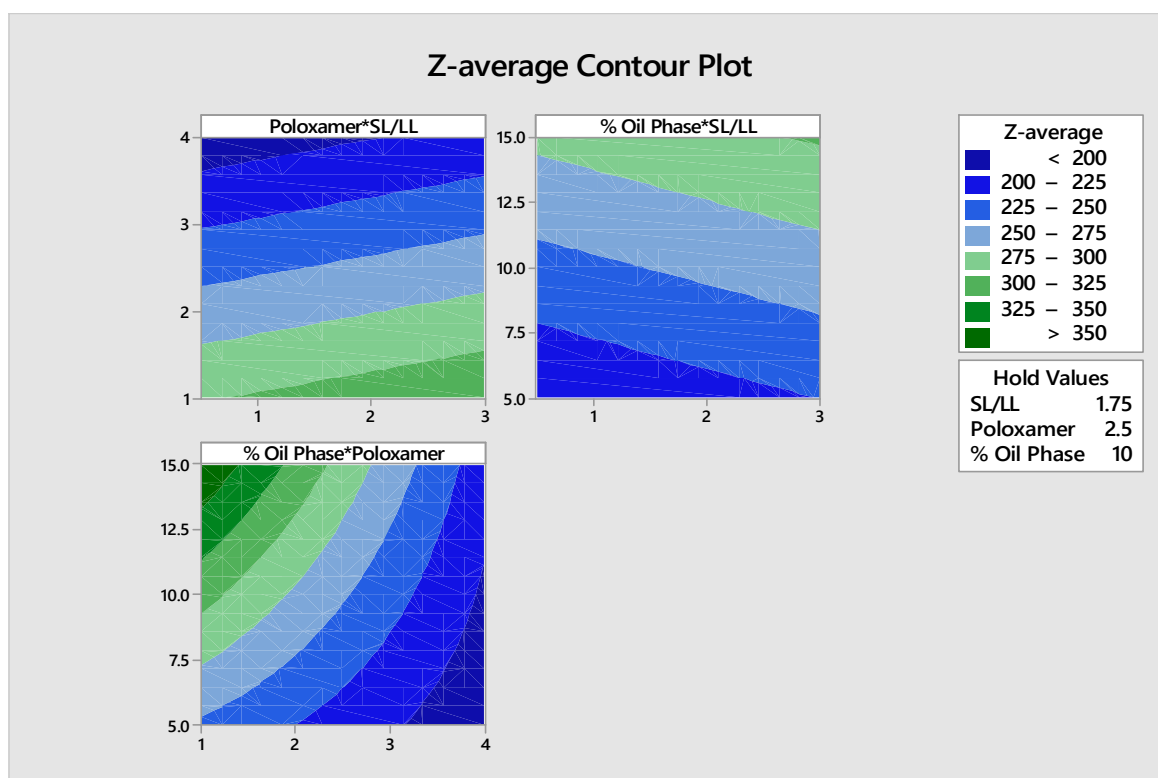


Figure 3.2 shows the contour plots of the Z-average data evaluation. This plot type is useful to observe the behavior of the variables when comparing a pair of them. It is also useful for observing the interactions among the variables.

Figure 3.2. Contour plots from Z-average data evaluation of buparvaquone nanostructured lipid carrier development.



Figures 3.3 and 3.4 show predicted formulations plots, which were used for mathematical model verification. The consistency of the statistical analysis was confirmed by using the model to prepare formulations with optimal Z-average. The observed and theoretical values are predicted to be similar (Table 3.4). The desirability tool was applied to achieve the lower Z-average as possible. Also, another formulation around 230 nm was calculated and prepared to test the model and aimed to yield formulation with higher %lipid phase, consequently, higher drug loading.

Table 3.4. Theoretical and experimental Z-average from formulations for mathematical model verification of buparvaquone nanostructured lipid carrier development

Formulation	Theoretical z-average (nm)	Experimental Z-average (nm)
<b>V1</b>	175.3 (146.6 to 203.9)	173.9±1.6*
<b>V2</b>	253.3 (206.40 to 300.2)	232.4±1.6

Theoretical Z-average range for confidence interval of 95%; V1: formulation (SL:LL=0.5 w/w;% lipid phase: 5.0% w/w; poloxamer 188= 4 % w/w); V2: formulation (SL:LL= 0.5 w/w; % lipid phase: 15.0% w/w; poloxamer 188= 3.0% w/w).

Figure 3.3. Profile for predicted values and desirability function of the V1 Z-average (185.6 nm), containing the following variables: solid and liquid lipid ratio (SL:LL) at 1.0, poloxamer 188 at 4.0% w/w and lipid phase at 5.0% w/w.

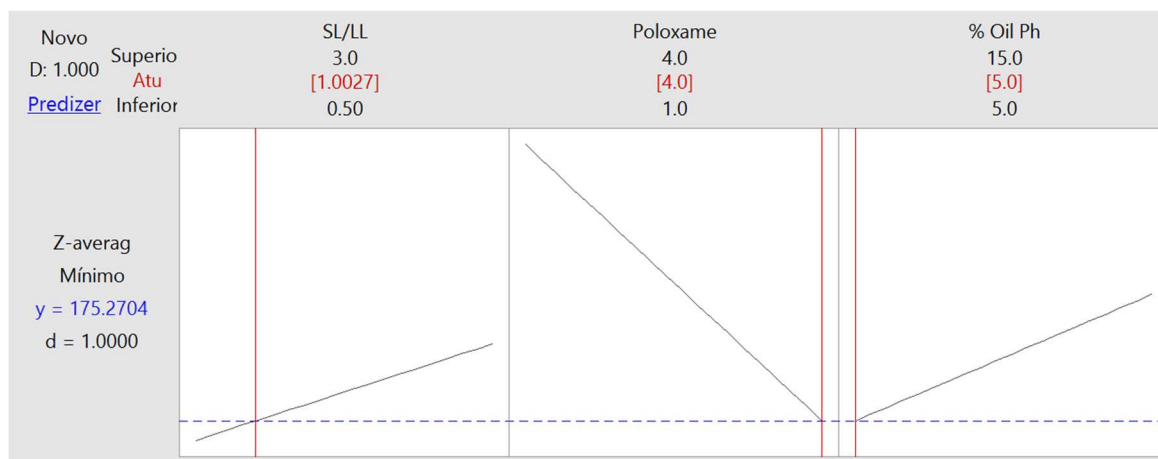
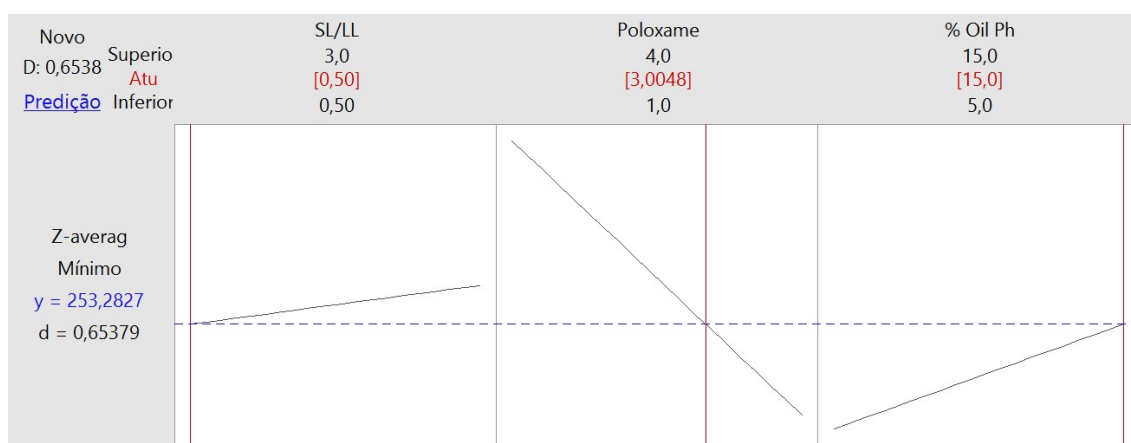


Figure 3.4. Profile for predicted values and desirability function of the V2 Z-average (232.4 nm), containing the following variables: solid and liquid lipid ratio (SL:LL) at 0.5, poloxamer 188 at 3.0% w/w and lipid phase at 15.0% w/w.



### 3.3.2. Determination of the Z-average, polydispersity index and particle size distribution

Table 3.4 shows the values for Z-average, both formulations showed monomodal size distribution. Regarding PDI, for V1, it was  $0.164 \pm 0.005$ , and for V2, it was  $0.132 \pm 0.007$ .

### 3.3.3. Drug loading and encapsulation efficiency (%EE)

Table 3.5 shows the values for drug loading and encapsulation efficiency for V1 and V2.

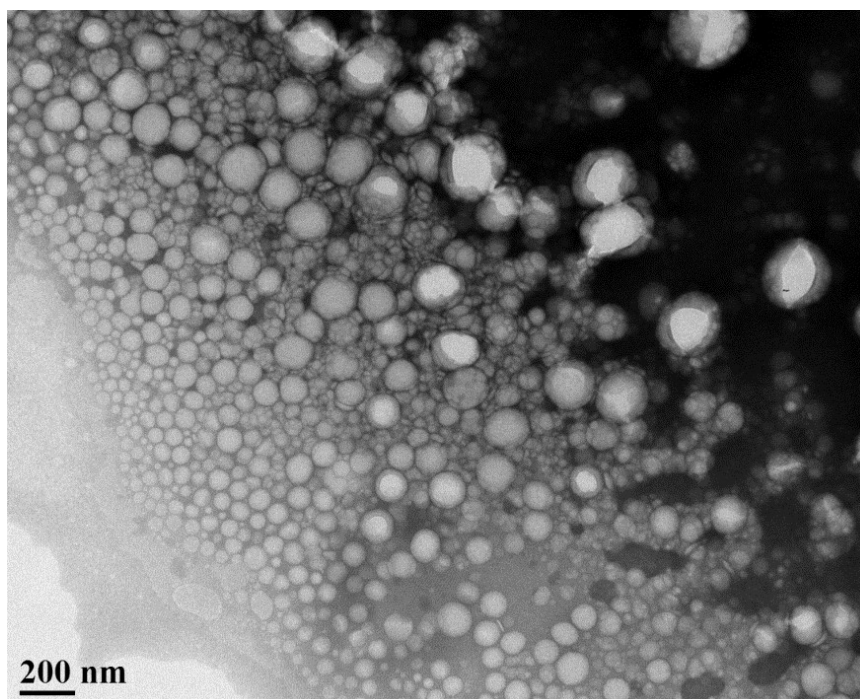
Table 3.5. Drug loading and encapsulation efficiency of V1 and V2 formulations from nanostructured lipid carrier development.

	<b>Drug loading (<math>\mu\text{g.mL}^{-1}</math>)</b>	<b>Supernatant (<math>\mu\text{g.mL}^{-1}</math>)</b>	<b>%EE</b>
<b>V1</b>	505.4 $\pm$ 10.8	1.40 $\pm$ 1.6	99.72 $\pm$ 0.32
<b>V2</b>	1393.5 $\pm$ 43.2	1.0 $\pm$ 0.1	99.93 $\pm$ 0.09

### 3.3.4. BPQ-NLC morphology by transmission electron microscopy

The BPQ-NLC morphology was evaluated at the fifth month of stability testing, the Z-average from the particles was slightly different from the initial determination. Figure 3.5 shows the morphology of V1 formulation by transmission electron microscopy.

Figure 3.5. Transmission electronic microscopy from formulation development V1: Z-average of 175.1 nm. Magnification 36kx.





### 3.3.5. BPQ-NLC Z-average and polydispersity index stability testing

Table 3.8 shows the values of Z-average (nm) and particle size distribution of V1 and V2 stability testing.

Table 3.6. Z-average (nm) and particle size distribution of V1 and V2 formulations from stability testing.

	Month				
	0	2	3	5	6
<b>V1</b>	173.9±1.6*	171.8±0.6*	173.9±1.7*	175.1±1.6*	178.8±6.2*
<b>V2</b>	232.4±1.6*	236.6±2.7*	237.9±12.3*	230.7±2.0*	239.8±10.4** (2 <sup>nd</sup> peak at 5µm)

Storage conditions: 8 ± 2°C, 8 mL clear glass vials, n=3. \* monomodal particle size distribution;

\*\* bimodal particle size distribution.

Regarding polydispersity index, the values of the stability testing are presented in Table 3.9.

Table 3.7. Polydispersity index stability test of V1 and V2 formulations from nanostructured lipid carrier development.

	Month				
	0	2	3	5	6
<b>V1</b>	0.164±0.005	0.144±0.033	0.133±0.031	0.122±0.011	0.147±0.032
<b>V2</b>	0.132±0.007	0.215±0.046	0.155±0.020	0.151±0.029	0.187±0.033

Storage conditions: 8 ± 2°C, 8 mL clear glass vials, n=3.

### 3.3.6. BPQ-NLC drug loading and encapsulation efficiency stability testing

Table 3.8 and 3.9 show the drug loading, supernatant BPQ content and encapsulation efficiency (%EE) of V1 and V2, respectively.

Table 3.8. Drug loading and encapsulation efficiency (%EE) stability test of V1 formulation from nanostructured lipid carrier development.

Month	Drug loading ( $\mu\text{g.mL}^{-1}$ )	Supernatant ( $\mu\text{g.mL}^{-1}$ )	%EE
0	505.4 $\pm$ 10.8	1.40 $\pm$ 1.6	99.72 $\pm$ 0.32
2	497.7 $\pm$ 7.7	3.26 $\pm$ 3.8	99.34 $\pm$ 0.77
4	495.3 $\pm$ 2.5	3.75 $\pm$ 4.5	99.24 $\pm$ 0.91
6	492.0 $\pm$ 7.2	0.53 $\pm$ 0.8	99.89 $\pm$ 0.16

Storage conditions: 8 $\pm$ 2°C, 8 mL clear glass vials. SD: standard deviation (n=3)

Table 3.9. Drug loading and encapsulation efficiency (%EE) stability test of V2 formulation from nanostructured lipid carrier development.

Month	Drug loading ( $\mu\text{g.mL}^{-1}$ )	Supernatant ( $\mu\text{g.mL}^{-1}$ )	%EE
0	1393.5 $\pm$ 43.2	1.0 $\pm$ 0.1	99.93 $\pm$ 0.09
2	1349.7 $\pm$ 38.0	0.5 $\pm$ 0.4	99.96 $\pm$ 0.03
4	1349.7 $\pm$ 47.9	2.7 $\pm$ 6.5	99.81 $\pm$ 0.046
6	1351.8 $\pm$ 56.5	2.2 $\pm$ 2.7	99.84 $\pm$ 0.20

Storage conditions: 8 $\pm$ 2°C, 8 mL clear glass vials. SD: standard deviation (n=3)

### 3.3.7. BPQ-NLC solubility evaluation

The solubility test was performed to evaluate the impact of pH and surfactant in the solubility behavior. Also, the data was used to select the suitable media for dissolution test. The values of solubility of free drug and BPQ-NLC are shown in Table 3.12.

Table 3.10 Solubility of buparvaquone (BPQ), and V1 and V2 formulations from nanostructured lipid carrier development.

<b>BPQ solubility (<math>\mu\text{g}.\text{mL}^{-1}</math>)</b>	<b>Free BPQ</b>	<b>V1</b>	<b>V2</b>
<b>Simulated gastric fluid pH 1.2</b>	0.05 $\pm$ 0.01	3.57 $\pm$ 1.72	3.64 $\pm$ 2.20
<b>Phosphate buffer pH 4.5</b>	0.06 $\pm$ 0.04	3.30 $\pm$ 0.98	2.78 $\pm$ 0.90
<b>Phosphate buffer pH 6.8</b>	0.08 $\pm$ 0.02	2.82 $\pm$ 1.41	2.77 $\pm$ 3.05
<b>Phosphate buffer pH 7.4</b>	0.19 $\pm$ 0.10	12.62 $\pm$ 1.52	2.16 $\pm$ 0.65
<b>Fed state simulated intestinal fluid pH 5.0 (FeSSIF)</b>	12.53 $\pm$ 1.85	24.98 $\pm$ 2.04	25.56 $\pm$ 1.12
<b>Fasted state simulated intestinal fluid pH 4.0 (FaSSIF)</b>	3.39 $\pm$ 0.24	26.30 $\pm$ 2.66	2.28 $\pm$ 0.85
<b>SBF – simulated body fluid</b>	0.02 $\pm$ 0.01	12.22 $\pm$ 6.53	15.32 $\pm$ 12.36
<b>Buffer pH 7.4 with sodium dodecyl sulfate 1.0% w/w</b>	11.68 $\pm$ 0.78	37.74 $\pm$ 10.66	17.08 $\pm$ 4.50
<b>Buffer pH 7.4 with tween 80 0.07% w/w</b>	3.39 $\pm$ 0.30	15.31 $\pm$ 7.05	9.19 $\pm$ 2.02

### 3.3.8. Free BPQ and BPQ- NLC dissolution profiles

Reimão and colleagues (2012) prepared BPQ liposomes and tested against *L. infantum*. They found that an intraperitoneal dose of 0.33 mg.kg<sup>-1</sup>.day<sup>-1</sup> for eight days reduced the number of amastigotes by 89.4% in the spleen and by 67.2% in the liver. However, 20 mg.kg<sup>-1</sup>.day<sup>-1</sup> of free BPQ failed to treat the hamsters. Considering the effectiveness of the BPQ-NLC at least as the same as liposome formulation, the HED (human equivalent dose) was calculated as described by FDA (2005) and Nair and Jacob (2016). The dose of 0.33 mg.kg<sup>-1</sup>.day<sup>-1</sup> was divided by 7.4 (hamster to human),

which results in a HED of  $0.045 \text{ mg.kg}^{-1}.\text{day}^{-1}$ . Considering 70 kg an average human weight, the daily dose would consist of 3.15 mg. However, the dose was increased to 4mg, when dissolution method for oral dosage, as depicted in Figure 3.6 and 3.7.

Figure 3.6. Dissolution of free buparvaquone (BPQ) (black circles) and formulations V1 and V2 with (grey triangles) and without (black circles) pancrelipase, containing 4 mg of BPQ; using USP II apparatus (900 mL phosphate buffer pH 7.4 0.05M, tween 80 0.07% w/v), 50 rpm, 37 °C. (A) V1 Z-average: 175.1 nm. (B) V2 Z-average: 230.7 nm.

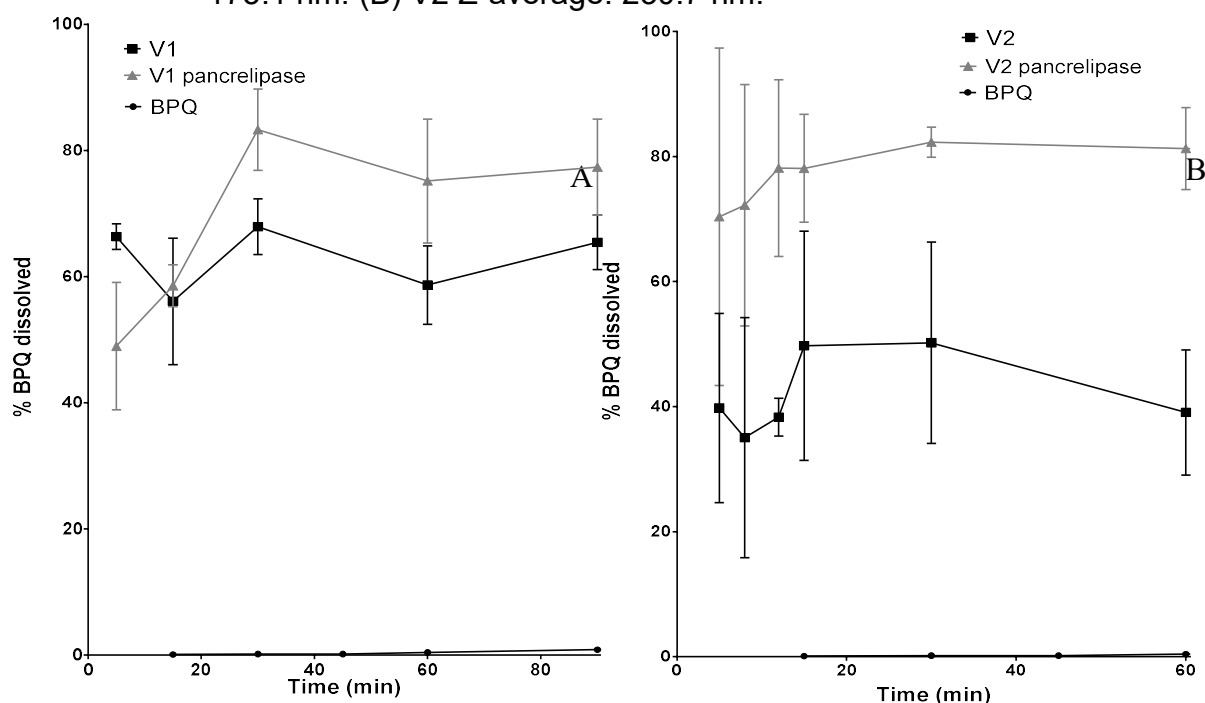
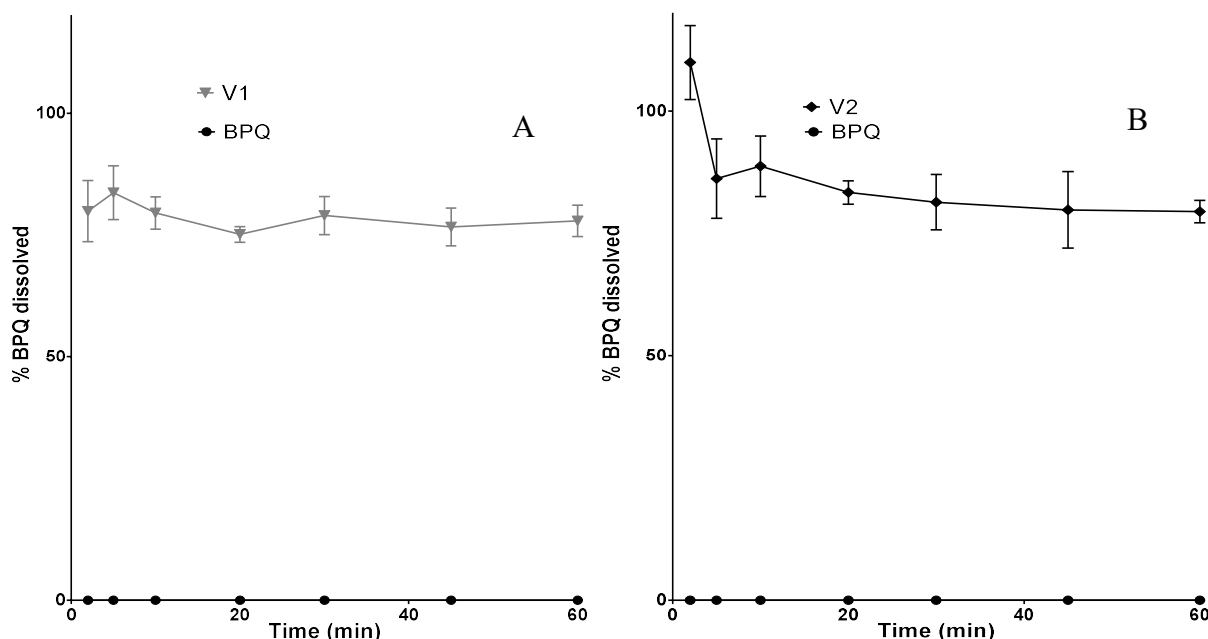


Figure 3.7. Dissolution of free buparvaquone (BPQ) (black circles) and formulations V1 and V2 containing 4 mg of BPQ; using USP II apparatus (900 mL phosphate buffer pH 7.4 0.05 M, sodium dodecyl sulfate 1.0% w/v), 50 rpm, 37 °C. (A) V1 Z-average: 175.1 nm (gray inverted triangle). (B) V2 Z-average: 230.7 nm. (black diamond).



### 3.3.9. Free BPQ and BPQ- NLC cytotoxicity

The cytotoxicity of BPQ and BPQ-NLC were accessed by MTT using peritoneal mouse macrophages. Free BPQ CC50 was 554.4  $\mu$ M (252.2 to 1090), and for V1, it was 583.4  $\mu$ M (362.6 to 938.6).

## 3.4. Discussion

### 3.4.1. BPQ-NLC formulation development

All the formulations presented Z-average lower than 300 nm, except the F4, which was prepared with the highest lipid phase content (15.0% w/w) and lowest concentration of the surfactant (1.0% w/w). Regarding the PDI, even for F4, the results were lower than 0.3, which shows a narrow particle size distribution (IBRAHIM,

ALOMRAN, and YASSIN, 2014; KASHANIAN, AZANDARYANI and DERA KHSHANDEH, 2011).

In ANOVA, when p-values are lower than 0.05, the obtained models are statistically significant, which demonstrates that the terms in the model have essential effects on the responses. When adjusted- $R^2$  and  $R^2$  differ dramatically, there is a good chance that non-significant terms were included in the model (TRINH and KANG, 2011). For the Z-average evaluation, the two values of  $R^2$  were similar. Therefore, for Z-average, the global first order model, as expressed in Equation 1, is significant and suitable. Also, the predicted- $R^2$  also does not differ substantially from the values of  $R^2$  and adjusted- $R^2$ . The observed value higher than 0.8 indicates the high probability of predicted values calculated by the model being close to the experimental values, that is, the mathematical model can be used for the optimization of the process with a substantial chance of reaching the desired results.

The higher content of poloxamer, the lower the Z-average because of the negative value of the coefficient (-56.11). Additionally, there was an interaction between the % lipid phase and poloxamer 188 (significant p-value <0.05), which favors the achievement of lower values for the response due to its negative value (-23.87). Even though the coefficient from SL:LL (p-value>0.05) was no significant, the removal of this term led to lower  $R^2$  coefficients, which implies that the changes in the SL:LL does not have a significant impact in the Z-average. Nevertheless, it is still part of the model. It can be seen in the Equation 3.1 that the term SS:LL was included. Therefore, the p-values are one piece of information, and all the available models should be compared regarding  $R^2$  coefficients for finding the most suitable one since valuable information can be lost by automatically removing terms that aren't significant.

Figure 3.2 shows the main effects plots, the variable SL:LL illustrates the no-significant p-value from the model using the levels of 0.5 (-1), 1.75 (0), 3.0 (+1), there is the low impact of this term in the Z-average. The plot from poloxamer 188 shows the effect of this variable, the higher poloxamer 188 concentration, the lower is the Z-average. The opposite behavior is depicted in the % lipid phase plot.

The plot % lipid phase and poloxamer 188 shows the nonlinear relationship between them (interaction). Observing the plot % lipid phase versus poloxamer, nanoparticles with Z-average lower than 220 nm can be achieved with a combination of lipid phase lower than 10.0% and poloxamer 188 higher than 3.5%. From the plot %

lipid phase versus SL:LL is possible to observe the low impact of SL:LL, when the % lipid phase is lower than 7.5% this variable, can change from 0.5 to 3, but the Z-average only changes from 200 to 225 nm. The absence of the <200 nm zone from this plot indicates that nanoparticles in this range are only possible to prepare when poloxamer 188 is above 2.5%.

Regarding the mathematical model verification and NLC optimization, experimental Z-average for both formulations presented Z-average in the range of the model, with a confidence interval of 95%. Also, the result for PDI was considered suitable (<0.3), indicating a narrow distribution of the particles. Therefore, the V1 and V2 confirmed the mathematical model suitability and was considered two optimized formulations due to low Z-average, low PDI, and monomodal distribution.

#### **3.4.2. BPQ-NLC morphology by transmission electron microscopy**

Figure 3.5 shows the morphology of V1 (175.1 nm). It was possible to confirm the round shape of the particles and size distribution compatible with the PCS results. This field showed a high number of nanoparticles. However, they kept their round shape and individuality. It can be explained by the gelling phenomena of the poloxamer 188, which can cover the particle with a robust physical barrier.

#### **3.4.3. BPQ-NLC Z-average polydispersity index stability testing**

Z-average of V1 did not change significantly during the six months, the variation is within the confidence interval for the method, and the monomodal particle size distribution was observed during the entire stability test. For V2, in the sixth month, the particle size distribution changed to bimodal, with a second peak around 5  $\mu\text{m}$  with 5% of total intensity, which indicates aggregation of the system. However, this aggregation did not have an impact in the Z-average, it is possible that a small number of particles were compromised.

Regarding polydispersity index, the values of the stability testing for both formulations were stable. Even for V2, the PDI did not increase, which indicates that the aggregation after six months occurred in a low fraction of particles.

#### **3.4.4. BPQ-NLC drug loading and encapsulation efficiency stability testing**

The %EE from V1 was near 100% and did not change over the six months stability testing. Due to the results of %EE and drug loading, V1 has a potential behavior for the development of a liquid formulation. Regarding V2, it showed EE% near 100% at all points, which strengthened the suitability of nanostructured lipid carrier for BPQ.

#### **3.4.5. BPQ-NLC solubility evaluation**

In both, the formulations BPQ was more soluble than the free drug. In media without surfactant, BPQ showed a rise in the solubility when the pH is above 6.8. The solubility was slightly increased from 0.05 to 0.08  $\mu\text{g.mL}^{-1}$  when the pH was changed from 1.2 to 6.8, but when the media was altered to pH 7.4, the BPQ solubility was 0.19  $\mu\text{g.mL}^{-1}$ . This behavior is consistent within simulated solubility versus pH profiles, as obtained from Chemaxon calculator.

Regarding the use of nanoparticles for oral administration, phosphate buffer pH 7.4 with 1.0% w/v of sodium dodecyl sulfate was tested to simulate fed condition and phosphate buffer pH 7.4 with Tween 80 0.07%w/v to simulate fasted condition since BPQ showed similar solubility in these media.

#### **3.4.6. BPQ- NLC dissolution profiles**

Free BPQ dissolution at phosphate buffer pH 7.4 0.05M with tween 80 0.07% w/v can be seen in Figure 3.10. Even after four hours, only 2.89% of 4.0 mg of free drug was dissolved, which means that the drug did not reach the solubility (3.39  $\mu\text{g.mL}^{-1}$ ) in this media. For sink conditions considering the BPQ solubility, one dose should be only 0.12 mg for 900 mL of medium or the volume should be 36 liters for a 4.0 mg dose. Even using an open-loop flow-through cell apparatus, this volume would not be feasible.

During the dissolution method development, the pancrelipase was tested to simulate the nanoparticle degradation from intestinal lipases. This media was chosen



due to the low content of surfactants, which could disrupt the nanoparticle structure and the effect of pancrelipases could be reduced.

Regarding V1 dissolution profile without pancrelipase, the drug release could reach 65.43% of the 4.0 mg drug dose after 90 minutes. Profile assessed with the use of the enzyme, the dissolution could reach 77.34%. However, it is important to note the drug precipitation of this formulation in this medium. After 30 minutes, the dissolution with and without lipase was 67.93% and 83.29%, respectively.

Formulation V2 had almost the same behavior as V1, but the increase of the BPQ dissolution was more prominent with pancrelipase. In this medium, after 60 minutes, 81.25% of the 4.0 mg dose was dissolved. As found for V1, in medium without enzyme, the drug started to precipitate after 30 minutes. The dissolution was 50.21% at 30 minutes point, and 60 minutes, it was only 39.07%.

Regarding the dissolution profiles using phosphate buffer pH 7.4 0.05M with sodium dodecyl sulfate 1.0% w/v, pancrelipase was tested, but no significant difference was found ( $p < 0.05$ ). From V1, the drug release could reach 83.71% at 5 minutes of the test, although some precipitation was found at 20 minutes, the dissolution at the end of the test (60 minutes) was 75.12%. The extent of the precipitation and variation among the samples (standard deviation) were minimized when comparing with phosphate buffer pH 7.4 0.05M with tween 80 0.07% w/v. The dissolution from V2 could reach 79.84% of 4.0 mg drug dose after 60 minutes, and as found from V1, the precipitation and standard deviation were reduced when compared with medium simulating fasted conditions.

Comparing the dissolution profiles is clear the increase and the sustained dissolution of the drug from the nanoparticles. Only with the use of NLCs, the oral administration of BPQ can be achieved. Those formulations, therefore, can be used as site-specific drug delivery system for BPQ or other lipophilic compounds, since the drug can be dissolved only in the duodenum, where the lipases and biliary salts are released. After the triglyceride degradation, the lipid and drug can be absorbed in the intestines, transferred to the lymphatic system and then, transported to lymph nodes, liver and spleen, which are the primary organs of infection by Leishmania parasites. Therefore, those formulations have a potential application for BPQ oral formulation, which can increase the patient's treatment compliance.

### 3.4.7. BPQ- NLC cytotoxicity

The CC<sub>50</sub> for V1 was 583.4  $\mu$ M and free BPQ 524.4  $\mu$ M. Those similar values show the low toxicity of the developed NLC since the drug presented no *in vitro* toxicity to mammalian cells, Reimão and colleagues (2012) found selectivity index higher than 150 using the *L. (L.) infantum chagasi* amastigotes. This behavior is a result of high compatibility and biodegradability of lipids and surfactant. MCT and poloxamer 188 are already used in products for injection, and the addition of Softisan did not compromise the safety of the developed formulations. Therefore, the BPQ-NLCs can be applied to develop safe and effective products for oral, topical and even parenteral administration.

### 3.5. Conclusions

This work presented the first steps in the development of an advanced nanotechnology formulations containing buparvaquone, which can be used to improve the safety and effectiveness of the anti-leishmaniasis treatment.

The high-pressure homogenization preparation was successfully applied in the development of the nanostructured lipid carriers, and it is a feasible method for industrial application. The formulation development by the response surface methodology and full 2<sup>3</sup> factorial designs showed that to obtain Z-averages less than 300 nm, the use of poloxamer 188 should be more than 2.0% w/w. Additionally, the % lipid phase is crucial to the achievement of low Z-averages, the lower the % lipid phase, the lower the Z-average. The use of a mathematical model allowed balancing the concentration of surfactants and lipid phase to achieve the desired particle size and drug loading. The mathematical model verification for all the formulations was satisfactory and within the 95% CI range.

The assessment of the stability testing data revealed the potential development of liquid formulations, which can avoid critical drying process. The BPQ solubility from NLCs showed increased values for all media tested when compared with the free drug.

Dissolution profiles revealed the improved BPQ dissolution from NLCs. Free BPQ could reach only 2.89% of a 4.0 mg dose when a fasted state was simulated. Both formulations in simulated fed and fasted conditions improved the drug dissolution at least 50% of the 4.0 mg for 60 minutes. These dissolution behaviors revealed the

potential use of the BPQ-NLCs for oral administration, followed by lymphatic absorption and distribution. Therefore, the drug can easily access at the lymph nodes, spleen, and liver. Cytotoxicity tests showed the safety and suitability of the NLCs as result of high compatibility and biodegradability of the lipids and surfactants.

Owing to the results of this work, the developed NLCs have potential application to improve the drug efficacy, reduce the toxicity of the treatment and improve the patient adherence. These formulations can be used as oral and parenteral drug dosage forms to fill the gaps of conventional leishmaniases treatment. As a consequence, the cost can be minimized by reduction of hospitalization for drug administration and side effects monitoring.

## Chapter 4

### **Co-encapsulation of buparvaquone and polymyxin B in nanostructured lipid carrier as a delivery system for leishmaniasis treatment**

This study was submitted as Lis Marie Monteiro, Raimar Löbenberg, Paulo Cesar Cotrim, Nádia Bou-Chacra. Co-encapsulation of buparvaquone and polymyxin B in nanostructured lipid carrier as a delivery system for leishmaniasis treatment at International Journal of Antimicrobial Agents.

## Abstract

Despite the high incidence of leishmaniasis, the most common treatment of the past 60 years shows severe toxicity, parasite resistance and variable efficacy. Buparvaquone (BPQ) showed promising activity against *Leishmania donovani*. However, due to its low water-solubility and bioavailability, it has failed in *in vivo* tests. Nanostructured lipid carrier (NLC) can improve therapeutic efficacy and overcome the low solubility of BPQ allowing a targeted drug delivery system for leishmaniasis through rapid internalization by macrophages. This work describes the preparation and the physicochemical characterization and *in vitro* leishmanicidal activity of BPQ nanostructured lipid carrier (BPQ-NLC), BPQ and polymyxin B co-encapsulated in NLC coated with chitosan and dextran sulfate (BPQ-NLC-POL[-]) and BPQ and polymyxin B co-encapsulated in NLC coated with DEAE-dextran (BPQ-NLC-POL[+]). The NLC preparation was performed by high-pressure homogenization and Z-average, polydispersity index (PDI) and zeta potential were accessed using photon correlation spectroscopy and electrophoretic mobility, respectively. The cytotoxicity was evaluated against mouse peritoneal macrophages and the leishmanicidal activity was evaluated on amastigotes of *L. infantum*. The Z-average of BPQ-NLC, BPQ-NLC-POL[-] and BPQ-NLC-POL[+] were  $173.9 \pm 1.6$ ,  $183.8 \pm 4.5$  and  $208.8 \pm 2.6$  nm, respectively. The PDI for all formulations were less than 0.3. The PZ were  $-19.6 \pm 1.5$ ,  $-20.1 \pm 1.1$  and  $+31.1 \pm 0.8$ , respectively. The  $CC_{50}$  from free BPQ, BPQ-NLC BPQ-NLC-POL[-] and BPQ-NLC-POL[+] were 524.4, 583.4, 203.1 and 5.7  $\mu$ M. The  $IC_{50}$  were 456.5, 229.0, 145.7 and 150.5 nM, respectively. Considering the improved leishmanicidal activity, the developed NLC proved to be a promising alternative for leishmaniasis treatment.

## 4.1 Introduction

Leishmaniasis are caused by protozoan parasites of the genus *Leishmania* and are transmitted to humans and other mammals by phlebotomine sandfly vectors. Around 350 million people in 88 countries globally are living at risk of developing one of the disease forms, mostly in South and Central America, Africa, Asia, and southern Europe (KAYE and SCOTT, 2011; NATEGHI ROSTAMI et al., 2016). The intracellular localization of leishmaniasis parasites hinders access of the chemotherapy to the site of action. Thereby, the treatment requires the administration of large and repeated doses, which rouses the appearance of toxicity and parasite resistance (COSTA LIMA et al., 2012).

The parasite's ability to survive and multiply within phagocytic cells is a prominent issue in developing new active compounds and drug-delivery systems for leishmaniasis. The intracellular parasites can protect themselves from exposure to drugs that do not readily diffuse into cells (CARRYN et al., 2003). Therefore, the use of drug carriers, such as nanoparticles, can improve the therapeutic efficacy by releasing leishmanicidal compound in its site of action (COSTA LIMA et al., 2012). Nanoparticles are preferentially taken up by macrophages following systemic or local administration.

The association of drugs with different mechanisms of action can provide synergistic effect aiming to reduce parasite resistance. Antimicrobial peptides (AMPs) are a non-conventional approach in the leishmaniasis therapy. These drugs can cause the disruption of the plasma membrane following increased cell permeability, interaction with intracellular targets and stimulation of biochemical modifications and apoptosis (MARR, MCGWIRE and MCMASTER, 2012). Thus, AMPs, as an adjuvant drug, have the potential to increase the therapeutic efficacy of a main drug when they are used in combination.

Biopolymers such as chitosan and dextran are recognized by SIGN-1 and mannan receptors (MR) from macrophages. These receptors interact with lipopolysaccharides (LPS) from Gram-negative bacteria for pathogen recognition, uptake and further induction of immune responses (KAWAUCHI, KURODA and KOJIMA, 2012; TAKAHARA et al, 2014). By exploring these features in drug delivery design, it is possible to enable more efficient and safer medicines.

Buparvaquone (BPQ) is a hydroxynaphthoquinone related to parvaquone, which is applied to treat theileriosis in cattle. The BPQ *in vitro* leishmanicidal activity of against *L. donovani* was revealed for the first time by Croft and colleagues (1992). However, due to drug very low water solubility ( $<300 \text{ ng.mL}^{-1}$ ), BPQ showed low *in vivo* activity against leishmaniasis by intramuscular injection (VEXENAT et al., 1998). There is a commercial BPQ product known as Butalex<sup>®</sup>; however, the high surfactant content (10.0 to 20.0%) and presence of N-methyl-2-pyrrolidone (50.0 to 60.0%), a toxic organic solvent, makes the formulation unsuitable for human application. Aiming to increase the BPQ solubility, while upholding the formulation biocompatibility, the use of nanostructured lipid carrier (NLC) is a promising approach. Also, a targeted drug delivery system to macrophage can be developed including specific molecules for cell recognition and internalization. Thus, this work describes the preparation and *in vitro* evaluation of buparvaquone and polymyxin B NLC coated with chitosan and dextran as moieties for site-specific delivery of buparvaquone, aiming to increase the therapeutic efficiency and to reduce the toxicity of leishmaniasis treatment.

## **4.2. Materials and methods**

### **4.2.1. Materials**

Softisan<sup>®</sup> 154 was kindly donated by Gattefossé (Lyon, France) and medium chain triglycerides (MCT) were kindly donated by Abitec (Columbus, USA). Buparvaquone was purchased from Uniwise (Hangzhou, China). Kolliphor<sup>®</sup> P188 was acquired from BASF (Ludwigshafen, Germany) and Tween 80 from MilliporeSigma (Ludwigshafen, Germany). Polymyxin B was purchased from Biotika (Slovenská Ľupča, Slovakia) ( $8106 \text{ units.mg}^{-1}$ ). Chitosan was purchased from NovaMatrix (Sandvika, Norway), dextran sulfate and DEAE-dextran were purchased from MilliporeSigma (Ludwigshafen, Germany). Purified water was obtained by Milli-Q system from Merck Millipore (Ludwigshafen, Germany). Organic solvents were HPLC grade and all other chemicals used were of at least analytical grade.

## **4.3. Methods**

#### **4.3.1. Analytical method for quantification of buparvaquone by HPLC**

A method described by Monteiro and colleagues (2017a) was used for the quantification of the BPQ in the encapsulation efficiency. The final conditions are Xterra Waters column, C8 100 x 4.6 mm, particle size 3.5  $\mu\text{m}$  (Waters Corporation, Milford, MA, USA). Mobile phase of 1% (v/v) glacial acetic acid, acetonitrile and methanol (25:65:10) (mobile phase A), 35 °C column temperature, 50  $\mu\text{L}$  injection volume and UV detection  $\lambda=252\text{ nm}$ . The HPLC method was performed in drug loading and encapsulation efficiency and formulations were evaluated in replicates of three.

#### **4.3.2. Preparation of buparvaquone nanostructured lipid carrier (BPQ-NLC)**

After the lipids selection, described by Monteiro and colleagues (2017a), the BPQ-NLC formulations were prepared by dispersing the heated lipid phase in the aqueous phase (70 °C) and pre-homogenized using high-performance disperser (8.000 RPM for 5 min) (T25 digital ULTRA-TURRAX, IKA, Staufen, Germany). Afterwards, the coarse emulsion was passed through high-pressure homogenizer (Nano DeBEE 45-2, Bee International, South Easton, MA, USA) at 600 bars for five cycles. The solid and liquid lipids were Softisan 154 and MCT (capric/caprylic triglyceride) (0.5:1), respectively. The surfactant was Kolliphor P188 4% w/v.

#### **4.3.3. Preparation of BPQ and polymyxin B co-encapsulated in NLC (BPQ-NLC-POL)**

The co-encapsulation was performed by the addition of a stock solution of polymyxin B to a final concentration of 1000 UI.mL<sup>-1</sup> diluted in 10 mL of BQP-NLC (diluted 3-fold), under magnetic stirring (100 rpm, 1h), with a negative charge endpoint.

#### **4.3.4. Preparation of BPQ-NLC-POL coated with chitosan + dextran sulfate (BPQ-NLC-POL[-]) and BPQ-NLC-POL coated with DEAE-dextran (BPQNLC-POL[+])**



The coating process delivered a negative and a positive charged nanoparticle depending on the biopolymer used: chitosan + dextran sulfate (BPQ-NLC-POL[-]) or a DEAE-dextran (BPQ-NLC-POL[+]), respectively. For the negative nanoparticles, chitosan was added a 10-mL aliquot of BPQ-NLC-POL to a final concentration of 0.05% w/v, under magnetic stirring (100 rpm, 1h). Following, the dextran sulfate was added to final concentration of (0.55% w/v), under magnetic stirring (100 rpm, 1h). For the cationic nanoparticles, DEAE-dextran was added a 10-mL aliquot of BPQ-NLC-POL to a final concentration of 0.05% w/v, under magnetic stirring (100 rpm, 1h).

#### **4.3.5. Determination of the Z-average, polydispersity index (PDI) and zeta potential (ZP)**

The Z-average and PDI were performed by photon correlation spectroscopy (PCS) and PZ by electrophoretic mobility. For both methods, Zetasizer Nano ZS90 (Malvern Instruments, Malvern, UK) was used. The measurements were carried out in purified water (n=3), with conductivity of 50  $\mu\text{S}\cdot\text{cm}^{-1}$ , pH  $6.5 \pm 0.2$  and 25 °C.

#### **4.3.6. Morphology by transmission electron microscopy (TEM) of BPQ-NLC, BPQ-NLC-POL[+] and BPQ-NLC-POL[-]**

Images were acquired using a Morgagni 268 transmission electron microscope with Gatan Digital Camera (Philips/FEI, Hillsboro, Oregon, USA). The samples were diluted in purified water in the ratio of 1:20. The diluted samples were placed over regular TEM grids and allowed to set for 15 seconds. The background was stained with phosphotungstic acid solution 10 % (w/v) (Sigma-Aldrich, St. Louis, Missouri, USA) for additional 15 seconds.

#### **4.3.7. Cytotoxicity and leishmanicidal activity of free BPQ, BPQ-NLC, BPQ-NLC-POL[-] and BPQ-NLC-POL [+] in *L. infantum* amastigotes**

Cytotoxicity and leishmanicidal activity were performed as described previously by Monteiro and colleagues (2017b). Cell cytotoxicity was determined using mouse

peritoneal macrophages. Briefly, macrophages were incubated in RPMI 1640 medium with increased concentrations free BPQ and nanostructured formulations, after 24 hours, MTT solution was added, and the optical density was recorded using plate reader ( $\lambda = 595$  nm). The test was performed in replicates of three and repeated twice independently.

Amastigote test was performed using *L.infantum*. Briefly, infected macrophages were incubated using RPMI 1640 medium at 37 °C for 24 hours with increased concentrations of free BPQ and nanostructured formulations. Then, the cells were washed, fixed with methanol and stained with Giemsa. The number of infected, uninfected cells and amastigotes per cell were counted (200 cells per sample) by microscopic examination. The test were performed in replicates of three and repeated twice independently. The selectivity index was calculated as described by Benedict and colleagues (2015).

#### **4.3.8. IC<sub>50</sub>, CC<sub>50</sub> and statistical analysis**

IC<sub>50</sub> and CC<sub>50</sub> values were expressed as the mean  $\pm$  standard deviation of parasite or cell viability. IC<sub>50</sub> and CC<sub>50</sub> were calculated by non-linear regression analysis using GraphPad Prism version 5.01. The significance of differences among values was determined using ANOVA (Minitab 17 software). The p-value of  $<0.05$  was considered statistically significant.

### **4.4. Results**

#### **4.4.1. Preparation of buparvaquone nanostructured lipid carrier (BPQ-NLC)**

BPQ-NLC showed Z-average of  $173.9 \pm 1.6$  nm with monomodal distribution. Regarding PDI, it was  $0.164 \pm 0.005$  and ZP was  $-19.6 \pm 1.5$  mV. BPQ loading and %EE were  $0.5054 \pm 0.0108$  mg.mL<sup>-1</sup> and  $99.72 \pm 0.33\%$ , respectively. All the parameters of this formulation were stable at least for four months.

#### **4.4.2. Preparation of BPQ-NLC with polymyxin B (BPQ-NLC-POL)**

BPQ-NLC-POL showed Z-average of  $171.9 \pm 1.6$  nm and monomodal distribution. Regarding PDI, it was  $0.110 \pm 0.003$  and ZP was  $-3.7 \pm 0.5$  mV. Due to zeta potential close to neutral, this formulation was not stable for more than one month. Therefore, only BPQ-NLC and coated nanoparticles were subject to cytotoxicity and leishmanicidal activities.

#### 4.4.3. Preparation of BPQ-NLC-POL coated with chitosan and dextran sulfate (BPQ-NLC-POL[-]) and BPQ-NLC-POL coated with DEAE-dextran (BPQ-NLC-POL[+])

Table 4.1 shows the mean values and standard deviation for Z-average, PDI, ZP, BPQ loading and %EE from BPQ-NLC-POL[-] and BPQ-NLC-POL[+]. Both formulations were stable for at least four months.

Table 4.1. Z-average, polydispersity index, zeta potential, buparvaquone (BPQ) drug loading and encapsulation efficiency BPQ-NLC-POL[-] and BPQ-NLC-POL[+] (n=3).

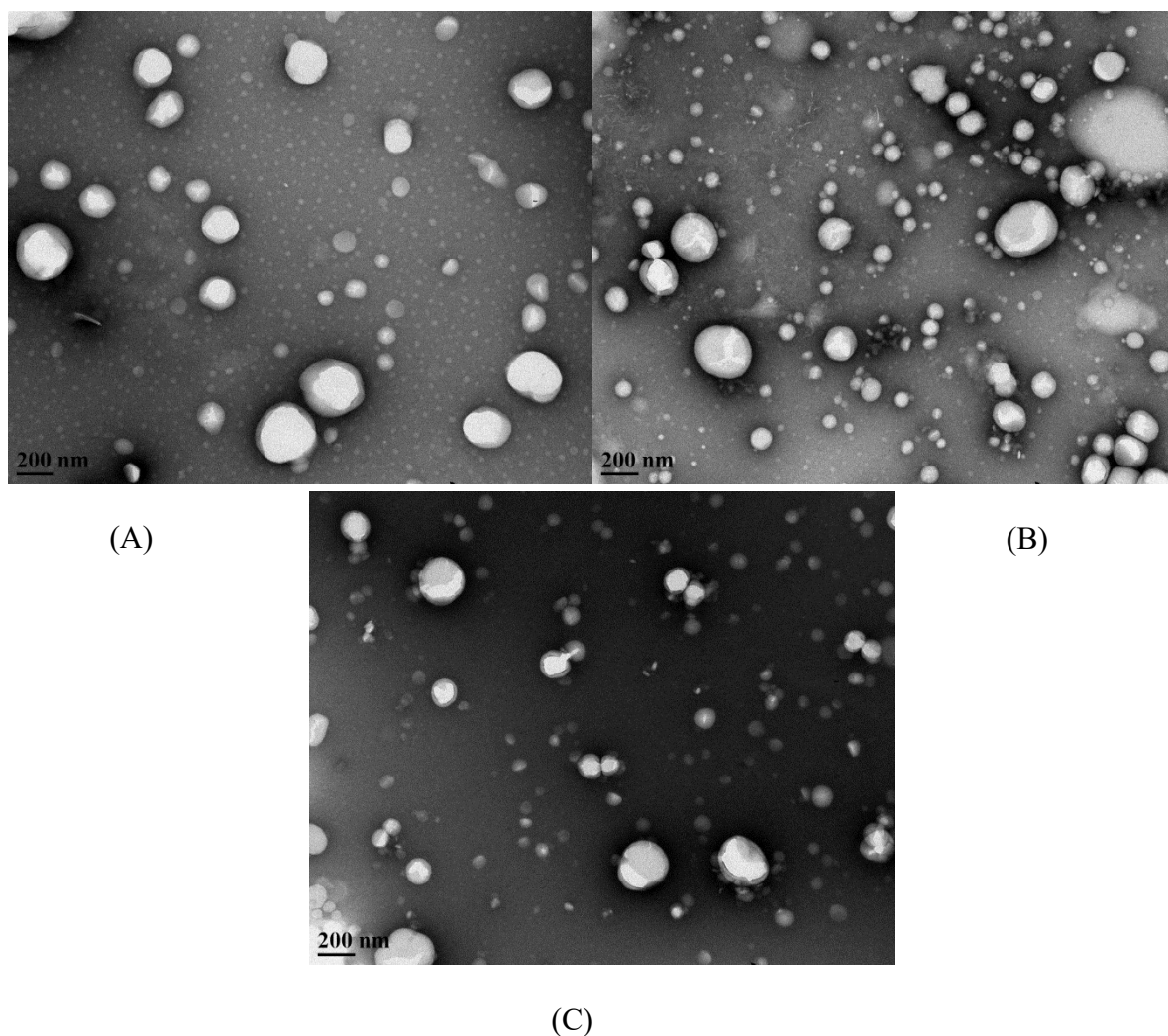
	BPQ-NLC-POL[-]	BPQ-NLC-POL[+]
<b>Z-average (nm)</b>	$183.8 \pm 4.5$ monomodal	$208.8 \pm 2.6$ monomodal
<b>Polydispersity</b>	$0.139 \pm 0.005$	$0.140 \pm 0.019$
<b>Zeta potential (mV)</b>	$-20.1 \pm 1.1$	$+31.1 \pm 0.8$
<b>BPQ drug loading (mg.mL<sup>-1</sup>)</b>	$0.1534 \pm 0.0064$	$0.1657 \pm 0.0025$
<b>BPQ encapsulation efficiency (%)</b>	$99.54 \pm 0.46$	$99.73 \pm 0.47$

BPQ-NLC-POL[-]: BPQ nanostructured lipid carrier and polymyxin B coated with chitosan and dextran sulfate; BPQ-NLC-POL[+]: BPQ nanostructured lipid carrier and polymyxin B coated with DEAE-dextran.

#### 4.4.4. Morphology by transmission electron microscopy (TEM) of BPQ-NLC, BPQ-NLC-POL[-] and BPQ-NLC-POL[+]

Figure 4.1 shows the microscopy of the developed formulations, except for BPQ-NLC-POL due to aggregation found in the first month of stability testing.

Figure 4.1. Transmission electron microscopy (36kx) of (A) Buparvaquone nanostructured lipid carrier ( $171.9 \pm 1.6$  nm). (B) Buparvaquone nanostructured lipid carrier with polymyxin B coated with chitosan and dextran sulfate ( $183.8 \pm 4.5$  nm). (C) Buparvaquone nanostructured lipid carrier with polymyxin B coated with DEAE-dextran ( $208.8 \pm 2.6$  nm).



#### 4.4.5. Cytotoxicity and leishmanicidal activity of free BPQ, BPQ-NLC, BPQ-NLC-POL[-] and BPQ-NLC-POL [+] in *L. infantum* amastigotes

Table 4.2 shows the cytotoxicity ( $CC_{50}$ ), leishmanicidal ( $IC_{50}$ ) and selectivity index of free BPQ and developed nanostructured formulations.

Table 4.21. Cytotoxicity, amastigote activity against *L.infantum* (CC<sub>50</sub> or IC<sub>50</sub> and 95% IC) and selectivity index of free buparvaquone (BPQ), BPQ nanostructured lipid carrier (BPQ-NLC), BPQ nanostructured lipid carrier with polymyxin B coated with chitosan and dextran sulfate (BPQ-NLC-POL[-]) and BPQ nanostructured lipid carrier with polymyxin B coated with DEAE-dextran (BPQ-NLC-POL[+]).

	<b>Cytotoxicity CC<sub>50</sub> (μM)</b>	<b>Amastigote IC<sub>50</sub> (nM)</b>	<b>Amastigote selectivity index</b>
<b>Free BPQ</b>	524.4 (252.2 to 1090.0)	456.5 (332.4 to 627.0)	1149
<b>BPQ-NLC</b>	583.4 (362.6 to 938.6)	229.0 (190.5 to 275.2)	2547
<b>BPQ-NLC-POL[-]</b>	203.1 (169.6 to 243.3)	145.7 (132.3 to 160.6)	1394
<b>BPQ-NLC-POL[+]</b>	5.7 (4.2 to 7.8)	150.5 (139.5 to 162.4)	38

## 4.5. Discussion

### 4.5.1. Preparation of buparvaquone nanostructured lipid carrier (BPQ-NLC)

High-pressure homogenization was applied successfully for BPQ-NLC preparation revealing Z-average <300 nm (monomodal), PDI<0.3, which indicates a homogenous and narrow size distribution formulation.

He and colleagues (2010) showed that nanoparticles larger than 300 nm tend to accumulate in the liver. On the other hand, the spleen nanoparticle distribution decreased with the increase of the particle size from 150 to 300 nm. Therefore, the Z-average of 173.9±1.6 nm for BPQ-NLC is suitable for targeting liver and spleen, since the nanoparticles in this range can accumulate in both organs, parasitized by amastigotes.

### 4.5.2. Preparation of BPQ-NLC with polymyxin B (BPQ-NLC-POL)

The electrostatic interaction between the polymyxin B and the BPQ-NLC allowed the co-encapsulation. The developed BPQ-NLC presented negative charges, which can electrostatically bind the positive charges of polymyxin B to the particle surface. The zeta potential decreased, in module, remaining negative in the end of process due to the polymyxin B concentration used. This ZP reduction indicated the success of the co-encapsulation. Unfortunately, the low ZP was inadequate to prevent aggregation of this formulation, which showed less than one month of stability (Z-average and PDI increased). Therefore, BPQ-NLC-POL was considered an intermediary product from BPQ-NLC-POL[-] and BPQ-NLC-POL[+].

#### **4.5.3. Preparation of BPQ-NLC-POL coated with chitosan and dextran sulfate (BPQ-NLC-POL[-]) and BPQ-NLC-POL coated with DEAE-dextran (BPQ-NLC-POL[+])**

The mechanism of coating was also by electrostatic interaction. Biopolymer with opposite charge was added to the nanoparticles, and the coating was confirmed by the ZP inversion. Regarding to Z-average, both formulations were in the nanometric range with low PDI (<0.3) and monomodal PSD, which indicates the narrow distribution of the particles.

Regarding the ZP, only BPQ-NLC-POL[+] formulation showed values  $<\pm 30$  mV as expected for a charge stabilized nanoparticles. However, BPQ-NLC and BPQ-NLC-POL[-], which showed ZP around -20 mV, were stable for at least four months. This finding can be explained by the presence of poloxamer 188 as a steric stabilizing agent, with in combination with the charges, assured the stability of Z-average, PDI and PSD.

#### **4.5.4. Morphology by transmission electron microscopy (TEM) of BPQ-NLC, BPQ-NLC-POL[+] and BPQ-NLC-POL[-]**

PCS method correlates the scattered light intensity with particle size for calculation of the Z-average. This is an indirect method, which calculates the equivalent spherical diameter, which is sensitive to the presence of agglomerates and optical parameters (KECK, 2010). Therefore, microscopy should be used to confirm

the shape and size of nanoparticles. The microscopy using TEM revealed the sphericity and the absence of agglomerated particles. Also, the size distribution was compatible with the PCS results for all formulations.

#### **4.5.5. Cytotoxicity and leishmanicidal activity of free BPQ, BPQ-NLC, BPQ-NLC-POL[-] and BPQ-NLC-POL [+] in *L. infantum* amastigotes**

BPQ-NLC showed cytotoxicity similar to free BPQ, respectively  $CC_{50}$  equal to 583.4  $\mu$ M and 524.4  $\mu$ M. BPQ-NLC-POL[-]  $CC_{50}$  showed a significant increase in toxicity (203.1  $\mu$ M). This finding was expected due to the action of the polymyxin B (data not shown).

Concerning BPQ-NLC-POL[+], the  $CC_{50}$  was only 5.7  $\mu$ M. The decreased value is explained by the interaction of cationic particles, which cause more pronounced disruption in the cell membrane integrity. Wang and colleagues (2013) showed that these nanoparticles are internalized and directed to lysosomes leading to membrane permeabilization and cell death from apoptosis. However, these interaction triggers the release of pro-inflammatory response by inducing Th1 cytokines expression (IL-2, IFN  $\gamma$  and TNF  $\alpha$ ) (KEDMI, BEN-ARIE, PEER, 2010) which can be a valuable tool to parasite elimination, since one of the main mechanisms of *Leishmania* survival is the innate immune response modulation (FALCÃO et al., 2016).

Regarding  $IC_{50}$  against *L. infantum* amastigotes from BPQ-NLC, the value was 2-fold (229.0 nM) higher than the free BPQ (456.5 nM). As a consequence of the low  $CC_{50}$  from BPQ-NLC, the selectivity index increased 2.2-fold. BPQ-NLC-POL[-] and BPQ-NLC-POL[+] showed similar activity, 145.7 and 150.5 nM, respectively, which are an increase of 3.0 and 3.1-fold when comparing to free BPQ. The improved  $IC_{50}$  of coated NLCs, when comparing with BPQ-NLC, can be explained by the activity of polymyxin B, combined with the interaction of the polysaccharides with the SIGN-R1 receptors of the macrophage cell membrane (PUSTYLNIKOV, SAGAR and KHAN, 2014; TAKAHARA et al., 2011) which helps the internalization of nanoparticles.

#### 4.6. Conclusions

This work provided the first steps for the co-encapsulation of buparvaquone as main drug and polymyxin B as adjuvant in NLC. These nanoparticles were coated with chitosan and dextran delivering anionic and cationic nanoparticles aiming an active targeted drug delivery system to macrophages. The developed formulations revealed suitable physicochemical attributes (Z-average, PDI, %EE) and increased *in vitro* leishmanicidal activity, when compared with free BPQ, while preserving the low cytotoxicity. Therefore, they will be investigated in further *in vivo* and immunological tests.

Owing to these preliminary results, the developed NLCs showed promising application to improve the drug efficacy, reduce the toxicity of the treatment and improve the patient adherence. As a parenteral drug dosage form, these NLCs have the potential to fill the gaps of conventional leishmaniases treatment.



## Chapter 5

### **General Conclusion and Future Prospective**

## General Conclusion

In recent years, few significant advances in the treatment of leishmaniasis have been achieved. The need to develop new drugs is urgent, since pentavalent antimonials used in standard therapy may be considered obsolete and available liposomal formulations have a prohibitive cost for the population in developing countries. Thus, the treatment of leishmaniasis remains a critical challenge. This work presented the first steps in the development of an advanced nanotechnology formulations containing buparvaquone, which can be used to improve the safety and effectiveness of the anti-leishmaniasis treatment.

Chapter 2 shows the first steps for NLC preparation and formulations using tween 80 and poloxamer 188 as surfactants. In the buparvaquone solubility tests for lipid screening, Softisan® 154 was found to be more suitable solid lipid for its encapsulation. MCT (medium chain triglycerides – capric and caprylic acid esters) was found as the best liquid lipid because of BPQ's higher solubility ( $11.5 \text{ g.kg}^{-1}$ ). The proportion of 1:2 was the best ratio to increase BPQ loading while preserving the blend melting point above  $40^\circ \text{C}$ . The high-pressure homogenization preparation was successfully applied in the development of the nanostructured lipid carriers and it is a feasible method for industrial application.

However, there is an interaction between the surfactants found by the mathematical model, which increases the Z-average. Therefore, in Chapter 3 is described a new formulation development by full  $2^3$  factorial design, due to the linear model found in Chapter 2. This investigation showed that to obtain Z-averages less than 300 nm, the use of poloxamer 188 should be more than 2% (w/v). Additionally, the % oil phase is crucial to the achievement of low Z-averages, the lower the % oil phase, the lower the Z-average. The use of a mathematical model allowed balancing the concentration of surfactants and oil phase to achieve the desired particle size. The mathematical model verification for the two predicted formulations was satisfactory and within the 95% CI range. The morphology evaluation by TEM confirmed particles with round shape and size distribution compatible with PCS results.

Still, in chapter 3, the formulations developed were tested for a possible oral administration. Dissolution profiles revealed the improved BPQ dissolution from NLC. Free BPQ could reach only 2.89% of a 4.0 mg dose in phosphate buffer pH7.4 with tween 80 0.07% w/v. In phosphate buffer, pH7.4 with dodecyl sodium sulfate 1.0% w/v, the free drug could not be dissolved because of precipitation. For V1 (Z-average: 185.6 nm), the dissolution in phosphate buffer pH7.4 with tween 80 0.07% w/v could reach 66.34% of the 4.0 mg dose in the first five minutes. The formulation V2 with higher Z-average (235.7 nm), the dissolution could reach 70.37% after five minutes of pancrelipase action. These dissolution behaviors revealed the potential use of the BPQ-NLC for oral administration, followed by lymphatic absorption and biodistribution. Therefore, the drug can easily access at the lymph nodes and spleen. Even the liver can be reached by the direct absorption via the intestines and by the remaining BPQ, which returns to the blood after leaving the lymphatic system.

Regarding Chapter 4, it describes the NLC co-encapsulation of BPQ and polymyxin B and a coating process with biopolymers, aiming specific target delivery for macrophages. Unlike formulations presented in Chapter 3, these coated formulations intended for intravenous administration for selective uptake by macrophages of the reticuloendothelial system, cells that are infected by *Leishmania* parasites.

Cationic coated formulation showed a decreased value for  $CC_{50}$ , which agrees with works found in the literature. Nevertheless, the cytotoxic effect of these particles can improve the *in vivo* leishmanicidal efficacy due to the intensification of the release of innate immune response mediators.

*In vitro* evaluation of the leishmanicidal activity against amastigotes showed the effectiveness of BPQ in nanomolar concentration against *L. infantum*. The  $IC_{50}$  for uncoated NLC were at least 2-fold lower, and coated formulations showed  $IC_{50}$  at least 3.0-fold lower than the free BPQ.

Owing to the results of this work, the hypothesis was answered, suitable NLCs for buparvaquone encapsulation were developed, which increased the drug water solubility and have potential application to improving the BPQ *in vivo* efficacy due to polymyxin B co-encapsulation and specific molecules for cell internalization.

## **Future prospective**

The current study highlighted the water solubility improvement of buparvaquone when a nanostructured lipid carrier formulation is applied. Also, the leishmanicidal activity from nanostructured buparvaquone was increased when compared with the free drug. However, the effects can be further validated using animal models. Based on the results of this thesis the following are my suggestions for future studies to verify and extend these findings.

### **Animal Studies**

#### **Visceral leishmaniasis model**

- I. Carry out the animal studies using hamsters infected with *L.infantum* and test oral and intravenous administration.
- II. Investigate the distribution of the particles in the mice body after injection.

#### **Cutaneous leishmaniasis**

- III. Carry out the animal studies using mice infected with *L.amazonensis* and test topical and wound injection administration.

### **Immunological Studies.**

- I. Investigate the changes in the cytokines profile after the administration of coated and uncoated nanoparticles.

### **Physicochemical studies**

- I. Investigate the chemical structure of the coated formulations.
- II. Perform long-term stability testing of liquid and dried formulations.

## References

- AGARWAL, R. et al. Liposomes in topical ophthalmic drug delivery: an update. **Drug Deliv**, v. 23, n. 4, p. 1075-91, May 2016. ISSN 1521-0464. Available at: < <https://www.ncbi.nlm.nih.gov/pubmed/25116511> .
- ALCOLEA, P. J. et al. Transcriptomics throughout the life cycle of *Leishmania infantum*: high down-regulation rate in the amastigote stage. **Int J Parasitol**, v. 40, n. 13, p. 1497-516, Nov 2010. ISSN 1879-0135. Available at: < <https://www.ncbi.nlm.nih.gov/pubmed/20654620> .
- ALJAEID, B. M.; HOSNY, K. M. Miconazole-loaded solid lipid nanoparticles: formulation and evaluation of a novel formula with high bioavailability and antifungal activity. **Int J Nanomedicine**, v. 11, p. 441-7, 2016. ISSN 1178-2013. Available at: < <https://www.ncbi.nlm.nih.gov/pubmed/26869787> .
- ALMOUAZEN, E. et al. Development of a nanoparticle-based system for the delivery of retinoic acid into macrophages. **Int J Pharm**, v. 430, n. 1-2, p. 207-15, Jul 2012. ISSN 1873-3476. Available at: < <https://www.ncbi.nlm.nih.gov/pubmed/22465633> .
- ALVAR, J. et al. Case study for a vaccine against leishmaniasis. **Vaccine**, v. 31 Suppl 2, p. B244-9, Apr 18 2013. ISSN 1873-2518 (Electronic)0264-410X (Linking). Available at: < <http://dx.doi.org/10.1016/j.vaccine.2012.11.080> .
- \_\_\_\_\_. Leishmaniasis worldwide and global estimates of its incidence. **PLoS One**, v. 7, n. 5, p. e35671, 2012. ISSN 1932-6203. Available at: < <https://www.ncbi.nlm.nih.gov/pubmed/22693548> .
- AMASYA, G. et al. Skin Localization of Lipid Nanoparticles (SLN/NLC): Focusing the Influence of Formulation Parameters. **Curr Drug Deliv**, v. 13, n. 7, p. 1100-1110, 2016. ISSN 1875-5704. Available at: < <https://www.ncbi.nlm.nih.gov/pubmed/26725723> .
- AMIDON, G. L. et al. A theoretical basis for a biopharmaceutical drug classification: the correlation of in vitro drug product dissolution and in vivo bioavailability. **Pharm Res**, v. 12, n. 3, p. 413-20, Mar 1995. ISSN 0724-8741 (Print)0724-8741 (Linking). Available at: < <http://dx.doi.org/> .
- ASTHANA, S. et al. Immunoadjuvant chemotherapy of visceral leishmaniasis in hamsters using amphotericin B-encapsulated nanoemulsion template-based chitosan nanocapsules. **Antimicrob Agents Chemother**, v. 57, n. 4, p. 1714-22, Apr 2013. ISSN 0066-4804. Available at: < <http://dx.doi.org/10.1128/aac.01984-12> .

- AVDEEF, A. **Absorption and Drug Development: Solubility, Permeability, and Charge State, 2nd Edition**. Wiley, John & Sons, Inc, 2012. 744
- AVERINA, E. S. et al. Physical and chemical stability of nanostructured lipid drug carriers (NLC) based on natural lipids from Baikal region (Siberia, Russia). **Pharmazie**, v. 66, n. 5, p. 348-56, May 2011. ISSN 0031-7144 (Print)0031-7144. Available at: &lt; <http://dx.doi.org/> .
- BALGURI, S. P.; ADELLI, G. R.; MAJUMDAR, S. Topical ophthalmic lipid nanoparticle formulations (SLN, NLC) of indomethacin for delivery to the posterior segment ocular tissues. **Eur J Pharm Biopharm**, v. 109, p. 224-235, Dec 2016. ISSN 0939-6411. Available at: &lt; <http://dx.doi.org/10.1016/j.ejpb.2016.10.015> .
- BAMRUNGSAP, S. et al. Nanotechnology in therapeutics: a focus on nanoparticles as a drug delivery system. **Nanomedicine (Lond)**, v. 7, n. 8, p. 1253-71, Aug 2012. ISSN 1748-6963. Available at: &lt; <http://www.ncbi.nlm.nih.gov/pubmed/22931450> .
- BEH, C. Y. et al. Development of erythropoietin receptor-targeted drug delivery system against breast cancer using tamoxifen-loaded nanostructured lipid carriers. **Drug Des Devel Ther**, v. 11, p. 771-782, 2017. ISSN 1177-8881. Available at: &lt; <https://www.ncbi.nlm.nih.gov/pubmed/28352153> .
- BELOQUI, A. et al. Nanostructured lipid carriers: Promising drug delivery systems for future clinics. **Nanomedicine**, v. 12, n. 1, p. 143-61, Jan 2016. ISSN 1549-9634. Available at: &lt; <http://dx.doi.org/10.1016/j.nano.2015.09.004> .
- BEN SALAH, A. et al. Topical paromomycin with or without gentamicin for cutaneous leishmaniasis. **N Engl J Med**, v. 368, n. 6, p. 524-32, Feb 2013. ISSN 1533-4406. Available at: &lt; <https://www.ncbi.nlm.nih.gov/pubmed/23388004> .
- BENEDICT, A. et al. Repurposing FDA-approved drugs as therapeutics to treat Rift Valley fever virus infection. **Front Microbiol**, v. 6, p. 676, 2015. ISSN 1664-302X. Available at: &lt; <https://www.ncbi.nlm.nih.gov/pubmed/26217313> .
- BENET, L. Z. The role of BCS (biopharmaceutics classification system) and BDDCS (biopharmaceutics drug disposition classification system) in drug development. **J Pharm Sci**, v. 102, n. 1, p. 34-42, Jan 2013. ISSN 1520-6017. Available at: &lt; <https://www.ncbi.nlm.nih.gov/pubmed/23147500> .
- BHUSHAN, B. **Springer Handbook of Nanotechnology**. 3. Springer-Verlag Berlin Heidelberg, 2010. 1964 ISBN 978-3-642-02525-9.
- BLUM, J. et al. LeishMan recommendations for treatment of cutaneous and mucosal leishmaniasis in travelers, 2014. **J Travel Med**, v. 21, n. 2, p. 116-29,

2014 Mar-Apr 2014. ISSN 1708-8305. Available at: &lt;  
<https://www.ncbi.nlm.nih.gov/pubmed/24745041> .

BOISSON, S. et al. Water, sanitation and hygiene for accelerating and sustaining progress on neglected tropical diseases: a new Global Strategy 2015-20. **Int Health**, v. 8 Suppl 1, p. i19-21, Mar 2016. ISSN 1876-3405. Available at: &lt; <https://www.ncbi.nlm.nih.gov/pubmed/26940305> .

BORRIN, T. R. et al. Curcumin-loaded nanoemulsions produced by the emulsion inversion point (EIP) method: An evaluation of process parameters and physico-chemical stability. **Journal of Food Engineering**. 169: 1-9 p. 2016.

BOUYER, E. et al. Proteins, polysaccharides, and their complexes used as stabilizers for emulsions: alternatives to synthetic surfactants in the pharmaceutical field? **Int J Pharm**, v. 436, n. 1-2, p. 359-78, Oct 15 2012. ISSN 0378-5173. Available at: &lt;  
<http://dx.doi.org/10.1016/j.ijpharm.2012.06.052> .

BRASIL, M. D. S. **Manual de vigilância e controle da leishmaniose visceral**. Série A. Normas e Manuais Técnicos. Brasília: 120 p. 2006.

\_\_\_\_\_. **Manual de Vigilância da Leishmaniose Tegumentar Americana**. Série A. Normas e Manuais Técnicos: 119 p. 2007.

BRUGÈ, F. et al. A comparative study on the possible cytotoxic effects of different nanostructured lipid carrier (NLC) compositions in human dermal fibroblasts. **Int J Pharm**, v. 495, n. 2, p. 879-85, Nov 2015. ISSN 1873-3476. Available at: &lt; <https://www.ncbi.nlm.nih.gov/pubmed/26392245> .

BUETTNER, M.; BODE, U. Lymph node dissection--understanding the immunological function of lymph nodes. **Clin Exp Immunol**, v. 169, n. 3, p. 205-12, Sep 2012. ISSN 0009-9104. Available at: &lt;  
<http://dx.doi.org/10.1111/j.1365-2249.2012.04602.x> .

BUNJES, H.; WESTESEN, K.; KOCH, M. H. J. Crystallization tendency and polymorphic transitions in triglyceride nanoparticles. **International Journal of Pharmaceutics**: Elsevier. 129: 159-173 p. 1996.

BUTLER, J. M.; DRESSMAN, J. B. The developability classification system: application of biopharmaceutics concepts to formulation development. **J Pharm Sci**, v. 99, n. 12, p. 4940-54, Dec 2010. ISSN 1520-6017. Available at: &lt; <https://www.ncbi.nlm.nih.gov/pubmed/20821390> .

CARRYN, S. et al. Intracellular pharmacodynamics of antibiotics. **Infectious Disease Clinics of North America**, v. 17, n. 3, p. 615-634, 2003. Available at: &lt;  
[https://www.researchgate.net/publication/8929580\\_Intracellular\\_pharmacodynamics\\_of\\_antibiotics](https://www.researchgate.net/publication/8929580_Intracellular_pharmacodynamics_of_antibiotics) .

- CARVALHO, L. P. et al. Lymph node hypertrophy following *Leishmania major* infection is dependent on TLR9. **J Immunol**, v. 188, n. 3, p. 1394-401, Feb 01 2012. ISSN 0022-1767. Available at: &lt;<http://dx.doi.org/10.4049/jimmunol.1101018> .
- CAVALLI, R. et al. Sterilization and freeze-drying of drug-free and drug-loaded solid lipid nanoparticles. **International Journal of Pharmaceutics**. 148: 47-54 p. 1997.
- CHANBUREE, S.; TIYABOONCHAI, W. Mucoadhesive nanostructured lipid carriers (NLCs) as potential carriers for improving oral delivery of curcumin. **Drug Dev Ind Pharm**, v. 43, n. 3, p. 432-440, Mar 2017. ISSN 1520-5762. Available at: &lt;<https://www.ncbi.nlm.nih.gov/pubmed/27808665> .
- CHAPMAN, N. et al. NEGLECTED DISEASE RESEARCH AND DEVELOPMENT: A PIVOTAL MOMENT FOR GLOBAL HEALTH. **The ninth G-FINDER report**, Brussels, Belgium, 2017. Available at: &lt;<http://www.policycuresresearch.org/downloads/Y9%20GFINDER%20full%20report%20web.pdf> . Accessed on: May 10th.
- CHARMAN, W. N. Lipids, lipophilic drugs, and oral drug delivery-some emerging concepts. **J Pharm Sci**, v. 89, n. 8, p. 967-78, Aug 2000. ISSN 0022-3549 (Print)0022-3549. Available at: &lt;<http://dx.doi.org/> .
- CHELLAT, F. et al. Therapeutic potential of nanoparticulate systems for macrophage targeting. **Biomaterials**, v. 26, n. 35, p. 7260-75, Dec 2005. ISSN 0142-9612 (Print)0142-9612. Available at: &lt;<http://dx.doi.org/10.1016/j.biomaterials.2005.05.044> .
- CHEN, H. et al. Nanonization strategies for poorly water-soluble drugs. **Drug Discov Today**, v. 16, n. 7-8, p. 354-60, Apr 2011. ISSN 1878-5832. Available at: &lt;<https://www.ncbi.nlm.nih.gov/pubmed/20206289> .
- CHEN, M. L. et al. The BCS, BDDCS, and regulatory guidances. **Pharm Res**, v. 28, n. 7, p. 1774-8, Jul 2011. ISSN 1573-904X. Available at: &lt;<https://www.ncbi.nlm.nih.gov/pubmed/21491148> .
- CHEN, P. C.; JUN-WEI, A. H.; JIMMY, A. P. An Investigation of Optimum NLC-Sunscreen Formulation Using Taguchi Analysis. **Journal of Nanomaterials**, v. 2013, p. 10, 2013.
- CHEN, Y. et al. Preparation and characterization of a nanostructured lipid carrier for a poorly soluble drug. **Colloids and Surfaces A: Physicochemical and Engineering Aspects**, v. 455, p. 36–43, 5 August 2014 2014. Available at: &lt;<https://doi.org/10.1016/j.colsurfa.2014.04.032> .
- CHINSRIWONGKUL, A. et al. Nanostructured lipid carriers (NLC) for parenteral delivery of an anticancer drug. **AAPS PharmSciTech**, v. 13, n. 1, p. 150-8, Mar 2012. ISSN 1530-9932. Available at: &lt;<https://www.ncbi.nlm.nih.gov/pubmed/22167418> .



- CHOI, H. J. et al. SIGN-R1, a C-type lectin, binds to Bip/GRP78 and this interaction mediates the regurgitation of T-cell-independent type 2 antigen dextran through the endoplasmic reticulum. **Immunobiology**, v. 216, n. 4, p. 437-46, Apr 2011. ISSN 1878-3279. Available at: &lt; <http://www.ncbi.nlm.nih.gov/pubmed/20951467> .
- CIRRI, M. et al. Development of a new delivery system consisting in;drug--in cyclodextrin--in nanostructured lipid carriers for ketoprofen topical delivery. **Eur J Pharm Biopharm**. Netherlands: 2011 Elsevier B.V. 80: 46-53 p. 2012.
- CORRIAS, F.; LAI, F. New methods for lipid nanoparticles preparation. **Recent Pat Drug Deliv Formul**, v. 5, n. 3, p. 201-13, Sep 2011. ISSN 2212-4039. Available at: &lt; <https://www.ncbi.nlm.nih.gov/pubmed/21834772> .
- COSTA, C. H. N. et al. Vaccines for the Leishmaniasis: Proposals for a Research Agenda. In: (Ed.). **PLoS Negl Trop Dis**, v.5, 2011. ISBN 1935-2727 (Print)1935-2735 (Electronic).
- COSTA LIMA, S. et al. In vitro evaluation of bisnaphthalimidopropyl derivatives loaded into pegylated nanoparticles against Leishmania infantum protozoa. **Int J Antimicrob Agents**, v. 39, n. 5, p. 424-30, May 2012. ISSN 1872-7913. Available at: &lt; <http://www.ncbi.nlm.nih.gov/pubmed/22398197> .
- CROFT, S. L. et al. The activity of hydroxynaphthoquinones against Leishmania donovani. **J Antimicrob Chemother**, v. 30, n. 6, p. 827-32, Dec 1992. ISSN 0305-7453. Available at: &lt; <https://www.ncbi.nlm.nih.gov/pubmed/1289357> .
- DA COSTA-SILVA, T. A. et al. Nanoliposomal Buparvaquone Immunomodulates Leishmania infantum-Infected Macrophages and Is Highly Effective in a Murine Model. **Antimicrob Agents Chemother**, v. 61, n. 4, Apr 2017. ISSN 0066-4804. Available at: &lt; <http://dx.doi.org/10.1128/aac.02297-16> .
- DAS, S.; NG, W. K.; TAN, R. B. Are nanostructured lipid carriers (NLCs) better than solid lipid nanoparticles (SLNs): development, characterizations and comparative evaluations of clotrimazole-loaded SLNs and NLCs? **Eur J Pharm Sci**. Netherlands: 2012 Elsevier B.V. 47: 139-51 p. 2012.
- DE PAIVA-CAVALCANTI, M. et al. Leishmaniasis diagnosis: an update on the use of immunological and molecular tools. **Cell Biosci**, v. 5, p. 31, 2015. Available at: &lt; <https://www.ncbi.nlm.nih.gov/pubmed/26097678> .
- DEMETZOS, C. **Introduction to Nanotechnology - Fundamentals and Practical Applications**. ADIS, 2016. 203.
- DERRINGER, G. C.; SUICH, R. Simultaneous Optimization of Several Response Variables. **Journal of Quality Technology**, v. 12, p. 214-219, 1980.

- DEVKAR, T. B.; TEKADE, A. R.; KHANDELWAL, K. R. Surface engineered nanostructured lipid carriers for efficient nose to brain delivery of ondansetron HCl using Delonix regia gum as a natural mucoadhesive polymer. **Colloids Surf B Biointerfaces**, v. 122, p. 143-50, Oct 1 2014. ISSN 1873-4367 (Electronic)0927-7765 (Linking). Available at: &lt; <http://dx.doi.org/10.1016/j.colsurfb.2014.06.037> .
- DOKTOROVOVA, S.; SOUTO, E. B.; SILVA, A. M. Nanotoxicology applied to solid lipid nanoparticles and nanostructured lipid carriers - a systematic review of in vitro data. **Eur J Pharm Biopharm**, v. 87, n. 1, p. 1-18, May 2014. ISSN 1873-3441. Available at: &lt; <https://www.ncbi.nlm.nih.gov/pubmed/24530885> .
- ELMOWAFY, M. et al. Enhancement of Bioavailability and Pharmacodynamic Effects of Thymoquinone Via Nanostructured Lipid Carrier (NLC) Formulation. **AAPS PharmSciTech**, v. 17, n. 3, p. 663-72, Jun 2016. ISSN 1530-9932. Available at: &lt; <http://dx.doi.org/10.1208/s12249-015-0391-0> .
- ESPOSITO, E. et al. Effect of nanostructured lipid vehicles on percutaneous absorption of curcumin. **Eur J Pharm Biopharm**, v. 86, n. 2, p. 121-32, Feb 2014. ISSN 1873-3441. Available at: &lt; <https://www.ncbi.nlm.nih.gov/pubmed/24361485> .
- FALCAO, S. A. C. et al. Leishmania infantum and Leishmania braziliensis: Differences and Similarities to Evade the Innate Immune System. **Front Immunol**, v. 7, p. 287, 2016. ISSN 1664-3224. Available at: &lt; <http://dx.doi.org/10.3389/fimmu.2016.00287> .
- FANG, C. et al. In vivo tumor targeting of tumor necrosis factor-alpha-loaded stealth nanoparticles: effect of MePEG molecular weight and particle size. **Eur J Pharm Sci**, v. 27, n. 1, p. 27-36, Jan 2006. ISSN 0928-0987. Available at: &lt; <http://www.ncbi.nlm.nih.gov/pubmed/16150582> .
- FARAJI, A. H.; WIPF, P. Nanoparticles in cellular drug delivery. **Bioorganic & Medicinal Chemistry**. 17: 2950–2962 p. 2009.
- FDA. **Guidance for Industry Estimating the Maximum Safe Starting Dose in Initial Clinical Trials for Therapeutics in Adult Healthy Volunteers**. (CDER), C. F. D. E. A. R. 2005.
- FDA. **Waiver of In Vivo Bioavailability and Bioequivalence Studies for Immediate-Release Solid Oral Dosage Forms Based on a Biopharmaceutics Classification System** 2015.
- FENG, J.; ZHAO, L.; YU, Q. Receptor-mediated stimulatory effect of oligochitosan in macrophages. **Biochem Biophys Res Commun**, v. 317, n. 2, p. 414-20, Apr 30 2004. ISSN 0006-291X (Print)0006-291x. Available at: &lt; <http://dx.doi.org/10.1016/j.bbrc.2004.03.048> .

- FREITAS, C.; MÜLLER, R. H. Correlation between long-term stability of solid lipid nanoparticles (SLN) and crystallinity of the lipid phase. **Eur J Pharm Biopharm**, v. 47, n. 2, p. 125-32, Mar 1999. ISSN 0939-6411. Available at: &lt; <https://www.ncbi.nlm.nih.gov/pubmed/10234536> .
- FRICKER, G. et al. Phospholipids and lipid-based formulations in oral drug delivery. **Pharm Res**, v. 27, n. 8, p. 1469-86, Aug 2010. ISSN 0724-8741. Available at: &lt; <http://dx.doi.org/10.1007/s11095-010-0130-x> .
- GAN, Y.; QIAO, L. Combustion characteristics of fuel droplets with addition of nano and micron-sized aluminum particles. **Combustion and Flame**: Elsevier. 158: 354–368 p. 2011.
- GARCIA-FUENTES, M. et al. A comparative study of the potential of solid triglyceride nanostructures coated with chitosan or poly(ethylene glycol) as carriers for oral calcitonin delivery. **Eur J Pharm Sci**, v. 25, n. 1, p. 133-43, May 2005. ISSN 0928-0987. Available at: &lt; <https://www.ncbi.nlm.nih.gov/pubmed/15854809> .
- GARG, N. J. Global health: neglected diseases and access to medicines. **Infect Dis Clin North Am**, v. 25, n. 3, p. 639-51, ix-x, Sep 2011. ISSN 1557-9824. Available at: &lt; <https://www.ncbi.nlm.nih.gov/pubmed/21896364> .
- GARG, N. K. et al. Nanostructured lipid carrier mediates effective delivery of methotrexate to induce apoptosis of rheumatoid arthritis via NF-kappaB and FOXO1. **Int J Pharm**, v. 499, n. 1-2, p. 301-20, Feb 29 2016. ISSN 0378-5173. Available at: &lt; <http://dx.doi.org/10.1016/j.ijpharm.2015.12.061> .
- GELDERBLOM, H. et al. Cremophor EL: the drawbacks and advantages of vehicle selection for drug formulation. **Eur J Cancer**, v. 37, n. 13, p. 1590-8, Sep 2001. ISSN 0959-8049 (Print)0959-8049.
- GHARIB, R. et al. Liposomes incorporating cyclodextrin-drug inclusion complexes: Current state of knowledge. **Carbohydr Polym**, v. 129, p. 175-86, Sep 2015. ISSN 1879-1344. Available at: &lt; <https://www.ncbi.nlm.nih.gov/pubmed/26050903>.
- GLOMME, A.; MÄRZ, J.; DRESSMAN, J. B. Comparison of a miniaturized shake-flask solubility method with automated potentiometric acid/base titrations and calculated solubilities. **J Pharm Sci**, v. 94, n. 1, p. 1-16, Jan 2005. ISSN 0022-3549. Available at: &lt; <https://www.ncbi.nlm.nih.gov/pubmed/15761925>.
- GOSWAMI, T. et al. In silico model of drug permeability across sublingual mucosa. **Arch Oral Biol**, v. 58, n. 5, p. 545-51, May 2013. ISSN 1879-1506. Available at: &lt; <https://www.ncbi.nlm.nih.gov/pubmed/23123066> .
- HAO, J. et al. Fabrication of a composite system combining solid lipid nanoparticles and thermosensitive hydrogel for challenging ophthalmic drug delivery.

**Colloids Surf B Biointerfaces**, v. 114, p. 111-20, Feb 01 2014. ISSN 0927-7765. Available at: &lt;  
<http://dx.doi.org/10.1016/j.colsurfb.2013.09.059> .

HE, C. et al. Effects of particle size and surface charge on cellular uptake and biodistribution of polymeric nanoparticles. v. 31, n. 13, p. 3657–3666, May 2010. Available at: &lt;  
<http://dx.doi.org/10.1016/j.biomaterials.2010.01.065> .

HE, Q. et al. A pH-responsive mesoporous silica nanoparticles-based multi-drug delivery system for overcoming multi-drug resistance. **Biomaterials**, v. 32, n. 30, p. 7711-20, Oct 2011. ISSN 1878-5905. Available at: &lt;  
<https://www.ncbi.nlm.nih.gov/pubmed/21816467> .

HE, W. et al. Nanoemulsion-templated shell-crosslinked nanocapsules as drug delivery systems. **Int J Pharm**, v. 445, n. 1-2, p. 69-78, Mar 2013. ISSN 1873-3476. Available at: &lt;  
<https://www.ncbi.nlm.nih.gov/pubmed/23396257> .

HEBISHY, E. et al. Physical and oxidative stability of whey protein oil-in-water emulsions produced by conventional and ultra high-pressure homogenization: Effects of pressure and protein concentration on emulsion characteristics. **Innovative Food Science & Emerging Technologies**: Elsevier. 32: 79-90 p. 2015.

HENTSCHEL, A. et al. Beta-carotene-loaded nanostructured lipid carriers. **J Food Sci**, v. 73, n. 2, p. N1-6, Mar 2008. ISSN 1750-3841. Available at: &lt;  
<https://www.ncbi.nlm.nih.gov/pubmed/18298743> .

HO, H. et al. Small molecule proprotein convertase inhibitors for inhibition of embryo implantation. **PLoS One**, v. 8, n. 12, p. e81380, 2013. ISSN 1932-6203. Available at: &lt; <https://www.ncbi.nlm.nih.gov/pubmed/24324690> .

HOLM, R. et al. Structured triglyceride vehicles for oral delivery of halofantrine: examination of intestinal lymphatic transport and bioavailability in conscious rats. **Pharm Res**, v. 19, n. 9, p. 1354-61, Sep 2002. ISSN 0724-8741 (Print)0724-8741. Available at: &lt; <http://dx.doi.org/> .

HOLMES, B. et al. Protection of phagocytized bacteria from the killing action of antibiotics. **Nature**, v. 210, n. 5041, p. 1131-2, Jun 1966. ISSN 0028-0836. Available at: &lt; <http://www.ncbi.nlm.nih.gov/pubmed/5964315> .

HOTEZ, P. J. et al. Eliminating the Neglected Tropical Diseases: Translational Science and New Technologies. **PLoS Negl Trop Dis**, v. 10, n. 3, p. e0003895, Mar 2016. ISSN 1935-2735. Available at: &lt;  
<https://www.ncbi.nlm.nih.gov/pubmed/26934395> .

HU, F. Q. et al. Preparation and characteristics of monostearin nanostructured lipid carriers. **Int J Pharm**, v. 314, n. 1, p. 83-9, May 2006. ISSN 0378-5173. Available at: &lt; <https://www.ncbi.nlm.nih.gov/pubmed/16563671> .

- IBRAHIM, W. M.; ALOMRANI, A. H.; AE, B. Y. Novel sulpiride-loaded solid lipid nanoparticles with enhanced intestinal permeability. In: (Ed.). **Int J Nanomedicine**, v.9, 2014. p.129-44. ISBN 1176-9114 (Print)1178-2013 (Electronic).
- ICH. **Guidance for Industry, Q8(R2) Pharmaceutical Development**. ICH HARMONISED TRIPARTITE GUIDELINE. 2009
- JOUBYBAN, A.; FAKHREE, M. A.; SHAYANFAR, A. Review of pharmaceutical applications of N-methyl-2-pyrrolidone. **J Pharm Pharm Sci**, v. 13, n. 4, p. 524-35, 2010. ISSN 1482-1826. Available at: &lt; http://dx.doi.org/ .
- JUNYAPRASERT, V. B.; MORAKUL, B. Nanocrystals for enhancement of oral bioavailability of poorly water-soluble drugs. **Asian Journal of Pharmaceutical Sciences**, v. 10, n. 1, p. 13-23, 2015.
- JUNYAPRASERT, V. B. et al. Q10-loaded NLC versus nanoemulsions: stability, rheology and in vitro skin permeation. **Int J Pharm**, v. 377, n. 1-2, p. 207-14, Jul 2009. ISSN 1873-3476. Available at: &lt; https://www.ncbi.nlm.nih.gov/pubmed/19465098 .
- KAITHWAS, V. et al. Nanostructured lipid carriers of olmesartan medoxomil with enhanced oral bioavailability. **Colloids Surf B Biointerfaces**, v. 154, p. 10-20, Jun 2017. ISSN 1873-4367. Available at: &lt; https://www.ncbi.nlm.nih.gov/pubmed/28284054 .
- KALEPU, S.; MANTHINA, M.; PADAVALA, V. Oral lipid-based drug delivery systems – an overview. v. 3, n. 6, p. 361–372, December 2013 2013. Available at: &lt; https://doi.org/10.1016/j.apsb.2013.10.001 .
- KANG, Y. S. et al. SIGN-R1, a novel C-type lectin expressed by marginal zone macrophages in spleen, mediates uptake of the polysaccharide dextran. **Int Immunol**, v. 15, n. 2, p. 177-86, Feb 2003. ISSN 0953-8178 (Print)0953-8178. Available at: &lt; http://intimm.oxfordjournals.org/content/15/2/177.full .
- KASHANIAN, S.; AZANDARYANI, A. H.; DERAKHSHANDEH, K. New surface-modified solid lipid nanoparticles using N-glutaryl phosphatidylethanolamine as the outer shell. In: (Ed.). **Int J Nanomedicine**, v.6, 2011. p.2393-401. ISBN 1176-9114 (Print)1178-2013 (Electronic).
- KASONGO, K. W. et al. Selection and characterization of suitable lipid excipients for use in the manufacture of didanosine-loaded solid lipid nanoparticles and nanostructured lipid carriers. **J Pharm Sci**, v. 100, n. 12, p. 5185-96, Dec 2011. ISSN 1520-6017 (Electronic)0022-3549 (Linking). Available at: &lt; http://dx.doi.org/10.1002/jps.22711 .

- KATZ, L. M.; DEWAN, K.; BRONAUGH, R. L. Nanotechnology in cosmetics. **Food Chem Toxicol**, v. 85, p. 127-37, Nov 2015. ISSN 1873-6351. Available at: &lt; <https://www.ncbi.nlm.nih.gov/pubmed/26159063> .
- KAWAUCHI, Y.; KURODA, Y.; KOJIMA, N. Preferences for uptake of carbohydrate-coated liposomes by C-type lectin receptors as antigen-uptake receptors. **Glycoconj J**, v. 29, n. 7, p. 481-90, Oct 2012. ISSN 1573-4986. Available at: &lt; <http://www.ncbi.nlm.nih.gov/pubmed/22733147> .
- \_\_\_\_\_. Comparison of the carbohydrate preference of SIGNR1 as a phagocytic receptor with the preference as an adhesion molecule. **Int Immunopharmacol**, v. 19, n. 1, p. 27-36, Mar 2014. ISSN 1878-1705. Available at: &lt; <https://www.ncbi.nlm.nih.gov/pubmed/24434373> .
- KAYE, P.; SCOTT, P. Leishmaniasis: complexity at the host-pathogen interface. **Nat Rev Microbiol**, v. 9, n. 8, p. 604-15, Jul 2011. ISSN 1740-1534. Available at: &lt; <https://www.ncbi.nlm.nih.gov/pubmed/21747391> .
- KECK, C. M. Particle size analysis of nanocrystals: improved analysis method. **Int J Pharm**, v. 390, n. 1, p. 3-12, May 2010. ISSN 1873-3476. Available at: &lt; <https://www.ncbi.nlm.nih.gov/pubmed/19733647> .
- KEDMI, R.; BEN-ARIE, N.; PEER, D. The systemic toxicity of positively charged lipid nanoparticles and the role of Toll-like receptor 4 in immune activation. **Biomaterials**, v. 31, n. 26, p. 6867-75, Sep 2010. ISSN 0142-9612. Available at: &lt; <http://dx.doi.org/10.1016/j.biomaterials.2010.05.027> .
- KHAN, S. et al. Chlorogenic acid stabilized nanostructured lipid carriers (NLC) of atorvastatin: formulation, design and in vivo evaluation. **Drug Dev Ind Pharm**, v. 42, n. 2, p. 209-20, 2016. ISSN 0363-9045. Available at: &lt; <http://dx.doi.org/10.3109/03639045.2015.1040414> .
- KOBETS, T.; GREKOV, I.; LIPOLDOVA, M. Leishmaniasis: prevention, parasite detection and treatment. In: (Ed.). **Curr Med Chem**. Netherlands, v.19, 2012. p.1443-74. ISBN 1875-533X (Electronic)0929-8673 (Linking).
- KOVACEVIC, A. et al. Polyhydroxy surfactants for the formulation of lipid nanoparticles (SLN and NLC): effects on size, physical stability and particle matrix structure. **Int J Pharm**, v. 406, n. 1-2, p. 163-72, Mar 2011. ISSN 1873-3476. Available at: &lt; <https://www.ncbi.nlm.nih.gov/pubmed/21219990> .
- KOVÁCS, A. et al. Development of nanostructured lipid carriers containing salicylic acid for dermal use based on the Quality by Design method. **Eur J Pharm Sci**, v. 99, p. 246-257, Mar 2017. ISSN 1879-0720. Available at: &lt; <https://www.ncbi.nlm.nih.gov/pubmed/28012940> .
- KUNIEDA, H. et al. Formation of microemulsions in mixed ionic-nonionic surfactant systems. **Langmuir**, v. 14, n. 2, p. 260–263, 1998.

- LAURENTI, M. D. et al. Asymptomatic dogs are highly competent to transmit *Leishmania (Leishmania) infantum chagasi* to the natural vector. **Vet Parasitol**, v. 196, n. 3-4, p. 296-300, Sep 23 2013. ISSN 0304-4017. Available at: &lt; <http://dx.doi.org/10.1016/j.vetpar.2013.03.017> .
- LE BARS, G. et al. Oral toxicity of Miglyol 812((R)) in the Gottingen((R)) minipig. **Regul Toxicol Pharmacol**, v. 73, n. 3, p. 930-7, Dec 2015. ISSN 0273-2300. Available at: &lt; <http://dx.doi.org/10.1016/j.yrtph.2015.09.022> .
- LEESON, P. D. Molecular inflation, attrition and the rule of five. **Adv Drug Deliv Rev**, v. 101, p. 22-33, Jun 2016. ISSN 1872-8294. Available at: &lt; <https://www.ncbi.nlm.nih.gov/pubmed/26836397> .
- LIESE, B.; ROSENBERG, M.; SCHRATZ, A. Programmes, partnerships, and governance for elimination and control of neglected tropical diseases. **Lancet**, v. 375, n. 9708, p. 67-76, Jan 2010. ISSN 1474-547X. Available at: &lt; <https://www.ncbi.nlm.nih.gov/pubmed/20109865> .
- LIN, B.; PEASE, J. H. A high throughput solubility assay for drug discovery using microscale shake-flask and rapid UHPLC-UV-CLND quantification. **J Pharm Biomed Anal**, v. 122, p. 126-40, Apr 2016. ISSN 1873-264X. Available at: &lt; <https://www.ncbi.nlm.nih.gov/pubmed/26855285> .
- LIN, C. et al. A novel oral delivery system consisting in &quot;drug-in cyclodextrin-in nanostructured lipid carriers&quot; for poorly water-soluble drug: vinpocetine. **Int J Pharm**, v. 465, n. 1-2, p. 90-6, Apr 2014. ISSN 1873-3476. Available at: &lt; <https://www.ncbi.nlm.nih.gov/pubmed/24530388> .
- LIN, Q. et al. Lipid-based nanoparticles in the systemic delivery of siRNA. **Nanomedicine (Lond)**, v. 9, n. 1, p. 105-20, Jan 2014. ISSN 1748-6963. Available at: &lt; <https://www.ncbi.nlm.nih.gov/pubmed/24354813> .
- LIN, X. et al. Preparation and characterization of monocaprato nanostructured lipid carriers. v. 311, n. Issues 1–3, p. 106–111, 1 December 2007 2007. Available at: &lt; <https://doi.org/10.1016/j.colsurfa.2007.06.003> .
- LIN, Y. et al. Delivery of large molecules via poly(butyl cyanoacrylate) nanoparticles into the injured rat brain. **Nanotechnology**, v. 23, n. 16, p. 165101, Apr 2012. ISSN 1361-6528. Available at: &lt; <http://www.ncbi.nlm.nih.gov/pubmed/22460562> .
- LINDOSO, J. A. L. et al. **Review of the current treatments for leishmaniasis.** Research and Reports in Tropical Medicine: Dove Press. 3: 69-77 p. 2012.
- LIU, D. et al. Potential advantages of a novel chitosan-N-acetylcysteine surface modified nanostructured lipid carrier on the performance of ophthalmic delivery of curcumin. **Sci Rep**, v. 6, p. 28796, Jun 28 2016. ISSN 2045-2322. Available at: &lt; <http://dx.doi.org/10.1038/srep28796> .

- LIU, J. L. et al. Sustained-release genistein from nanostructured lipid carrier suppresses human lens epithelial cell growth. **Int J Ophthalmol**, v. 9, n. 5, p. 643-9, 2016. ISSN 2222-3959 (Print)2222-3959. Available at: &lt; <http://dx.doi.org/10.18240/ijo.2016.05.01> .
- LIU, X.; HUANG, G. Formation strategies, mechanism of intracellular delivery and potential clinical applications of pH-sensitive liposomes. **Asian Journal of Pharmaceutical Sciences**. 8: 319–328 p. 2013.
- LIU, Z. et al. Mixed polyethylene glycol-modified breviscapine-loaded solid lipid nanoparticles for improved brain bioavailability: preparation, characterization, and in vivo cerebral microdialysis evaluation in adult Sprague Dawley rats. **AAPS PharmSciTech**, v. 15, n. 2, p. 483-96, Apr 2014. ISSN 1530-9932 (Electronic)1530-9932 (Linking). Available at: &lt; <http://dx.doi.org/10.1208/s12249-014-0080-4> .
- LOUTET, S. A.; VALVANO, M. A. Extreme antimicrobial peptide and polymyxin B resistance in the genus Burkholderia. **Front Cell Infect Microbiol**, v. 1, p. 6, 2011. ISSN 2235-2988. Available at: &lt; <http://dx.doi.org/10.3389/fcimb.2011.00006> .
- LOVELYN, C.; ATTAMA, A. A. Current State of Nanoemulsions in Drug Delivery. **Journal of Biomaterials and Nanobiotechnology**, v. 02, n. 05, p. 626-639, 2011-12-09 2011. ISSN 2158-70272158-7043. Available at: &lt; <https://www.scirp.org/journal/PaperInformation.aspx?PaperID=9112> .
- LUNOV, O. et al. Differential uptake of functionalized polystyrene nanoparticles by human macrophages and a monocytic cell line. **ACS Nano**, v. 5, n. 3, p. 1657-69, Mar 22 2011. ISSN 1936-0851. Available at: &lt; <http://dx.doi.org/10.1021/nn2000756> .
- MADANE, R. G.; MAHAJAN, H. S. Curcumin-loaded nanostructured lipid carriers (NLCs) for nasal administration: design, characterization, and in vivo study. **Drug Deliv**, v. 23, n. 4, p. 1326-34, May 2016. ISSN 1521-0464. Available at: &lt; <https://www.ncbi.nlm.nih.gov/pubmed/25367836> .
- MAROLI, M. et al. Phlebotomine sandflies and the spreading of leishmaniasis and other diseases of public health concern. **Med Vet Entomol**, v. 27, n. 2, p. 123-47, Jun 2013. ISSN 1365-2915. Available at: &lt; <https://www.ncbi.nlm.nih.gov/pubmed/22924419> .
- MARR, A. K.; MCGWIRE, B. S.; MCMASTER, W. R. Modes of action of Leishmanicidal antimicrobial peptides. **Future Microbiol**, v. 7, n. 9, p. 1047-59, Sep 2012. ISSN 1746-0913. Available at: &lt; <http://dx.doi.org/10.2217/fmb.12.85> .
- MCELFRESH, P. M.; HOLCOMB, D. L.; ECTOR, D. Application of Nanofluid Technology to Improve Recovery in Oil and Gas Wells. **SPE Conference Paper**. The Netherlands: Society of Petroleum Engineers. 2012.



- MCGWIRE, B. S.; SATOSKAR, A. R. Leishmaniasis: clinical syndromes and treatment. **QJM**, v. 107, n. 1, p. 7-14, Jan 2014. ISSN 1460-2393. Available at: &lt; <https://www.ncbi.nlm.nih.gov/pubmed/23744570> .
- MEHNERT, W.; MÄDER, K. Solid lipid nanoparticles: production, characterization and applications. **Adv Drug Deliv Rev**, v. 47, n. 2-3, p. 165-96, Apr 2001. ISSN 0169-409X. Available at: &lt; <https://www.ncbi.nlm.nih.gov/pubmed/11311991> .
- MENDES, A. I. et al. Miconazole-loaded nanostructured lipid carriers (NLC) for local delivery to the oral mucosa: improving antifungal activity. **Colloids Surf B Biointerfaces**, v. 111, p. 755-63, Nov 1 2013. ISSN 1873-4367 (Electronic)0927-7765 (Linking). Available at: &lt; <http://dx.doi.org/10.1016/j.colsurfb.2013.05.041> .
- MOLOUGHNEY, J. G.; WEISLEDER, N. Poloxamer 188 (p188) as a membrane resealing reagent in biomedical applications. **Recent Pat Biotechnol**, v. 6, n. 3, p. 200-11, Dec 2012. ISSN 2212-4012. Available at: &lt; <https://www.ncbi.nlm.nih.gov/pubmed/23092436> .
- MONTEIRO, L. M. et al. Buparvaquone Nanostructured Lipid Carrier: Development of an Affordable Delivery System for the Treatment of Leishmaniasis. **Biomed Res Int**, v. 2017, p. 9781603, 2017. ISSN 2314-6141. Available at: &lt; <https://www.ncbi.nlm.nih.gov/pubmed/28255558> .
- \_\_\_\_\_. Targeting Leishmania amazonensis amastigotes through macrophage internalisation of a hydroxymethylnitrofurazone nanostructured polymeric system. **Int J Antimicrob Agents**, v. 50, n. 1, p. 88-92, Jul 2017. ISSN 1872-7913. Available at: &lt; <https://www.ncbi.nlm.nih.gov/pubmed/28454918> .
- MONTGOMERY, D. C. **Design and analysis of experiments**. 6. John Wiley & Sons, Inc, 2004. 660 ISBN 047148735X
- MORAN, M. et al. Neglected disease research and development: how much are we really spending? **PLoS Med**, v. 6, n. 2, p. e30, Feb 2009. ISSN 1549-1676. Available at: &lt; <https://www.ncbi.nlm.nih.gov/pubmed/19192946> .
- MOREL, S. et al. Thymopentin in solid lipid nanoparticles **International Journal of Pharmaceutics**: Elsevier. 132: 259-261 p. 1996.
- MUCHOW, M. et al. Testosterone undecanoate – increase of oral bioavailability by nanostructured lipid carriers (NLC). **Journal of Pharmaceutical Technology & Drug Research**, v. 2013, p. 10, 2013.
- MULLER, R. H. et al. Oral bioavailability of cyclosporine: solid lipid nanoparticles (SLN) versus drug nanocrystals. In: (Ed.). **Int J Pharm**. Netherlands, v.317, 2006. p.82-9. ISBN 0378-5173 (Print)0378-5173 (Linking).

- MULVANEY, P. Nanoscience vs nanotechnology--defining the field. **ACS Nano**, v. 9, n. 3, p. 2215-7, Mar 2015. ISSN 1936-086X. Available at: &lt;<https://www.ncbi.nlm.nih.gov/pubmed/25802086> .
- MUNIR, A. et al. Structure-Based Pharmacophore Modeling, Virtual Screening and Molecular docking for the Treatment of ESR1 Mutations in Breast Cancer. **Drug Designing** v.5 ,2016.
- MYERS, R. H. et al. **Response Surface Methodology: Process and Product Optimization Using Designed Experiments, 3rd Edition**. 3. John Wiley & Sons, 2009. 704 ISBN 978-0-470-17446-3.
- MÜLLER, J. et al. Buparvaquone is active against *Neospora caninum* in vitro and in experimentally infected mice. **Int J Parasitol Drugs Drug Resist**, v. 5, n. 1, p. 16-25, Apr 2015. Available at: &lt;<https://www.ncbi.nlm.nih.gov/pubmed/25941626> .
- \_\_\_\_\_. Repurposing of antiparasitic drugs: the hydroxy-naphthoquinone buparvaquone inhibits vertical transmission in the pregnant neosporosis mouse model. **Vet Res**, v. 47, p. 32, Feb 2016. ISSN 1297-9716. Available at: &lt;<https://www.ncbi.nlm.nih.gov/pubmed/26883424> .
- NAHAR, M. et al. In vitro evaluation of surface functionalized gelatin nanoparticles for macrophage targeting in the therapy of visceral leishmaniasis. **J Drug Target**, v. 18, n. 2, p. 93-105, Feb 2010. ISSN 1026-7158. Available at: &lt;<http://dx.doi.org/10.3109/10611860903115290> .
- NAIR, A. B.; JACOB, S. A simple practice guide for dose conversion between animals and human. **J Basic Clin Pharm**, v. 7, n. 2, p. 27-31, Mar 2016. ISSN 0976-0105 (Print)0976-0113. Available at: &lt;<http://dx.doi.org/10.4103/0976-0105.177703> .
- NAKAGAWA, J. et al. Towards effective prevention and control of helminth neglected tropical diseases in the Western Pacific Region through multi-disease and multi-sectoral interventions. **Acta Trop**, v. 141, n. Pt B, p. 407-18, Jan 2015. ISSN 1873-6254. Available at: &lt;<https://www.ncbi.nlm.nih.gov/pubmed/23792012> .
- NATARAJAN, U.; PERIYANAN, P. R.; YANG, S. H. Multipleresponse optimization for micro-endmilling process using response surface methodology. **International Journal of Advanced Manufacturing Technology**, v. 56, n. 1, p. 177–185, 2011.
- NATEGHI ROSTAMI, M. et al. Tumour Necrosis Factor-alpha (TNF- $\alpha$ ) and its soluble receptor type 1 (sTNFR I) in human active and healed leishmaniasis. **Parasite Immunol**, v. 38, n. 4, p. 255-60, Apr 2016. ISSN 1365-3024. Available at: &lt;<https://www.ncbi.nlm.nih.gov/pubmed/26813918> .

- NEGI, L. M.; JAGGI, M.; TALEGAONKAR, S. Development of protocol for screening the formulation components and the assessment of common quality problems of nano-structured lipid carriers. **Int J Pharm**, v. 461, n. 1-2, p. 403-10, Jan 2014. ISSN 1873-3476. Available at: &lt;<https://www.ncbi.nlm.nih.gov/pubmed/24345574> .
- NGUYEN, M. et al. Effects of the physical state of nanocarriers on their penetration into the root and upward transportation to the stem of soybean plants using confocal laser scanning microscopy. **Crop Protection**, v. 87, p. 25–30, September 2016 2016. Available at: &lt;<https://doi.org/10.1016/j.cropro.2016.04.012> .
- NIKOLIC, S. et al. Skin photoprotection improvement: synergistic interaction between lipid nanoparticles and organic UV filters. **Int J Pharm**, v. 414, n. 1-2, p. 276-84, 2011. ISSN 1873-3476 (Electronic)0378-5173 (Linking). Available at: &lt;<http://dx.doi.org/10.1016/j.ijpharm.2011.05.010> .
- NOGARA, P. A. et al. Virtual screening of acetylcholinesterase inhibitors using the Lipinski's rule of five and ZINC databank. **Biomed Res Int**, v. 2015, p. 870389, 2015. ISSN 2314-6141. Available at: &lt;<https://www.ncbi.nlm.nih.gov/pubmed/25685814> .
- OLIVEIRA, L. F. et al. Systematic review of the adverse effects of cutaneous leishmaniasis treatment in the New World. **Acta Trop**, v. 118, n. 2, p. 87-96, May 2011. ISSN 1873-6254. Available at: &lt;<https://www.ncbi.nlm.nih.gov/pubmed/21420925> .
- OPS, O. P. D. L. S. **Leishmaniasis en las Américas: recomendaciones para el tratamiento** 2013.
- OTAROLA, J. et al. Capillary electrophoresis to determine entrapment efficiency of a nanostructured lipid carrier loaded with piroxicam. **Journal of Pharmaceutical Analysis**, v. 5, n. 1, p. 70–73, February 2015 2015. Available at: &lt;<https://doi.org/10.1016/j.jpha.2014.05.003> .
- OZAK, S. T.; OZKAN, P. Nanotechnology and dentistry. **Eur J Dent**, v. 7, n. 1, p. 145-51, Jan 2013. ISSN 1305-7456. Available at: &lt;<https://www.ncbi.nlm.nih.gov/pubmed/23408486> .
- PAAVER, U. et al. Electrospun nanofibers as a potential controlled-release solid dispersion system for poorly water-soluble drugs. **Int J Pharm**, v. 479, n. 1, p. 252-60, Feb 2015. ISSN 1873-3476. Available at: &lt;<https://www.ncbi.nlm.nih.gov/pubmed/25549852> .
- PARDEIKE, J. et al. Development of an itraconazole-loaded nanostructured lipid carrier (NLC) formulation for pulmonary application. **Int J Pharm**, v. 419, n. 1-2, p. 329-38, 2011. ISSN 1873-3476 (Electronic)0378-5173 (Linking). Available at: &lt;<http://dx.doi.org/10.1016/j.ijpharm.2011.07.040> .

- \_\_\_\_\_. Itraconazole-loaded nanostructured lipid carriers (NLC) for pulmonary treatment of aspergillosis in falcons. **Eur J Pharm Biopharm**, v. 108, p. 269-276, Nov 2016. ISSN 0939-6411. Available at: &lt; <http://dx.doi.org/10.1016/j.ejpb.2016.07.018> .
- PARVEEN, S.; MISRA, R.; SAHOO, S. K. Nanoparticles: a boon to drug delivery, therapeutics, diagnostics and imaging. **Nanomedicine**, v. 8, n. 2, p. 147-66, Feb 2012. ISSN 1549-9634. Available at: &lt; <http://dx.doi.org/10.1016/j.nano.2011.05.016> .
- PATIL-GADHE, A.; POKHARKAR, V. Montelukast-loaded nanostructured lipid carriers: part I oral bioavailability improvement. **Eur J Pharm Biopharm**, v. 88, n. 1, p. 160-8, Sep 2014. ISSN 1873-3441 (Electronic)0939-6411 (Linking). Available at: &lt; <http://dx.doi.org/10.1016/j.ejpb.2014.05.019> .
- PEZESHKI, A. et al. Encapsulation of Vitamin A Palmitate in Nanostructured Lipid Carrier (NLC)-Effect of Surfactant Concentration on the Formulation Properties. **Adv Pharm Bull**, v. 4, n. Suppl 2, p. 563-8, Dec 2014. ISSN 2228-5881 (Print)2228-5881. Available at: &lt; <http://dx.doi.org/10.5681/apb.2014.083> .
- PIGOTT, D. M. et al. Global distribution maps of the leishmaniases. **Elife**, v. 3, Jun 2014. ISSN 2050-084X. Available at: &lt; <https://www.ncbi.nlm.nih.gov/pubmed/24972829> .
- POKHREL, S.; REIDPATH, D.; ALLOTEY, P. Social sciences research in neglected tropical diseases 3: Investment in social science research in neglected diseases of poverty: a case study of Bill and Melinda Gates Foundation. **Health Res Policy Syst**, v. 9, p. 2, Jan 2011. ISSN 1478-4505. Available at: &lt; <https://www.ncbi.nlm.nih.gov/pubmed/21210999> .
- PORTER, C. J.; CHARMAN, W. N. Intestinal lymphatic drug transport: an update. **Adv Drug Deliv Rev**, v. 50, n. 1-2, p. 61-80, Aug 23 2001. ISSN 0169-409X (Print)0169-409x. Available at: &lt; <http://dx.doi.org/> .
- PUSTYLNIKOV, S. et al. Targeting the C-type lectins-mediated host-pathogen interactions with dextran. **J Pharm Pharm Sci**, v. 17, n. 3, p. 371-92, 2014. ISSN 1482-1826. Available at: &lt; <http://www.ncbi.nlm.nih.gov/pubmed/25224349> .
- RAJINIKANTH, P. S.; CHELLIAN, J. Development and evaluation of nanostructured lipid carrier-based hydrogel for topical delivery of 5-fluorouracil. **Int J Nanomedicine**, v. 11, p. 5067-5077, 2016. ISSN 1176-9114. Available at: &lt; <http://dx.doi.org/10.2147/ijn.s117511> .
- RANPISE, N. S.; KORABU, S. S.; GHODAKE, V. N. Second generation lipid nanoparticles (NLC) as an oral drug carrier for delivery of lercanidipine hydrochloride. **Colloids Surf B Biointerfaces**, v. 116, p. 81-7, Apr 01 2014. ISSN 0927-7765. Available at: &lt; <http://dx.doi.org/10.1016/j.colsurfb.2013.12.012> .

- RAVANI, L. et al. Clotrimazole-loaded nanostructured lipid carrier hydrogels: thermal analysis and in vitro studies. **Int J Pharm**, v. 454, n. 2, p. 695-702, Oct 01 2013. ISSN 0378-5173. Available at: &lt;<http://dx.doi.org/10.1016/j.ijpharm.2013.06.015> .
- REIMÃO, J. Q. et al. Effectiveness of liposomal buparvaquone in an experimental hamster model of Leishmania (L.) infantum chagasi. **Exp Parasitol**, v. 130, n. 3, p. 195-9, Mar 2012. ISSN 1090-2449. Available at: &lt;<https://www.ncbi.nlm.nih.gov/pubmed/22281156> .
- REUS, M. et al. Visceral leishmaniasis: diagnosis by ultrasound-guided fine needle aspiration of an axillary node. **Br J Radiol**, v. 78, n. 926, p. 158-60, Feb 2005. ISSN 0007-1285 (Print)0007-1285. Available at: &lt;<http://dx.doi.org/10.1259/bjr/33263789> .
- RIBEIRO, L. N. et al. Nanostructured lipid carriers as robust systems for topical lidocaine-prilocaine release in dentistry. **Eur J Pharm Sci**, v. 93, p. 192-202, Oct 2016. ISSN 1879-0720. Available at: &lt;<https://www.ncbi.nlm.nih.gov/pubmed/27543066> .
- SACHAN, A. K.; GUPTA, A.; ARORA, M. FORMULATION & CHARACTERIZATION OF NANOSTRUCTURED LIPID CARRIER (NLC) BASED GEL FOR TOPICAL DELIVERY OF ETORICOXIB. **Journal of Drug Delivery and Therapeutics**, v. 6, n. 2, 2016-03-15 2016. Available at: &lt;<http://jddtonline.info/index.php/jddt/article/view/1222> .
- SAVJANI, K. T.; GAJJAR, A. K.; SAVJANI, J. K. Drug solubility: importance and enhancement techniques. **ISRN Pharm**, v. 2012, p. 195727, 2012. ISSN 2090-6153. Available at: &lt;<https://www.ncbi.nlm.nih.gov/pubmed/22830056> .
- SCHUCK, D. C. et al. Biological evaluation of hydroxynaphthoquinones as anti-malarials. **Malar J**, v. 12, p. 234, Jul 2013. ISSN 1475-2875. Available at: &lt;<https://www.ncbi.nlm.nih.gov/pubmed/23841934> .
- SCHWARZ, C. et al. Solid lipid nanoparticles (SLN) for controlled drug delivery. I. Production, characterization and sterilization - ScienceDirect. **Journal of Controlled Release**: Elsevier. 30: 83-96 p. 1994.
- SCHWARZ, J. C. et al. Ultra-small NLC for improved dermal delivery of coenzyme Q10. **Int J Pharm**, v. 447, n. 1-2, p. 213-7, Apr 2013. ISSN 1873-3476. Available at: &lt;<https://www.ncbi.nlm.nih.gov/pubmed/23438979> .
- SEO, W. G. et al. Synergistic cooperation between water-soluble chitosan oligomers and interferon-gamma for induction of nitric oxide synthesis and tumoricidal activity in murine peritoneal macrophages. **Cancer Lett**, v. 159, n. 2, p. 189-95, Oct 31 2000. ISSN 0304-3835 (Print)0304-3835. Available at: &lt;<http://dx.doi.org/> .

- SEVERINO, P. et al. Polymorphism, crystallinity and hydrophilic-lipophilic balance of stearic acid and stearic acid-capric/caprylic triglyceride matrices for production of stable nanoparticles. **Colloids Surf B Biointerfaces**, v. 86, n. 1, p. 125-30, 2011. ISSN 1873-4367 (Electronic)0927-7765 (Linking). Available at: <http://dx.doi.org/10.1016/j.colsurfb.2011.03.029 .
- SEVERINO, P.; SANTANA, M. H.; SOUTO, E. B. Optimizing SLN and NLC by 2(2) full factorial design: effect of homogenization technique. **Mater Sci Eng C Mater Biol Appl**, v. 32, n. 6, p. 1375-9, 2012. ISSN 1873-0191 (Electronic)0928-4931 (Linking). Available at: <http://dx.doi.org/10.1016/j.msec.2012.04.017 .
- SEZER, A. D. **Application of Nanotechnology in Drug Delivery**. 2014. ISBN 978-953-51-1628-8.
- SHEGOKAR, R.; MÜLLER, R. H. Nanocrystals: industrially feasible multifunctional formulation technology for poorly soluble actives. **Int J Pharm**, v. 399, n. 1-2, p. 129-39, Oct 2010. ISSN 1873-3476. Available at: <https://www.ncbi.nlm.nih.gov/pubmed/20674732 .
- SHETE, H.; PATRAVALE, V. Long chain lipid based tamoxifen NLC. Part I: preformulation studies, formulation development and physicochemical characterization. **Int J Pharm**, v. 454, n. 1, p. 573-83, Sep 15 2013. ISSN 0378-5173. Available at: <http://dx.doi.org/10.1016/j.ijpharm.2013.03.034 .
- SHUKLA, A. K.; PATRA, S.; DUBEY, V. K. Nanospheres encapsulating anti-leishmanial drugs for their specific macrophage targeting, reduced toxicity, and deliberate intracellular release. **Vector Borne Zoonotic Dis**, v. 12, n. 11, p. 953-60, Nov 2012. ISSN 1530-3667. Available at: <http://dx.doi.org/10.1089/vbz.2011.0948 .
- SIEKMANN, B.; WESTESEN, K. Thermoanalysis of the recrystallization process of melt-homogenized glyceride nanoparticles. **Colloids and Surfaces B: Biointerfaces**, v. 3, n. 3, p. 159-175, 1994.
- SINGH, R. K. et al. Targeting Leishmania Species: Nanotechnological Prospects. **Advanced Science Letters**, v. 5, n. 1, p. 11-20, January 2012 2012. Available at: <http://www.ingentaconnect.com/content/asp/asl/2012/00000005/00000001/art00002 .
- SINGH, Y. et al. Nanoemulsion: Concepts, development and applications in drug delivery. **J Control Release**, v. 252, p. 28-49, Mar 2017. ISSN 1873-4995. Available at: <https://www.ncbi.nlm.nih.gov/pubmed/28279798 .
- SOUTO, E. B.; MULLER, R. H. Solid Lipid Nanoparticles and Nanostructured Lipid Carriers-Lipid Nanoparticles for Medicals and Pharmaceutica. **Encyclopedia of Nanoscience and Nanotechnology**, Valencia-US,

2011. ISSN 1-58883-188-4. Available at: < http://www.muller-berlin.com/Download/more\_pdf/chapter/68.PDF .

SOUTO, E. B.; MÜLLER, R. H. SLN and NLC for topical delivery of ketoconazole. **J Microencapsul**, v. 22, n. 5, p. 501-10, Aug 2005. ISSN 0265-2048. Available at: < https://www.ncbi.nlm.nih.gov/pubmed/16361193 .

STRICKLEY, R. G. Solubilizing excipients in oral and injectable formulations. **Pharm Res**, v. 21, n. 2, p. 201-30, Feb 2004. ISSN 0724-8741 (Print)0724-8741. Available at: < http://dx.doi.org/ .

STROPPIA, P. H. F. et al. Effect of 1,2,3-triazole salts, non-classical bioisosteres of miltefosine, on *Leishmania amazonensis*. **Bioorg Med Chem**, Mar 2017. ISSN 1464-3391. Available at: < https://www.ncbi.nlm.nih.gov/pubmed/28433512 .

SUNDAR, S.; CHAKRAVARTY, J. Liposomal amphotericin B and leishmaniasis: dose and response. **J Glob Infect Dis**, v. 2, n. 2, p. 159-66, May 2010. ISSN 0974-8245. Available at: < https://www.ncbi.nlm.nih.gov/pubmed/20606972 .

SÁNCHEZ-LÓPEZ, E. et al. Lipid nanoparticles (SLN, NLC): Overcoming the anatomical and physiological barriers of the eye - Part II - Ocular drug-loaded lipid nanoparticles. **Eur J Pharm Biopharm**, v. 110, p. 58-69, Jan 2017. ISSN 1873-3441. Available at: < https://www.ncbi.nlm.nih.gov/pubmed/27789359 .

TAKAHARA, K. et al. C-type lectin SIGNR1 enhances cellular oxidative burst response against *C. albicans* in cooperation with Dectin-1. **Eur J Immunol**, v. 41, n. 5, p. 1435-44, May 2011. ISSN 0014-2980. Available at: < http://dx.doi.org/10.1002/eji.200940188 .

\_\_\_\_\_. Functional comparison of the mouse DC-SIGN, SIGNR1, SIGNR3 and Langerin, C-type lectins. **Int Immunol**, v. 16, n. 6, p. 819-29, Jun 2004. ISSN 0953-8178. Available at: < http://www.ncbi.nlm.nih.gov/pubmed/15096474 .

TAMJID, F. et al. Nanostructured lipid carriers (NLC): A potential delivery system for bioactive food molecules. **Innovative Food Science & Emerging Technologies**: Elsevier. 19: 29–43 p. 2013.

TEERANACHAIDEEKUL, V.; CHANTABURANAN, T.; JUNYAPRASERT, V. P. Influence of state and crystallinity of lipid matrix on physicochemical properties and permeation of capsaicin-loaded lipid nanoparticles for topical delivery. **Journal of Drug Delivery Science and Technology**, v. 39, p. 300-307, 2017.

THORAT, A. A.; DALVI, S. V. Liquid antisolvent precipitation and stabilization of nanoparticles of poorly water soluble drugs in aqueous suspensions:

Recent developments and future perspective. **Chemical Engineering Journal**. 181-182: 1–34 p. 2012.

- TILA, D. et al. Functional liposomes in the cancer-targeted drug delivery. **J Biomater Appl**, v. 30, n. 1, p. 3-16, Jul 2015. ISSN 1530-8022. Available at: &lt; <https://www.ncbi.nlm.nih.gov/pubmed/25823898> .
- TIUMAN, T. S. et al. Recent advances in leishmaniasis treatment. **Int J Infect Dis**, v. 15, n. 8, p. e525-32, 2011. ISSN 1878-3511 (Electronic)1201-9712 (Linking). Available at: &lt; <http://dx.doi.org/10.1016/j.ijid.2011.03.021> .
- TRINH, T. K.; KANG, L. S. Response surface methodological approach to optimize the coagulation–flocculation process in drinking water treatment. v. 89, n. 7, p. 1126–1135, July 2011 2011. Available at: &lt; <http://dx.doi.org/10.1016/j.cherd.2010.12.004> .
- TSUME, Y. et al. The Biopharmaceutics Classification System: subclasses for in vivo predictive dissolution (IPD) methodology and IVIVC. **Eur J Pharm Sci**, v. 57, p. 152-63, Jun 2014. ISSN 1879-0720. Available at: &lt; <https://www.ncbi.nlm.nih.gov/pubmed/24486482> .
- UENO, N.; WILSON, M. E. Receptor-mediated phagocytosis of Leishmania: implications for intracellular survival. **Trends Parasitol**, v. 28, n. 8, p. 335-44, Aug 2012. ISSN 1471-5007. Available at: &lt; <https://www.ncbi.nlm.nih.gov/pubmed/22726697> .
- UNER, M. Preparation, characterization and physico-chemical properties of solid lipid nanoparticles (SLN) and nanostructured lipid carriers (NLC): their benefits as colloidal drug carrier systems. **Pharmazie**, v. 61, n. 5, p. 375-86, May 2006. ISSN 0031-7144 (Print)0031-7144.
- VAN DE VEN, H. et al. Intracellular drug delivery in Leishmania-infected macrophages: Evaluation of saponin-loaded PLGA nanoparticles. **J Drug Target**, v. 20, n. 2, p. 142-54, Feb 2012. ISSN 1026-7158. Available at: &lt; <http://dx.doi.org/10.3109/1061186x.2011.595491> .
- VENKATESH, G. et al. In vitro and in vivo evaluation of self-microemulsifying drug delivery system of buparvaquone. **Drug Dev Ind Pharm**, v. 36, n. 6, p. 735-45, Jun 2010. ISSN 1520-5762. Available at: &lt; <https://www.ncbi.nlm.nih.gov/pubmed/20136493> .
- VEXENAT, J. A. et al. Failure of buparvaquone (Butalex) in the treatment of canine visceral leishmaniosis. **Vet Parasitol**, v. 77, n. 1, p. 71-3, May 1998. ISSN 0304-4017. Available at: &lt; <https://www.ncbi.nlm.nih.gov/pubmed/9652385> .
- VO, C. L.; PARK, C.; LEE, B. J. Current trends and future perspectives of solid dispersions containing poorly water-soluble drugs. **Eur J Pharm Biopharm**, v. 85, n. 3 Pt B, p. 799-813, Nov 2013. ISSN 1873-3441. Available at: &lt; <https://www.ncbi.nlm.nih.gov/pubmed/24056053> .



- WANG, F. et al. The biomolecular corona is retained during nanoparticle uptake and protects the cells from the damage induced by cationic nanoparticles until degraded in the lysosomes. **Nanomedicine**, v. 9, n. 8, p. 1159-68, Nov 2013. ISSN 1549-9634. Available at: &lt;<http://dx.doi.org/10.1016/j.nano.2013.04.010> .
- WANG, H. et al. Application of response surface methodology to optimise supercritical carbon dioxide extraction of essential oil from *Cyperus rotundus* Linn. **Food Chem**, v. 132, n. 1, p. 582-7, May 2012. ISSN 0308-8146. Available at: &lt;<https://www.ncbi.nlm.nih.gov/pubmed/26434335> .
- WANG, K. et al. Effect of solid lipid's structure on nanostructured lipid carriers encapsulated with sun filter: characterisation, photo-stability and in vitro release. **J Microencapsul**, v. 34, n. 1, p. 104-110, Feb 2017. ISSN 0265-2048. Available at: &lt;<http://dx.doi.org/10.1080/02652048.2017.1290156> .
- WANG, L. et al. PEGylated nanostructured lipid carriers (PEG-NLC) as a novel drug delivery system for biochanin A. **Drug Dev Ind Pharm**, v. 41, n. 7, p. 1204-12, 2015. ISSN 1520-5762. Available at: &lt;<https://www.ncbi.nlm.nih.gov/pubmed/25010850> .
- WARING, M. J. et al. An analysis of the attrition of drug candidates from four major pharmaceutical companies. **Nat Rev Drug Discov**, v. 14, n. 7, p. 475-86, Jul 2015. ISSN 1474-1784. Available at: &lt;<https://www.ncbi.nlm.nih.gov/pubmed/26091267> .
- WASAN, E. K. et al. A novel tropically stable oral amphotericin B formulation (iCo-010) exhibits efficacy against visceral Leishmaniasis in a murine model. **PLoS Negl Trop Dis**, v. 4, n. 12, p. e913, Dec 07 2010. ISSN 1935-2727. Available at: &lt;<http://dx.doi.org/10.1371/journal.pntd.0000913> .
- WEBER, S.; ZIMMER, A.; PARDEIKE, J. Solid Lipid Nanoparticles (SLN) and Nanostructured Lipid Carriers (NLC) for pulmonary application: a review of the state of the art. **Eur J Pharm Biopharm**, v. 86, n. 1, p. 7-22, Jan 2014. ISSN 1873-3441. Available at: &lt;<https://www.ncbi.nlm.nih.gov/pubmed/24007657> .
- WHO. Control of the leishmaniasis: report of a meeting of the WHO Expert Committee on the Control of Leishmaniasis. **WHO technical report series**, Geneva, 2010. Available at: &lt;[http://whqlibdoc.who.int/trs/WHO\\_TRS\\_949\\_eng.pdf](http://whqlibdoc.who.int/trs/WHO_TRS_949_eng.pdf) . Accessed on: 05 May.
- \_\_\_\_\_. **Frequently Asked Questions on Visceral Leishmaniasis (Kala-azar)**: World Health Organization: 15 p. 2013.
- \_\_\_\_\_. Third WHO report on neglected tropical diseases: "Investing to overcome the global impact of neglected tropical diseases. Geneva, 2015.

Available at: <br>[http://www.who.int/neglected\\_diseases/9789241564861/en/](http://www.who.int/neglected_diseases/9789241564861/en/) . Accessed on: May 15th.

\_\_\_\_\_. **Integrating neglected tropical diseases in global health and development - Fourth WHO report on neglected tropical diseases.** World Health Organization, p.vi. 2017

WILLIAMS, H. D. et al. Strategies to address low drug solubility in discovery and development. **Pharmacol Rev**, v. 65, n. 1, p. 315-499, Jan 2013a. ISSN 1521-0081. Available at: <br><https://www.ncbi.nlm.nih.gov/pubmed/23383426> .

\_\_\_\_\_. Strategies to address low drug solubility in discovery and development. **Pharmacol Rev**, v. 65, n. 1, p. 315-499, Jan 2013b. ISSN 1521-0081. Available at: <br><https://www.ncbi.nlm.nih.gov/pubmed/23383426> .

WU, C. Y.; BENET, L. Z. Predicting drug disposition via application of BCS: transport/absorption/ elimination interplay and development of a biopharmaceutics drug disposition classification system. **Pharm Res**, v. 22, n. 1, p. 11-23, Jan 2005. ISSN 0724-8741. Available at: <br><https://www.ncbi.nlm.nih.gov/pubmed/15771225> .

XU, W.; LING, P.; ZHANG, T. Polymeric micelles, a promising drug delivery system to enhance bioavailability of poorly water-soluble drugs. **J Drug Deliv**, v. 2013, p. 340315, 2013a. ISSN 2090-3014. Available at: <br><https://www.ncbi.nlm.nih.gov/pubmed/23936656> .

\_\_\_\_\_. Polymeric micelles, a promising drug delivery system to enhance bioavailability of poorly water-soluble drugs. **J Drug Deliv**, v. 2013, p. 340315, 2013b. ISSN 2090-3014. Available at: <br><https://www.ncbi.nlm.nih.gov/pubmed/23936656> .

YANEZ, J. A. et al. Intestinal lymphatic transport for drug delivery. **Adv Drug Deliv Rev**, v. 63, n. 10-11, p. 923-42, Sep 10 2011. ISSN 0169-409x. Available at: <br><http://dx.doi.org/10.1016/j.addr.2011.05.019> .

YINGCHONCHAROEN, P.; KALINOWSKI, D. S.; RICHARDSON, D. R. Lipid-Based Drug Delivery Systems in Cancer Therapy: What Is Available and What Is Yet to Come. **Pharmacol Rev**, v. 68, n. 3, p. 701-87, 07 2016. ISSN 1521-0081. Available at: <br><https://www.ncbi.nlm.nih.gov/pubmed/27363439> .

YOSTAWONKUL, J. et al. Surface modification of nanostructure lipid carrier (NLC) by oleoyl-quaternized-chitosan as a mucoadhesive nanocarrier. **Colloids Surf B Biointerfaces**, v. 149, p. 301-311, Jan 01 2017. ISSN 0927-7765. Available at: <br><http://dx.doi.org/10.1016/j.colsurfb.2016.09.049> .

- YU, S. et al. Nanostructured lipid carrier (NLC)-based novel hydrogels as potential carriers for nepafenac applied after cataract surgery for the treatment of inflammation: design, characterization and *in vitro* cellular inhibition and uptake studies. **RSC Adv**, v. 7, n. 27, p. 16668-16677, 2017.
- YUAN, H. et al. Preparation and characteristics of nanostructured lipid carriers for control-releasing progesterone by melt-emulsification. **Colloids Surf B Biointerfaces**, v. 60, n. 2, p. 174-9, Nov 2007. ISSN 0927-7765. Available at: &lt; <https://www.ncbi.nlm.nih.gov/pubmed/17656075> .
- ZHANG, Y. et al. Ethyl oleate-containing nanostructured lipid carriers improve oral bioavailability of trans-ferulic acid as compared with conventional solid lipid nanoparticles. **Int J Pharm**, v. 511, n. 1, p. 57-64, Sep 10 2016. ISSN 0378-5173. Available at: &lt; <http://dx.doi.org/10.1016/j.ijpharm.2016.06.131> .
- ZHOU, L. et al. Development of a high throughput equilibrium solubility assay using miniaturized shake-flask method in early drug discovery. **J Pharm Sci**, v. 96, n. 11, p. 3052-71, Nov 2007. ISSN 0022-3549. Available at: &lt; <https://www.ncbi.nlm.nih.gov/pubmed/17722003> .

## Appendices



**Universidade de São Paulo**  
**Faculdade de Ciências Farmacêuticas**

**Documento sem validade oficial**

**FICHA DO ALUNO**

---

**9139 - 7348244/2 - Lis Marie Monteiro**

<b>Email:</b>	lismarie@usp.br
<b>Data de Nascimento:</b>	12/08/1983
<b>Cédula de Identidade:</b>	RG - 6.218.177 0 - PR
<b>Local de Nascimento:</b>	Estado do Paraná
<b>Nacionalidade:</b>	Brasileira
<b>Graduação:</b>	Farmacêutico - Universidade Estadual de Londrina - Paraná - Brasil - 2006
<b>Mestrado:</b>	Mestra em Ciências - Área: Produção e Controle Farmacêuticos - Faculdade de Ciências Farmacêuticas - Universidade de São Paulo - São Paulo - Brasil - 2013

---

<b>Curso:</b>	Doutorado
<b>Programa:</b>	Fármaco e Medicamentos
<b>Área:</b>	Produção e Controle Farmacêuticos
<b>Data de Matrícula:</b>	07/06/2013
<b>Início da Contagem de Prazo:</b>	07/06/2013
<b>Data Limite para o Depósito:</b>	07/06/2017
<b>Orientador na USP:</b>	Prof(a). Dr(a). Nádía Araci Bou Chacra - 07/06/2013 até o presente. Email: chacra@usp.br
<b>Co-orientador:</b>	Prof(a). Dr(a). Paulo Cesar Cotrim - 10/06/2015 até o presente. Email: pccotrim@usp.br

**Aluno USP em convênio de dupla titulação com instituição estrangeira**

<b>Instituição Conveniada:</b>	University of Alberta, Canadá
<b>Orientador na Instituição Conveniada:</b>	Raimar Loebenberg
<b>Proficiência em Línguas:</b>	Inglês, Aprovado em 07/06/2013
<b>Data de Aprovação no Exame de Qualificação:</b>	Aprovado em 30/07/2015
<b>Data do Depósito do Trabalho:</b>	
<b>Título do Trabalho:</b>	
<b>Data Máxima para Aprovação da Banca:</b>	
<b>Data de Aprovação da Banca:</b>	
<b>Data Máxima para Defesa:</b>	
<b>Data da Defesa:</b>	
<b>Resultado da Defesa:</b>	
<b>Histórico de Ocorrências:</b>	Primeira Matrícula em 07/06/2013

---

Aluno matriculado no Regimento da Pós-Graduação USP (Resolução nº 6542 em vigor a partir de 20/04/2013).

**Última ocorrência:** Matrícula de Acompanhamento em 06/02/2017



**Universidade de São Paulo**  
**Faculdade de Ciências Farmacêuticas**  
**Documento sem validade oficial**  
**FICHA DO ALUNO**

**9139 - 7348244/2 - Lis Marie Monteiro**

Sigla	Nome da Disciplina	Início	Término	Carga Horária	Cred.	Freq.	Conc.	Exc.	Situação
FBF5810-1/1	Tópicos Avançados em Fármaco e Medicamentos. Espectroscopias Raman e no Infravermelho Próximo Associadas à Quimiometria: Aplicação no Desenvolvimento e no Controle em Processo de Medicamentos com Base Nanotecnológica	24/06/2013	30/06/2013	30	2	100	A	N	Concluída
FBF5805-1/2	Delineamento de Experimentos e Ferramentas Estatísticas Aplicadas às Ciências Farmacêuticas	14/08/2013	17/09/2013	45	3	80	A	N	Concluída
FBF5779-2/1	Preparo de Artigos Científicos na Área de Farmácia	16/08/2013	17/10/2013	90	6	90	A	N	Concluída
FBF5794-2/4	Tópicos Gerais de Fármaco e Medicamentos II	11/09/2013	19/11/2013	30	2	100	A	N	Concluída
FBF5813-1/1	Tecnologias de Caracterização de Sistemas Nanoestruturados	04/09/2014	15/10/2014	90	6	100	A	N	Concluída
FBF5766-3/2	Biodisponibilidade e Bioequivalência de Medicamentos	30/09/2014	01/12/2014	90	0	-	-	N	Matrícula cancelada
FBF5819-1/1	Tópicos Avançados em Fármaco e Medicamentos (Tecnologia Analítica de Processo - PAT e Qualidade por Design - QbD)	22/06/2015	30/06/2015	30	2	100	A	N	Concluída
FBF5821-1/1	Tópicos Avançados em Fármaco e Medicamentos (Avanços e Desafios no Desenvolvimento de Sistemas Nanoestruturados para a Liberação Modificada de Fármacos)	23/09/2015	21/10/2015	30	2	100	A	N	Concluída
FBA5758-1/1	Fundamentos do Planejamento Experimental e Otimização Simplex	26/01/2016	01/02/2016	30	2	75	A	N	Concluída

	Créditos mínimos exigidos		Créditos obtidos
	Para exame de qualificação	Para depósito de tese	
<b>Disciplinas:</b>	0	20	25
<b>Estágios:</b>			
<b>Total:</b>	0	20	25

**Créditos Atribuídos à Tese:** 167

Conceito a partir de 02/01/1997:
A - Excelente, com direito a crédito; B - Bom, com direito a crédito; C - Regular, com direito a crédito; R - Reprovado; T - Transferência.
Um(1) crédito equivale a 15 horas de atividade programada.

**Última ocorrência:** Matrícula de Acompanhamento em 06/02/2017

**Impresso em:** 05/06/2017 09:33:13

**9139 - 7348244/2 - Lis Marie Monteiro**

Comissão julgadora da tese de doutorado:			
NUSP	Nome	Vínculo	Função
1231705	Nádia Araci Bou Chacra	FCF - USP	Presidente

**Última ocorrência:** Matrícula de Acompanhamento em 06/02/2017

**Impresso em:** 05/06/2017 09:33:13



*Certificate of Completion*  
*The United States Pharmacopeial Convention*

recognizes

*Lis Marie Monteiro*

*to certify successful completion with excellence of the*

*USP Visiting Scientist Program*

May 2, 2014

A handwritten signature in black ink, appearing to read "R. Piervincenzi", written over a horizontal line.

Ronald T. Piervincenzi, Ph.D.  
Chief Executive Officer

